Characterization of redox proteins using electrochemical methods

Marc F.J.M. Verhagen

1

Promotor: Dr C. Veeger
          Hoogleraar in de Biochemie

Co-Promotor: Dr W.R. Hagen
          Universitair hoofddocent, vakgroep Biochemie

Marc Verhagen

Characterization of redox proteins using electrochemical methods

Proefschrift
ter verkrijging van de graad van doctor
in de landbouw- en milieuwetenschappen
op gezag van de rector magnificus,
Dr C.M. Karssen,
in het openbaar te verdedigen
op maandag 1 mei 1995
des namiddags te vier uur in de Aula
van de Landbouwuniversiteit te Wageningen

III

IV

Stellingen

1   De constatering dat het afwezig zijn van een mengsel van twee N-termini in het desulfoferrodoxine preparaat van Verhagen *et al.* te wijten is aan een te stringente zuiveringsprocedure gaat voorbij aan het uiteindelijke doel van eiwitzuivering.

> Chen, L., Sharma, P., Le Gall, J., Mariano, A.M., Teixeira, M., & Xavier, A.V., *Eur. J. Biochem.*, (1994) 226, 613-618.
> Hoofdstuk 4 van dit proefschrift.

2   Met het bepalen van een halfwaarde potentiaal uit een irreversibel voltammogram geven de auteurs aan dat ze het niet zo nauw nemen met de Nernst vergelijking.

> Tan, J. & Cowan, J.A., *Biochemistry*, (1990) 29, 4886-4892.

3   Een diffusiecoefficient van 0.3 cm^2/s voor het dissimilatoire sulfietreductase van *Desulfovibrio vulgaris* (Mw: 200 kD), zoals berekend kan worden uit de door Lui en Cowan gepresenteerde electrochemische data, is fysisch onmogelijk.

> Lui, S.M. & Cowan, J.A., *J. Am. Chem. Soc.*, (1994) 116, 11538-11549.

4   In de bepaling van de stabiliteitsparameters van cytochroom *c* met behulp van "hydrogen exchange" experimenten gaan Bai *et al.* voorbij aan het bestaan van verschillende pH en temperatuur afhankelijke conformatietoestanden zoals beschreven voor dit eiwit door Ikeshoji *et al.*

> Bai, Y., Milne, J.S., Mayne, L. & Englander, S.W., *Proteins: Structure, Function and Genetics*, (1994) 20, 4-14.
> Ikeshoji, T., Taniguchi, I., Hawkridge, F.M., *J. Electroanal. Chem.*, (1989) 270, 297-308.

5   Met de vermelding dat *Pyrococcus furiosus* sporenelementen nodig heeft aangezien het onder andere Zn gesubstitueerd rubredoxine bevat geven de auteurs aan dat ze de strekking van het door hen geciteerde artikel niet begrepen hebben.

               Hoaki, T., Nishijima, M., Kato, M., Adachi, K., Mizobuchi, S., Hanzawa, N. & Maruyama, T., *Applied and Environmental Microbiology*, (1994) 60, 2898-2904.

6   Gezien de overvloed aan nietszeggende artikelen verdient het aanbeveling de "kleinst publiceerbare eenheid" als officiële SI standaard vast te leggen.

7   De term gedoogbeleid suggereert ten onrechte dat acceptatie van de status quo een vorm van beleid is.

8   Bij het vergelijken van drie verschillende eiwit bepalingsmethoden draait de fabrikant van een van deze methoden de gebruiker een "Bio Rad" voor de ogen door vermelding van de spreiding in de gemiddelde waarde achterwege te laten.

               Gebruiksaanwijzing Bio Rad protein assay

9   In het huidige regeringsbeleid worden de begrippen doel en middel nogal eens door elkaar gehaald.

Marc Verhagen
Characterization of redox proteins using electrochemical methods
Wageningen, 1 mei 1995

Voorwoord

Het voorwoord: Het laatste stukje tekst dat aan het proefschrift wordt toegevoegd maar het eerste dat door de meeste mensen wordt gelezen. Na bijna 6 jaar is het einde van de promotie in zicht en heb ik nog een laatste kans om de mensen die een bijdrage geleverd hebben aan dit proefschrift te bedanken:

In de eerste plaats mijn co-promotor Fred Hagen. Zijn ideeën en visie hebben als fundament voor dit proefschrift gediend. Ook de vele evaluaties zowel binnen als buiten het lab hebben veel bijgedragen aan het uiteindelijke resultaat. Vervolgens mijn promotor Professor Veeger die mijn artikelen voor publicatie nauwgezet doornam en met een kritische blik de puntjes op de i zette. En natuurlijk Antonio Pierik, Ronnie Wolbert, Dirk Heering, Sander Arendsen en Yvonne Bulsink die als labgenoten een belangrijke bijdrage leverden aan de plezierige en enthousiaste werksfeer op lab I/II (voorheen lab V).

Met veel plezier denk ik terug aan de tijd waarin een aantal studenten bij het lab kwam voor een afstudeervak. Aangezien ze bijna allemaal tegelijk kwamen was het een drukke tijd waarin bij tijd en wijle zoveel geluid geproduceerd werd in het lab dat het met recht een dierentuin genoemd kon worden. Ingeborg Kooter, Richard van Kranenburg, Peter Schenkels, Bart van de Beek, Joost Kolkman, Wilfried Voorhorst en Elise Meussen; jullie bijdrage is essentieel geweest voor de totstandkoming van dit boekje. Ik heb veel van jullie geleerd en ik hoop dat dat ook omgekeerd het geval is geweest.

De leden van de vakgroep Biochemie voor de hulp en de getoonde interesse. Ik heb altijd met veel plezier mijn werk kunnen doen op de vakgroep. Met name Laura, Martin en Beri die alle administratieve zaken voor hun rekening namen; Jacques Benen en Adrie Westphal, die mij in eerste instantie belangeloos lipoamide dehydrogenase ter beschikking stelden en later de overproduktiekloon; en Axel Berg, Frank Vergeldt en Martina Duyvis, voor de hulp tijdens het afronden van de promotie (wat in het laatste jaar op afstand moest gebeuren), de gastvrijheid, de etentjes en hun bondgenootschap bij "ludieke acties". In ieder geval voor mij overtuigend bewijs dat goede collega's ook goede vrienden kunnen zijn.

Dr Thomas Link for the fruitful collaboration concerning the soluble fragment of the Rieske protein the results of which are described in chapter 8.

Maurice Franssen die als een van de opstarters van het oorspronkelijke project de vinger aan de pols hield met betrekking tot de voortgang van het onderzoek tijdens halfjaarlijkse "werklunches".

v

De groep "moleculaire wetenschappers" waarmee vele expedities zijn ondernomen, discussies gevoerd en vakantiehuisjes bezocht. Het voltooien van dit proefschrift betekent overigens niet dat ik nu een stapje verder ben.

Mijn ouders voor de mogelijkheden en de vrijheden die ze me gegeven hebben en het optimisme waarmee ze me altijd hebben gestimuleerd. Vincent, Paul, Marja, Michiel, Marjo en Maril voor hun hulp en interesse en de vergevingsgezindheid wanneer ik weer eens een paar uur later op kwam duiken dan verwacht.

Finally, I want to thank Professor Mike Adams for allowing me to finish this thesis while working in his lab.

CONTENTS

Abbreviations

A	surface area or hyperfine constant
Ac	Acetate
A	absorbance
AMP	adenosine 5'-monophosphate
AdoPSO$_4$	adenosine 5'-phosphosulfate
ATCC	American Type Culture Collection
B	magnetic field
Caps	3-(cyclohexylamino)-1-propanesulfonic acid
Ches	2-(N-cyclohexylamino)-ethanesulphonic acid
CoA	Coenzyme A
D	axial zero-field splitting parameter
DEAE	Diethylaminoethyl
DSM	Deutsche Sammlung für Mikroorganismen
DTPA	diethylenetriaminepentaacetate
E	redox potential or rhombic zero-field splitting parameter
E_m	midpoint potential
E/D	rhombicity
EDTA	ethylenediaminetetraacetate
EPR	Electron Paramagnetic Resonance
F	Faraday constant
FAD	Flavin Adenine Dinucleotide
FMN	Flavin Adenine Mononucleotide
FPLC	fast protein liquid chromatography
GC	glassy carbon or gas chromatograph
H	Hamiltonian operator
Hepes	4-(2-hydroxyethyl)-1-piperazineethane sulfonic acid
I	current or nuclear spin quantum number
IEF	isoelectric focusing
K_m	Michaelis-Menten constant
k	second order rate constant
k_s	standard heterogeneous rate constant
kDa	kilodalton
MCD	Magnetic circular dichroism
Mes	2-(N-morpholino)ethanesulphonic acid
Mops	3-(N-morpholino)propanesulfonic acid
mT	millitesla
n	number of electrons involved in a redox reaction

| NAD(P)H | reduced nicotinamide-adenine dinucleotide (phosphate) |
NCIB	National Collection of Industrial and marine Bacteria
NHE	Normal Hydrogen Electrode
PAGE	polyacrylamide gel electrophoresis
pI	isoelectric point
R	gas constant
S	spin (operator)
SCE	saturated calomel electrode
sd	standard deviation
SDS	sodium dodecyl sulfate
SHE	Standard Hydrogen Electrode
T	absolute temperature
Tris	tris(hydroxymethyl)aminoethane
U	unit of enzymatic activity (1 μmol product per minute)
UV	ultraviolet
v	potential scan rate
VIS	visible
W	linewidth
α	transfer coefficient
ϵ	extinction coefficient
Γ	surface concentration

Chapter 1

introduction

Introduction

Redox proteins

Proteins involved in electron transfer reactions are collectively known as redox proteins. This very diverse group ranges from small proteins, which generally serve as shuttles for the transport of electrons, to complex enzymes involved in e.g. the generation of energy in the living cell. A common property of these proteins is the presence of a redox active group. This group is often present as a cofactor and can be composed of transition elements (e.g. Fe, Cu), organic molecules (e.g. flavin, pyrroloquinoline quinone (PQQ)) or a combination of the two (e.g. heme, molybdopterin). Dependent on the function of a redox protein a different cofactor is encountered. Both its capability to coordinate certain substrates and the value of its redox potential determine the usefulness of a cofactor for a specific reaction. The redox potential of a cofactor can be modulated by changing its direct environment. In a protein the redox potential can, therefore, be regulated through the supply of different amino acid side chains. In this way it is possible to tune redox potentials over a wide potential range. In the living cell at pH 7 the upper limit for the redox potentials is set by the redox couple H_2O/O_2 (+830 mV) and for most organisms the lower limit by the couple H_2/H^+ (-420 mV). An illustration of the variety of redox potentials encountered with redox proteins is given in fig 1.
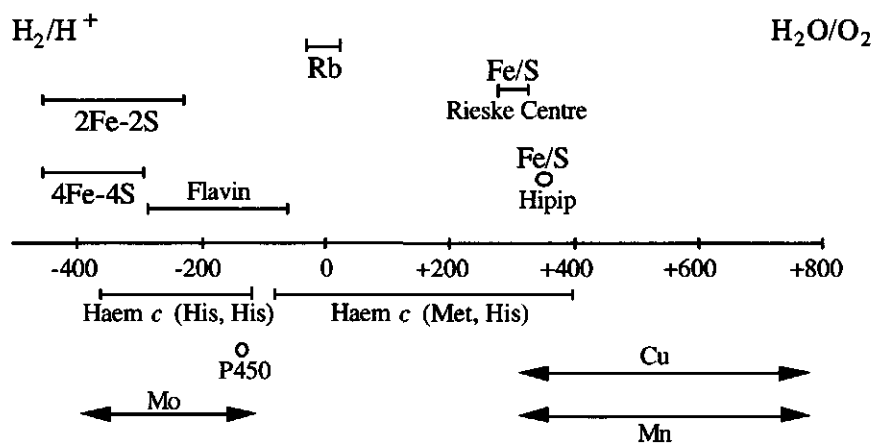
Figure 1: Potential ranges in mV versus SHE of several redox cofactors in redox proteins. Rb, rubredoxin; P450, cytochrome P450; HiPIP, High potential iron protein; Mo, Molybdenum proteins; Flavin, Flavoproteins; Cu, Copper proteins; Mn, Manganese containing proteins. Modified from ref [1]

The proteins indicated in fig. 1 can be divided in three major classes dependent on the type of redox cofactor present. Some of the characteristic properties of these different classes are summarized below:

Iron sulfur proteins : These proteins contain clusters consisting of iron and acid-labile sulfide ions in different stoichiometries. The iron ion is coordinated to the protein through cysteine residues cf. [2] or, in some cases, histidine residues ([3] and refs. therein). An overview of structures of some iron-sulfur clusters is given below in fig. 2

[1Fe]   [2Fe-2S]   [3Fe-4S]   [4Fe-4S]
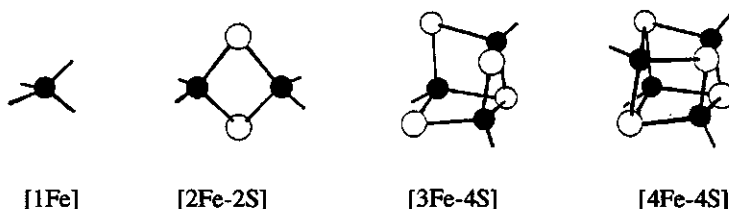
Figure 2: Examples of the coordination in iron-sulfur proteins. From left to right: rubredoxin-type center; 2Fe-2S; 3Fe-4S and 4Fe-4S cluster (modified from [4]).

Heme proteins: These proteins contain Fe-protoporphyrin IX (heme) as the cofactor. The heme is sometimes covalently bound to the protein through thioether bonds like in cytochrome c . The iron ion in the heme can be pentacoordinate (Cytochrome P450) or hexacoordinate (cytochrome c) with four ligands provided by the heme and one or two ligands provided by the protein matrix or the substrate [5; 6].

Flavoproteins: These proteins carry the cofactor flavin adenine dinucleotide (FAD) or the comparable flavin adenine mononucleotide (FMN) in their active site. This cofactor is, in most cases, non-covalently bound to the protein and can, therefore, dissociate [7]. FAD and FMN can be reduced by 2 electrons. The protein matrix, however, can stabilize the semiquinone state as in flavodoxin thus making it a one electron transferring group [8; 9].

The classification given above is far from complete. Several examples exist of proteins which contain multiple cofactors. These cofactors can be from the same class (e.g. the enzyme hydrogenase contains two cubane type [4Fe-4S] clusters and one putative [6Fe-6S] cluster

with unknown structure ([10] and refs therein) or from different classes (e.g. AdoPSO4 reductase contains one Fe-S cluster and one FAD as cofactors [chapter 9]).


Electrochemistry

Electrochemical techniques were originally part of the toolbox of physical chemists. They used these techniques to study the redox properties of metal ions both free in solution and in complexes with coordination compounds. It enabled them to obtain a dynamical picture of the redox compound in solution and determine properties like the formal redox potential, the stability of the compound, its electron transfer reactivity, and chemical reactivity in the presence of other reagents. For this purpose a vast number of electrochemical techniques were designed and over the years the theory for these techniques has been sorted out to a great extent [11; 12; 13]. A frequently used technique is cyclic voltammetry.

In a cyclic voltammetry (CV) experiment the potential of the working electrode is swept linearly between two limiting potential values with respect to a reference electrode with constant potential. A counter electrode is present to obtain a circuit with low resistance to avoid the ohmic potential drop. If it is assumed that the redox couple in solution is always in equilibrium with the working electrode the Nernst equation applies.

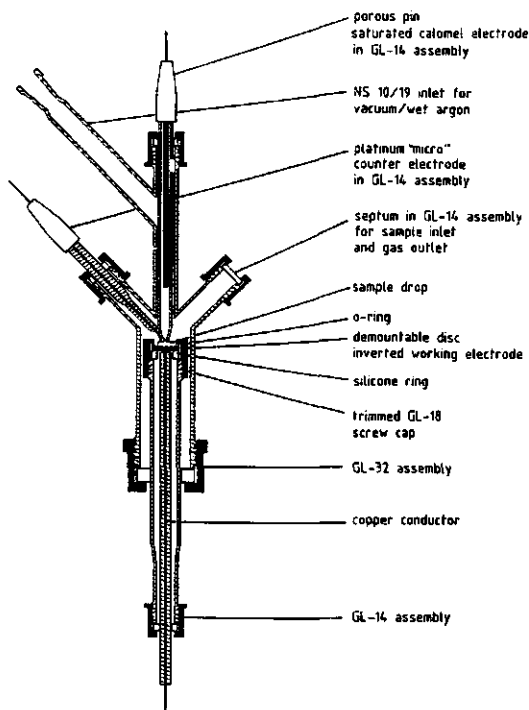$$E = E^{\circ} + RT/nF \cdot \ln\{[ox]/[red]\}$$

E is the solution potential, E° is the midpoint potential of the redox couple, n is the number of electrons, R is the gas constant, T is the temperature, F is the charge of one mol electrons (Faraday constant) and [ox] and [red] represent the concentration in solution of the oxidized and the reduced species, respectively. A change of the potential of the electrode (E) results in a change of the concentration ratio of the oxidized over the reduced species. The current, which consequently flows through the circuit formed by the working electrode and the counter electrode, can be recorded as a function of the potential. A graph of the current versus the potential is called a cyclic voltammogram. From the voltammogram the midpoint potential of the redox couple can be calculated as the average of the cathodic (reduction) and anodic (oxidation) peak potentials. Furthermore, the shape of the voltammogram and the behaviour of the peak current at different scan rates indicate whether a redox couple is adsorbed to the electrode or free in solution. Examples of cyclic voltammograms for an adsorbed and a free redox couple are given in fig. 3
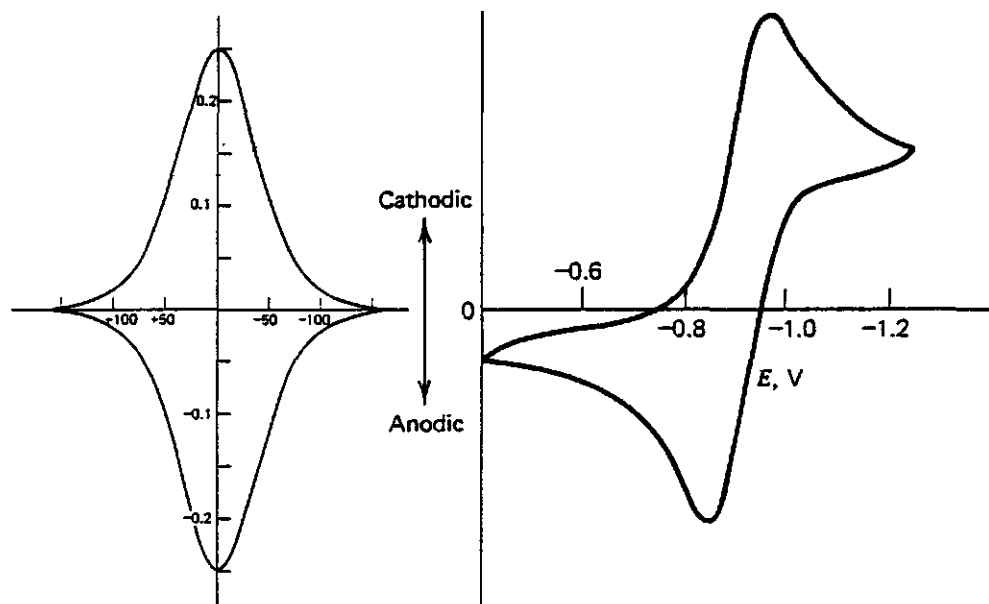
Figure 3: Cyclic voltammograms for a redox couple adsorbed onto the electrode (left) and a couple free in solution (right).

The study of redox proteins also requires methods to determine the behaviour of the redox cofactor in the protein. It is, therefore, not surprising that bioinorganic chemists started to explore the use of electrochemical techniques to study the properties of redox proteins. The adaptation of the new technique went hand in hand with some necessary changes in the experimental setup. Cells were designed in which the sample volume for an experiment was decreased a hundred fold fig. 4 [14]. Also the frequently used mercury electrodes, the site of the redox reaction, were replaced by solid electrodes like gold, platinum, or carbon. Despite the changes and the increasing effort it took several years before the first successful experiments were reported with horse heart cytochrome c at a gold electrode modified with 4,4'-bipyridyl [15]. This breakthrough was the result of the work of Hill and coworkers. In their subsequent work they showed that 4,4'-bipyridyl adsorbed to the gold electrode thus creating a surface suitable for the electrochemistry of the cytochrome [15; 16; 17]. However, the combination of 4,4'-bipyridyl with gold could only be used for cytochromes. With other proteins different combinations had to be made and a voltammetric response were only obtained when a 'compatible' surface could be created.

6

porous pin
saturated calomel electrode
in GL-14 assembly

NS 10/19 inlet for
vacuum/wet argon

platinum "micro"
counter electrode
in GL-14 assembly

septum in GL-14 assembly
for sample inlet
and gas outlet

sample drop

o-ring
demountable disc
inverted working electrode

silicone ring

trimmed GL-18
screw cap

GL-32 assembly

copper conductor

GL-14 assembly

Figure 4: Electrochemical cell for direct electrochemistry with small sample volumes as designed by Hagen [14].

A number of compounds ranging from small divalent and trivalent metal ions (Mg^{2+}, $Cr(NH_3)_6^{3+}$) to complex organic molecules (neomycin) were tested and found to be useful in protein electrochemistry [18]. These compounds were called 'promotors' since there presence was essential for the redox reaction of a protein at a solid electrode and unlike mediators they were not directly involved in the electron transfer. In this way a number of recipes for the electrochemistry of small electron carrier proteins like ferredoxin, plastocyanin and rubredoxin were designed [*ibid.*]. Unfortunately, although some general rules for the combination of protein, electrode material and promotor were postulated, finding the best combination remained a matter of trial and error. A different approach was, therefore, followed by Hagen [14]. He suggested that it should be possible to use an electrode material suitable for the electrochemistry of different proteins without the need for promotors. Indeed, he showed that several proteins could be studied with a bare glassy carbon electrode pretreated by immersion in concentrated nitric acid. The active surface created in this way is believed to be represented by fig. 5
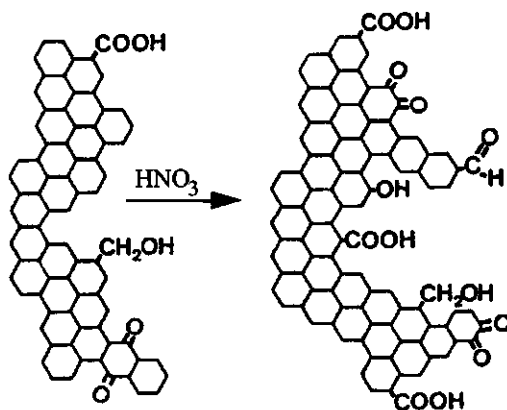
7

Figure 5: Schematic representation of glassy carbon and its functional groups. Modified from ref [19]

Dynamics of redox cofactors in proteins

The possibility to follow the reduction and oxidation reactions at room temperature makes it possible to study the dynamics of these reactions. A good example is the elegant voltammetric study by Armstrong and coworkers of the 7 Fe ferredoxin from *Desulfovibrio africanus*. This protein contains one [4Fe-4S] and one [3Fe-4S] cluster. During reduction of these clusters in the presence of Fe^{2+} the [3Fe-4S] cluster is converted to a [4Fe-4S] cluster. This directly follows from the voltammogram since the two clusters have different potentials and, therefore, it is possible to study the kinetics of cluster transformation [20]. The physiological relevance of cluster conversions is obvious from studies on the enzyme aconitase. This catalyst, which is part of the citric acid cycle, has a [4Fe-4S] cluster in its active site. This iron sulfur cluster, however, does not have a redox function but serves to bind and activate the substrate [21]. The conversion of the [4Fe-4S] cluster into an [3Fe-4S] cluster was found to inactivate the enzyme. The enzyme was activated again upon addition of Fe^{2+} and reducing equivalents. The activation was found to coincide with the regeneration of the [4Fe-4S] cluster [22]. Cyclic voltammetry experiments with the ferredoxin were also used to determine the binding constant of 2-mercaptoethanol to the "removable" iron in the [4Fe-4S] cluster. This iron atom is not coordinated to the protein matrix and can, therefore, bind other ligands [23]. Again aconitase can be used as the example that binding of extraneous ligands can have an important physiological function.

Another example of the use of electrochemistry to study the dynamic behavior of proteins is the work of Haladjian et al. and Barker and Mauk on horse heart and yeast

8

cytochrome *c* at high pH values. The redox potential of this protein changes above pH 8 due to the replacement of a methionine, the sixth ligand to the heme iron, by a lysine [24; 25]. Using cyclic voltammetry at high pH values it was found that the reduced forms of the "alkaline" and the "native" cytochrome *c* were in equilibrium. When a slow scan rate was used a distorted voltammogram was observed with a cathodic peak shifted to negative potential and a cathodic peak at almost unchanged position compared to the voltammogram at neutral pH. Upon increasing the scan rate the anodic peak potential also shifted to negative potential values, thus restoring the shape of the voltammogram expected for one redox couple. Representative voltammograms and a scheme of the electrochemical behaviour of yeast iso-1-cytochrome *c* are shown in fig. 6.
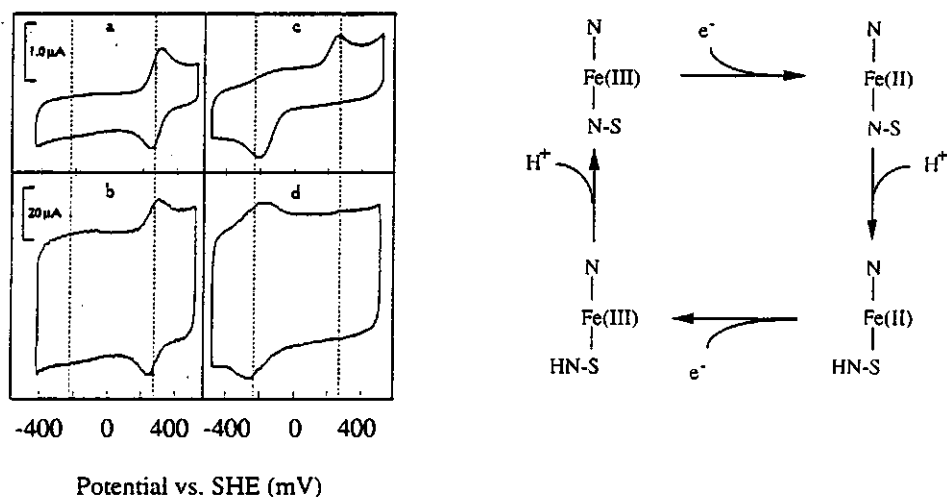

Figure 6: Cyclic voltammograms and a scheme describing the conformations of yeast iso-1-cytochrome *c* at a pyrolytic graphite electrode at different pH intervals. Panel a and b: pH 7.1 and sweep rates 20 mV s^{-1} (a) and 2 V s^{-1} (b). Panel c and d: pH 10.3 and sweep rates 20 mV s^{-1} (c) and 2 V s^{-1} (d). Modified from refs. [24; 25]

The oxidized cytochrome at high pH readily interconverts from the Met/His ligation to the Lys/His ligation [26]. This results in a decrease of the redox potential and a subsequent shift of the cathodic peak potential. The reduced protein favours the Met/His ligation and the change of ligation results in an oxidation potential similar to the native protein. If the rate of this interconversion is fast compared to the time scale of cyclic voltammetry a distorted voltammogram will appear as shown above in fig. 6 c. However, at high scan rates the interconversion cannot take place during an oxidation reduction cycle. For cytochrome *c* this means that the alkaline state is "frozen". Therefore, the voltammogram indicates the presence of only one redox couple. From this voltammogram the midpoint potential of the alkaline form of cytochrome *c* can be determined.

9

Electrochemistry of redox enzymes

The use of electrochemical techniques to probe the active site of redox enzymes remains not straightforward. Some reports have been published on the voltammetry of enzymes e.g. lysyl oxidase [27], *p* -cresolmethylhydroxylase [28] cytochrome *c* peroxidase from yeast mitochondria [29], superoxide dismutase [chapter 7][30; 31] and succinate dehydrogenase [32]. The obtained voltammetric response of these enzymes is without exceptions difficult to interpret. The oxidase, peroxidase and dehydrogenase only give a detectable current in the presence of a substrate. Furthermore, the voltammograms of the dehydrogenase have an unusual shape. It was suggested that this was caused by diode like behaviour of this protein. However, kinetic and possibly spectroscopic studies will be necessary to confirm this [32]. The conditions necessary to obtain a voltammogram with superoxide dismutase are rather extreme and, therefore, it is not certain if the results have any physiological significance [chapter 7].

In our laboratory considerable effort was made to determine whether it was possible to study the enzyme lipoamide dehydrogenase from *Azotobacter vinelandii* with direct electrochemical techniques. The enzyme is part of the pyruvate dehydrogenase complex and is involved in the regeneration of the lipoyl group of the complex. In this reaction NAD^+ is reduced to NADH [33; 34] The enzyme is a homodimer of 100,000 Da and contains besides two redox active disulfide bridges also two FAD molecules in the active site [35; 36; 37]. The initial trials with this enzyme resulted in well-defined voltammograms as shown in fig. 7.
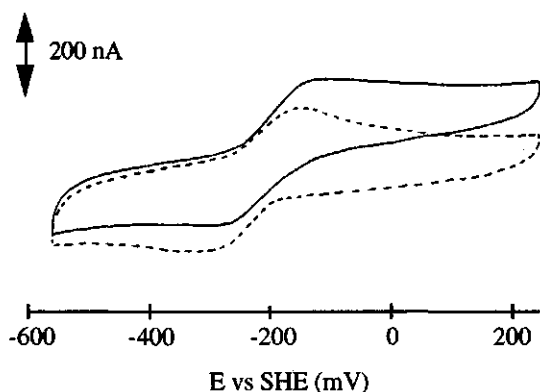

Figure 7: Cyclic voltammograms of Lipoamide dehydrogenase from *Azotobacter vinelandii* in the absence (---) and presence (——) of NADH. Voltammograms were recorded between -800 and 0 mV versus SCE. at a scan rate of 5 mV s^{-1}. Conditions: working/counter/reference electrodes, glassy carbon/ platinum/ saturated calomel. Temperature 23 °C.

From these voltammograms a midpoint potential of -240 mV was determined, comparable to the potential of free flavin. This potential value is suspect, since the cofactor is not covalently bound to the protein. Natural substrates like NADH, NAD$^+$, and reduced lipoamide were added during the electrochemical experiments to check if the enzyme was still catalytically active. NADH and reduced lipoamide indeed changed the shape of the voltammogram indicating that re-reduction by the substrate took place after oxidation of the enzyme at the electrode (fig. 6). However, it was not possible to reduce NAD$^+$ with the "electrochemically reduced" enzyme. An overview of the reactions tested is given in fig. 8.
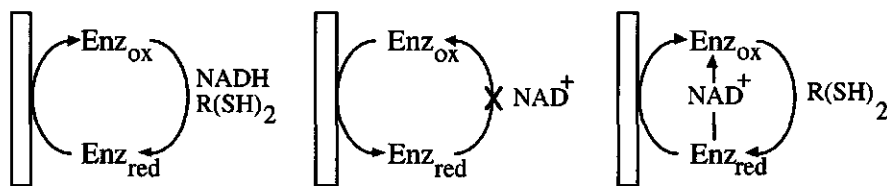
Figure 8: Scheme of catalytic reactions of lipoamide dehydrogenase reduced (red) or oxidized (ox) at a bare glassy carbon electrode in the presence of substrates. R(SH)$_2$ indicates reduced lipoamide.

The problems with establishing if the voltammetric response was significant or not were followed by problems with reproducibility. The electrochemistry of the enzyme was dependent on the preparation used and again numerous experiments were performed to find the reason for this inconsistency. The observation that FAD in the presence of catalytic amounts of lipoamide dehydrogenase and NADH gives rise to small catalytic currents suggests that the observed electrochemical behaviour was in fact a mediated response in which unbound flavin served as a shuttle between the electrode and enzyme molecules in solution. A schematic representation of this process is given in fig. 9.
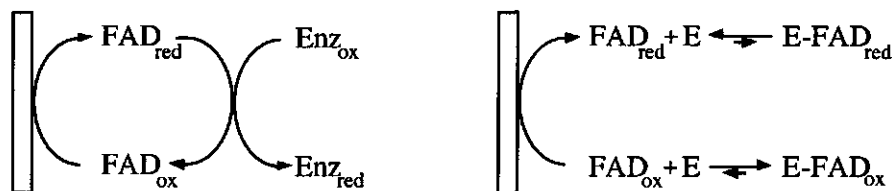
Figure 9: Possible mechanism of the electrochemistry of lipoamide dehydrogenase at a bare glassy carbon electrode. Unbound FAD can either function as a mediator between the electrode and the enzyme (left) or can dissociate and associate during reduction and oxidation (right).

The work on lipoamide dehydrogenase provided us with a rule of thumb for the prediction whether a voltammetric response of an enzyme can be expected to occur at a solid state electrode. The redox center in lipoamide dehydrogenase is not meant to transfer electrons to the surface. Instead it is meant to isolate the electrons from the environment until a suitable substrate binds, which can be reduced or oxidized. Our current working hypothesis is, therefore, that direct electrochemistry can best be applied to enzymes which are part of an electron transfer chain and involved in some electron transfer process. *In vivo* these enzymes are reduced by electron carrier proteins and for this purpose they possess "docking places" on their surface. The electron carrier binds at these places and electrons can be transferred to the redox center of the enzyme. With these enzymes one can expect that the electrode can serve as a substrate when proper circumstances are applied.

Redox titrations

Although electrochemistry has evolved to a valuable technique for the determination of redox properties of redox proteins there are some disadvantages. A voltammogram will only show the current as a function of the potential. In case of reversible stable voltammograms one can assume that the redox couple observed is caused by the redox protein in solution. However with multiple electron transfer proteins, in case adsorption of the protein takes place or when the electron transfer is quasi reversible the voltammograms can become difficult to interpret or might not reflect the solution potentials. Confirmation of the observed redox potentials in these cases is necessary to verify and help interpret the obtained results. An independent way to verify redox potentials of metalloenzymes is a redox titration monitored by e.g. Electron Paramagnetic Resonance spectroscopy. For a more detailed description of EPR spectroscopy and its applications in the characterization of metalloproteins the reader is referred to [38]. Different iron-sulfur clusters generally have very characteristic EPR spectra which change upon reduction or oxidation. Some representative spectra are shown in fig 10.

The spectral differences between the reduced and oxidized forms of a protein can be used to determine its redox potential. A titration is performed by adding small aliquots of reductant or oxidant to the solution containing the protein. After equilibration samples are drawn at different potentials and frozen in EPR tubes. A plot of the relative peak intensity of the EPR spectrum of the samples as a function of the solution potential results in a Nernst curve from which the midpoint potential and the number of transferred electrons can be determined. During the titration of the protein it is generally necessary to have mediators present in the solution. These small organic molecules can be easily reduced and oxidized and guarantee a rapid equilibrium between the reductant or oxidant and the protein [39; 40]. Furthermore, the presence of these redox dyes is necessary for the establishment of a good

equilibrium between the solution and the electrodes present to determine the solution potential.
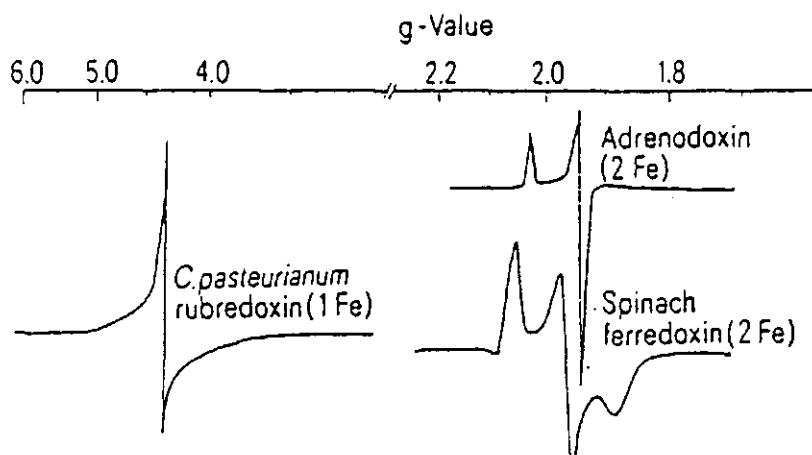

Figure 10: EPR spectra of rubredoxin (1 Fe) adrenodoxin (2Fe-2S) and Spinach ferredoxin (2Fe-2S).

For colored proteins with absorption maxima in the visible range of a UV/VIS spectrum it is possible to perform an optically monitored redox titration. This can be done by adding aliquots of reductant or oxidant to the protein solution while measuring the potential with two electrodes or setting the potential of the solution with a potentiostat [41; 42]. However, it is not possible to add a number of mediators since these tend to have bright colors. Their presence will make the interpretation of the successive spectra very difficult. This problem can be circumvented to a certain extent by the use of circular dichroism. The contribution of the protein is greatly enhanced with respect to the dye. For a more detailed description of circular dichroism and its use in redox titrations the reader is referred to [43]. Massey described the use of a closed system in which the reducing equivalents were supplied by xanthine and xanthine oxidase [44]. To determine the redox potential of the solution a redox dye was added with its midpoint potential close to the value expected for the protein under study. The major difficulty with this method is to find a suitable redox dye which has both the correct potential and an optical spectrum which does not interfere with the spectrum of the protein.

One of the general problems with redox titrations is that it is very difficult to determine whether the redox dye interferes with the protein or vice versa. Most of the commonly used dyes are known to bind to the protein and sometimes this can have

unpredictable effects on the protein's redox properties c.f. [45]. Another problem is one of equilibrium. However, this can be independently checked performing both an oxidative as well as a reductive titration and varying the ratio of dye over protein. The different Nernst curves obtained should, obviously, result in the same redox potential. The major disadvantage of EPR monitored redox titrations is the need for relatively large amounts of protein. Furthermore, it is necessary to record the spectra at low temperature using frozen solutions. The dynamics of the redox reaction are, therefore, difficult to study since this requires the use of elaborate rapid-freeze techniques. Despite its disadvantages it is reasonable to say that EPR and optical monitored redox titrations have contributed significantly to the insight in behavior of redox cofactors in proteins.

Conclusion

Direct electrochemistry allows the determination of dynamical properties without the interference of any other substances. However, the interpretation of the current voltage characteristic is not always straightforward. The addition of substrates can provide further evidence that the potential observed in the voltammogram indeed originates from the expected center of the enzyme. Furthermore, the validity of the electrochemical results can be checked by comparison with the EPR or optical titration. In the case of comparable results one can safely assume that the electrochemistry provides the correct answer.

Electrochemistry of proteins using solid electrodes has certainly deserved its place as a technique to study the redox behavior of, especially, small redox proteins. The possibility to work with a small sample size at physiological temperatures as well as the easiness of the determinations can be exploited in studies of genetically altered redox proteins. Examples are the use of the technique in investigations of the influence of the protein matrix on the regulation of the redox potential of redox cofactors in proteins [46]. and its use in the characterization of electron transfer pathways within and between proteins [chapter 3]. Unfortunately, an important drawback of direct electrochemistry is the fact that it is not yet generally applicable to all proteins due to the limitations mentioned earlier in this chapter. In order to overcome these limitations, the future development of this technique should be focused on the following two issues:

1) Extending the use of direct electrochemical methods to larger proteins and enzymes. The goal of this is to reach a stage in which it will be possible to determine the conditions favourable for protein electrochemistry from a number of physical parameters of the enzyme or protein under study. Properties like pI, hydrophobicity, surface charge and physiological function seem to be important although so far it has not been possible to use these parameters to predict the conditions necessary to obtain a voltammogram.

2) Combining electrochemical and spectroscopic methods in such a way that it is possible to monitor the sample with a spectroscopic method during or directly after the electrochemical experiment. The spectroelectrochemical setups designed up till now are all based on transparent indium tinoxide electrodes (ITO glass) or gold grid electrodes. The combination of the, for protein electrochemistry, favourable carbon electrodes with a spectroscopic technique has still to be made.

Outline of this thesis

The goal of the research described in this thesis was to establish the conditions necessary for the electrochemistry of proteins and enzymes. The research started with the enzyme lipoamide dehydrogenase, a 100 kDa flavoprotein. The gene coding for this enzyme was cloned and sequenced by Benen and coworkers and several mutants were available [47; 48; 49; 50; 33]. It is obvious that direct electrochemistry could serve as a very useful tool to study the redox properties of the different mutants and compare them to the wild-type enzyme. Unfortunately, the potentials obtained with the wild-type enzyme were different from the reported values from solution titrations. The effects of substrate additions on the voltammogram indicated that the enzyme "communicated" with the electrode. However, it was established that mediation by unbound FAD could cause this effect as described in the introduction. Since most flavoproteins contain non-covalently bound FAD it is reasonable to assume that during electrochemical experiments with flavoproteins a small amount of unbound FAD will be present. It is, therefore, important to know the behaviour of this cofactor at the glassy carbon electrode. This has been described in chapter 2.

The function of the periplasmic Fe-hydrogenase from *Desulfovibrio vulgaris* (Hildenborough) is still controversial. It has been postulated that the enzyme functions in the hydrogen uptake reaction donating its electrons to cytochrome c 3. The results of cyclic voltammetry experiments of cytochrome c 553 and cytochrome c 3 in the presence and absence of hydrogenase and hydrogen are described in chapter 3.

During purifications of several proteins from *Desulfovibrio vulgaris* (H) a purple protein was found as a side fraction of one of the proteins under study. This protein had been purified previously and it was described that it contained two Fe atoms with unusual coordination. A reinvestigation of the EPR properties, redox titrations and electrochemical characterization led to a new proposal for the coordination of one of the iron atoms as described in chapter 4.

The problems encountered with the electrochemistry of lipoamide dehydrogenase could not easily be overcome. The idea evolved that the use of an enzyme which was part of an electron transfer chain would possibly be easier to study with direct electrochemistry. Therefore the research focused on the bacterial enzyme cytochrome P-450. This enzyme is relatively small and has a [2Fe-2S] ferredoxin as the natural electron donor. Although well developed voltammograms were obtained as shown in chapter 5 the observed potential differed significantly from the potential obtained in EPR monitored redox titrations.

The work on superoxide dismutase, as described in chapter 6, was initiated after reports that reversible electron transfer was possible between this enzyme and bare electrodes. We were not able to reproduce these results and we showed that the reported potentials were different from the values obtained in EPR monitored redox titrations.

The difficulties with the electrochemistry of enzymes made us decide to focus on the electrochemical characterization of a number of small redox proteins. The results of a study on rubredoxin is described in chapter 7. The reports published on the electrochemistry of this protein indicated that the voltammetry was almost irreversible and the electron transfer between the protein and the electrode slow. In the presence of the lanthanide europium, however, reversible and fast electron transfer between the protein and the electrode was obtained. The pH dependence of the voltammetry indicates that the currently used models to describe the working mechanism of promotors can not be applied to europium.

The study of the soluble fragment of the bc_1 complex from beef heart, containing the Rieske cluster, is described in chapter 8. Upon extension of the potential scan range to - 1 V a second redox couple was discovered at -840 mV versus SHE. Although it is unclear if the second reduction is physiological significant, the phenomenon of "superreduction" contributes to our understanding of multiple electron transfer by iron sulfur clusters. The potential of this couple can not be reached with chemical reductants and this indicates the importance of a technique like direct electrochemistry.

The final part of this thesis consists of two chapters in which biochemical and spectroscopic studies of two proteins of *Desulfovibrio vulgaris* (H) are described. In chapter 9 the results obtained with the enzyme $AdoPSO_4$ reductase are presented. This enzyme was reported to contain two iron -sulfur clusters and one FAD as cofactors. Redox titrations, metal analysis and EPR studies indicated that only one iron sulfur cluster is present possibly with an iron nuclearity greater than four.

Chapter 10 contains the results obtained with high molecular weight cytochrome c . A reinvestigation of the redox properties of this protein which has an unknown function and contains 16 hemes resulted in midpoint potentials different from the values reported previously. Furthermore, spin quantitations and analysis of the EPR spectra were used to establish the nature of the ligands to the different heme iron atoms present in the protein.

[1]   Fraústo da Silva, J. J. R. & Williams, R. J. P. (1991) in *The Biological Chemistry of the Elements,* Oxford University Press, Oxford.

[2]   Cammack, R. C. (1992) in *Advances in Inorganic Chemistry, Vol 38: Iron-Sulfur Proteins,* (R. C. Cammack and A. G. Sykes, eds.) Academic Press, San Diego, Ca, 281-322.

[3]   Link, T. A., Hagen, W. R., Pierik, A. J., Assmann, C. & von Jagow, G. (1992), *Eur. J. Biochem.,* 208, 685-691.

[4]   Armstrong, F. A. (1990), *Structure and Bonding,* 72, 137-221.

[5]   Lemberg, R. & Barrett, J. (1973) in *Cytochromes,* Academic Press, London & New York.

[6]   Yamanaka, T. (1992) in *The biochemistry of the bacterial cytochromes,* Springer Verlag, Berlin.

[7]   van Berkel, W. J. H. (1989), Agricultural University, The Netherlands.

[8]   Ludwig, M. L. & Luschinsky, C. L. (1992) in *Chemistry and biochemistry of flavoenzymes, Vol III,* (F. Müller, ed.) CRC Press, Inc., Boca Raton, Fl., 427-466.

[9]   Mayhew, S. G. & Tollin, G. (1992) in *Chemistry and biochemistry of flavoenzymes, Vol III,* (F. Müller, ed.) CRC Press, Inc., Boca Raton, Fl, USA, 389-426.

[10]   Pierik, A. J., Hagen, W. R., Redeker, J. S., Wolbert, R. B. G., Boersma, M., Verhagen, M. F. J. M., Grande, H. J., Veeger, C., Mutsaers, P. H. A., Sands, R. H. & Dunham, W. R. (1992), *Eur. J. Biochem.,* 209, 63-72.

[11]   Nicholson, R. S. & Shain, I. (1964), *Anal. Chem.,* 36, 706-723.

[12]   Nicholson, R. S. (1965), *Anal. Chem.,* 37, 1351-1354.

[13]   Bard, A. J. & Faulkner, L. (1980) in *Electrochemical methods; fundamentals and applications.,* J. Wiley & Sons, New York.

[14]   Hagen, W. R. (1989), *Eur. J. Biochem.,* 182, 523-530.

[15]   Eddowes, M. J. & Hill, H. A. O. (1977), *J. Chem. Soc. Chem. Commun.,* 771-772.

[16]   Eddowes, M. J. & Hill, H. A. O. (1979), *J. Amer. Chem. Soc.,* 101, 4461-4464.

[17]   Albery, W. J., Eddowes, M. J., Hill, H. A. O. & Hillman, A. R. (1981), *J. Amer. Chem. Soc.,* 103, 3904-3910.

[18]   Armstrong, F. A., Cox, P. A., Hill, H. A. O., Lowe, V. J. & Oliver, B. N. (1987), *J. Electroanal. Chem.,* 217, 331-366.

[19]   Schreurs, J. & Barendrecht, E. (1984), *Recl. Trav. Chim. Pays-Bas,* 103, 205-219.

[20]   George, S. J., Armstrong, F. A., Hatchikian, E. C. & Thomson, A. J. (1989), *Biochem. J.,* 264, 275-.

[21]   Beinert, H. & Kennedy, M. C. (1989), *Eur. J. Biochem.,* 186, 5-15.

[22]   Kennedy, M. C. & Stout, C. D. (1992) in *Advances in Inorganic Chemistry, Vol. 38: Iron -Sulfur Proteins,* (R. Cammack and A. G. Sykes, eds.) Acad. press, San Diego, 323-339.

[23] Butt, J. N., Sucheta, A., Armstrong, F. A., Breton, J., Thomson, A. J. & Hatchikian, E. C. (1993), *J. Am. Chem. Soc.*, 115, 1413-1421.

[24] Haladjian, J., Pilard, R., Bianco, P. & Serre, P.-A. (1982), *Bioelectrochem. Bioenerg.*, 9, 91-101.

[25] Barker, P. D. & Mauk, A. G. (1992), *J. Am. Chem. Soc.*, 114, 3619-3624.

[26] Ferrer, J. C., Guillemette, J. G., Bogumil, R., Inglis, S., Smith, M. & Mauk, A. G. (1993), *J. Inorg. Biochem.*, 51, 95.

[27] Govindaraju, K., Unni Nair, B., Ramasami, T. & Ramaswamy, D. (1987), *J. Inorg. Biochem.*, 29, 111-118.

[28] Guo, L. H., Hill, H. A. O., Lawrance, G. A., Sanghera, G. S. & Hopper, D. J. (1989), *J. Electroanal. Chem.*, 266, 379-396.

[29] Armstrong, F. A. & Lannon, A. M. (1987), *J. Amer. Chem. Soc.*, 109, 7211.

[30] Borsari, M. & Azab, H. A. (1992), *Bioelectrochem. Bioenerg.*, 27, 229-233.

[31] Iyer, R. N. & Schmidt, W. E. (1992), *Bioelectrochem. Bioenerg.*, 27, 393-404.

[32] Sucheta, A., Ackrell, B. A. C., Cochran, B. & Armstrong, F. A. (1992), *Nature*, 356, 361-362.

[33] Benen, J. A. E. (1992), Studies on Lipoamide Dehydrogenase. Agricultural University, Wageningen The Netherlands.

[34] Williams, C. H. J. (1992) in *Chemistry and Biochemistry of Flavoenzymes, Vol III*, (F. Muller, ed.) CRC Press, Boca Raton, Fl, USA, 121-211.

[35] Massey, V. & Veeger, C. (1961), *Biochim Biophys Acta*, 48, 33-47.

[36] Mattevi, A., Obmolova, G., Sokatch, J. R., Betzel, C. & Hol, W. G. J. (1992), *Proteins Structure Function and Genetics*, 13, 336-351.

[37] Mattevi, A., Obmolova, G., Kalk, K. H., Van Berkel, W. J. H. & Hol, W. G. J. (1993), *J. Mol. Biol.*, 230, 1200-1215.

[38] Hagen, W. R. (1992) in *Advances in Inorganic Chemistry, Vol 38: Iron-Sulfur Proteins*, (R. Cammack and A. G. Sykes, eds.) Acad. Press, San Diego, 165-222.

[39] Dutton, P. L. (1978) in *Methods in Enzymology, Vol 54:*, (S. Fleischer and L. Packer, eds.) 411-435.

[40] Pierik, A. J. & Hagen, W. R. (1991), *Eur. J. Biochem.*, 195, 505-516.

[41] Stankovich, M. (1980), *Anal. Biochem.*, 109, 295-308.

[42] Jarbawi, T. B. & Stankovich, M. T. (1994), *Anal. Chim. Acta*, 292, 71-76.

[43] Ke, B., Bulen, W. A., Shaw, E. R. & Breeze, R. H. (1974), *Arch. Biochem. Biophys.*, 162, 301-309.

[44] Massey, V. (1990) in *Flavins and Flavoproteins: proceedings of the Tenth International Symposium on Flavins and Flavoproteins*, (B. Curti, S. Ronchi and G. Zanetti, eds.) Walter de Gruyter & Co., Berlin, 59-66.

[45] Surerus, K. K., Chen, M., Van der Zwaan, J. W., Rusnak, F. M., Kolk, M., Duin, E. C., Albracht, S. P. J. & Münck, E. (1994), *Biochemistry*, 33, 4980-4993.

[46]   Burrows, A. L., Guo, L.-H., Hill, H. A. O., McLendon, G. & Sherman, F. (1991), *Eur. J. Biochem.*, 202, 543-549.

[47]   Westphal, A. H. & De Kok, A. (1988), *Eur. J. Biochem.*, 172, 299-305.

[48]   Benen, J., van Berkel, W., Zak, Z., Visser, T., Veeger, C. & de Kok, A. (1991), *Eur. J. Biochem.*, 202, 863-872.

[49]   Benen, J., Van Berkel, W., Zak, Z., Visser, T., Veeger, C. & De Kok, A. (1991), *Eur. J. Biochem.*, 202, 863-872.

[50]   Benen, J., van Berkel, W., Dieteren, N., Arscott, D., Williams, C. H. J., Veeger, C. & de Kok, A. (1992), *Eur. J. Biochem.*, 207, 487-497.

Chapter 2

Electron transfer mechanisms of flavin adenine dinucleotide at the glassy carbon electrode; a model study for protein electrochemistry

Marc F.J.M. Verhagen and Wilfred R. Hagen

Electron transfer mechanisms of flavine adenine dinucleotide at the glassy carbon electrode; a model study for protein electrochemistry

Marc F.J.M. Verhagen and Wilfred R. Hagen *

Department of Biochemistry, Agricultural University, Dreijenlaan 3, NL-6703 HA Wageningen (The Netherlands)

(Received 2 January 1992; in revised form 2 March 1992)

Abstract

The electrochemical properties of flavine adenine dinucleotide (FAD) were studied using a glassy carbon electrode. The nature of the electrochemical reaction proved to be concentration dependent. A change from adsorbed to completely diffusion-controlled was observed when changing the FAD concentration from 1 μM to 1 mM at constant pH.

The concentration dependence revealed a possible mechanism of self-mediation. In this mechanism adsorption causes formation of a stable monolayer of FAD on the electrode. These adsorbed molecules can act as mediators through which electron transfer from FAD molecules in solution to the electrode can occur. The heterogeneous rate constant of the surface charge transfer of the adsorbed film was unusually high, $k_{sc}^{\circ} \approx 219$ s^{-1} and $k_{sa}^{\circ} \approx 191$ s^{-1}, for the cathodic and anodic reaction, respectively. The transfer coefficient for the same reaction gave a rather low value $\alpha_c \approx 0.31$ and $\alpha_a \approx 0.37$.

The mechanism of self-mediation has some implications for the electrochemistry of biomolecules. Fast and reversible electron transfer between these molecules and solid electrodes requires compatible (self-mediating) surfaces.

INTRODUCTION

Interest in the electrochemistry of biological molecules, e.g. enzymes and cofactors, has increased considerably over the past decade. An obvious reason is that for the elucidation of electron transfer pathways in the living cell it is important to know the midpoint potentials of different redox proteins. Another reason is that electrochemistry, in combination with sensitive and stereospecific enzymes, clears the way for the construction of a variety of biosensors.

---

* To whom correspondence should be addressed: Laboratorium voor Biochemie, Landbouwuniversiteit, Dreijenlaan 3, NL-6703 HA Wageningen, The Netherlands.

Quite a number of redox-enzymes carry the cofactor flavine adenine dinucleotide (FAD) in their active site (flavoproteins). A well known example is glucose oxidase, which is commonly used for the construction of glucose sensors [1]. Knowledge of the behaviour of the isolated cofactor near an electrode surface is necessary for the correct interpretation of the electrochemistry of flavoproteins, especially when it is realized that the cofactor FAD is not covalently bound to these enzymes. Solutions of flavoproteins always contain a small portion of unbound cofactor, which can disturb the electrochemical measurements.

When FAD is bound to a protein it can exist in three states. The flavoquinone form is fully oxidized, the flavosemiquinone form is one-electron reduced and the flavohydroquinone form is two-electron reduced. The free cofactor in neutral aqueous solutions mainly exists in two states; completely oxidized or two-electron reduced. This is caused by the very fast disproportionation reaction of the flavosemiquinone, which results in the formation of one oxidized and one completely reduced flavin out of two flavosemiquinones. However, the semiquinone concentration can be increased considerably by adding divalent metal ions [2].

FAD has been studied quite extensively with several electrochemical techniques and several electrode materials [3–5]. However, there is considerable discrepancy between the results of different authors. Miyawaki and Wingard observed a significant shift of the midpoint potential when FAD was adsorbed on, or covalently attached to, a glassy carbon surface [5,6]. Although the authors did not determine the actual rate constants, they concluded that the resulting electron transfer was rather slow. Similar slow rates were obtained by Ueyama et al. with a flavin monolayer adsorbed on a gold electrode [7]. The resulting voltammograms were very broad and only partial analysis was possible. Gorton and Johansson found a slow rate constant for FAD adsorbed on a graphite electrode [8]. In their experiments gold, platinum and glassy carbon electrodes gave very poor voltammograms, and strong adsorption did not occur. These authors also found an unusual behaviour of the midpoint potential as a function of the pH above pH 6.0. They could not detect the pK of the reduced species and concluded that FAD did not become deprotonated up to pH 8.0, due to its adsorption [8]. Several other reports exist about the pH dependence of the midpoint potential of FAD. Ke [9] and Lowe and Clark [10] found that their plots of midpoint potential vs. pH conformed to the theoretical equation with two pK values.

Ksenzhek and Petrova [11] (and refs. quoted therein) conclude from their experiments that, especially in neutral solutions, an appreciable amount of semiquinone is formed during the reduction of FAD. This resulted in an extra peak in the cyclic voltammogram. However these results have never been confirmed by any other group and are contradicted by the work of Müller [2]. He concluded from EPR studies that in aqueous neutral solutions only 2% semiquinone is formed.

From all these reports we can conclude that up till now the electrochemistry of FAD has been found to be slow and complicated. In contrast, in this paper we show that FAD gives sharp, well-defined voltammograms with a glassy carbon

electrode. The formation of a surface layer of FAD through adsorption appears to be essential for fast electron transfer. Formation of the semiquinone as a stable intermediate during reduction is not observed.

MATERIALS AND METHODS

Flavin adenine dinucleotide (FAD) grade III was obtained from Sigma as the disodium salt and was used as received. FAD solutions were made fresh and stored in the dark until they were used. The electrochemical experiments were performed in daylight. Water was purified with a Nanopure II system from Sybron/Barnstead, Boston. This system was set at an output resistivity of > 16.7 MΩ cm^{-1}. For the determination of the pH dependence, 100 mM solutions of different buffers were used: sodium acetate (pK 4.7), 2-(N-morpholino)ethane-sulphonic acid (MES, pK 6.1), N-(2-hydroxyethyl)piperazine-N'-(2-ethane-sulphonic acid) (HEPES, pK 7.5), 2-(N-cyclohexylamino)-ethanesulphonic acid (CHES, pK 9.3) and 3-(cyclohexylamino)-1-propanesulphonic acid (CAPS, pK 10.4). The buffers were obtained from Sigma.

Cyclic voltammetry was performed using a potentiostat (Wenking POS 73, Bank Elektronik, FRG) connected to a Philips PM 8043 x–y–t recorder (Philips, Eindhoven, NL). A Fluka 8022-A digital multimeter (Fluka, Tilburg, NL) was used to calibrate the potential axis. The voltammograms at high scan rates were recorded with a transient recorder (Datalab transient recorder DL 905) connected to a Philips PM 3200 oscilloscope (Philips, Eindhoven, NL) and subsequently plotted on the Philips PM 8043 x–y–t recorder. The time constant of the potentiostat up to a scan rate of 160 V s^{-1} was tested with a dummy cell and no deviation from linearity was observed. The electrochemical experiments were performed at a temperature of 23 ± 1°C with the three-electrode microcell described by Hagen [12]. The working electrode was a glassy carbon disc (Le Carbon Lorraine, Rotterdam, NL). Prior to each measurement a glassy carbon disc was polished with 6-μm diamond lapping compound (Engis Ltd, Kent, UK), washed thoroughly with water, immersed for a few minutes in 65% nitric acid at ambient temperature, washed with 0.1 M K$_2$HPO$_4$, washed again with water and dried; the P1312 platinum microelectrode (Radiometer, Copenhagen) served as the counter electrode. The potential was measured with reference to a Radiometer K-401 saturated calomel electrode. All reported potentials have been recalculated with reference to the SHE.

RESULTS

Concentration dependence

We have studied the concentration dependence of the electrochemical response of FAD in the range of 1 μM to 1 mM. The voltammograms and the corresponding scan rate dependences show a significant change in the nature of the electron transfer reaction (Fig. 1).

With a concentration of 1 μM (Fig. 1(A)) the peak current is proportional to the potential scan rate, and is described by [13]

$$I_{pa} = -I_{pc} = n^2 F^2 A \Gamma v / 4RT \tag{1}$$

Γ is the surface concentration of the redox active species (mol cm^{-2}), A is the electrode surface area (cm^2), n the number of electrons and v the potential scan rate (V s^{-1}). The subscripts a and c stand for the anodic and cathodic reaction. The other symbols have their usual meaning. The peak-to-peak separation is calculated from Fig. 1(A) to be less than 10 mV and independent of the scan rate. The observed reaction is therefore a reversible surface charge transfer. On the other hand, with a 1000-fold higher concentration of 1 mM (Fig. 1(D)) the peak current is proportional to the square root of the scan rate and is described by [14]

$$I_{pa} = -I_{pc} = 0.4463 nFAc (nF/RT)^{1/2} v^{1/2} D^{1/2} \tag{2}$$

Here c is the bulk concentration of the redox active species (mol cm^{-3}) and D is the diffusion coefficient (cm^2 s^{-1}) The peak-to-peak separation is 55 mV at $v = 0.01$ V s^{-1} and increases with increasing scan rate. The reaction has become a quasi-reversible, diffusion-controlled electron transfer. With intermediate concentrations a combination of the two reaction patterns is observed.

From the slope of Fig. 1(A) it can be calculated, using eqn. (1), that the surface concentration of adsorbed FAD is $\Gamma = 3.0 \times 10^{-11}$ mol cm^{-2}. It is known from previous measurements that one single molecule of FAD covers an area of 1 nm^2 when the isoalloxazine ring is adsorbed in a flat position [7,8,15]. A monolayer coverage of FAD would therefore correspond to $\Gamma_{mono} = 17 \times 10^{-11}$ mol cm^{-2}. Thus, in the experiment of Fig. 1(A), approximately 18% of the electrode surface is covered with FAD. The effective surface area of the electrode in our setup is 0.2 cm^2. The absolute amount of adsorbed FAD is therefore calculated to be 0.6×10^{-11} mol. This is only 24% of the total amount of FAD, which is 2.5×10^{-11} mol in the 25 μl cell. At a scan rate of 0.01 V s^{-1} this 24% gives a peak current of 247 nA (Fig. 1(A)). Using eqn. (2) and a diffusion coefficient $D = 3.8 \times 10^{-6}$ cm^2 s^{-1} for FAD (calculated from the rotational correlation time [16]), we can calculate that the remaining FAD in solution should give rise to a diffusion controlled peak current of $I_p^{diffusion} = 23$ nA. Since this is almost 1/10 of the measured peak current of the surface reaction, a detectable deviation from linearity in the current vs. scan rate plot is expected. From Fig. 1(A) it is obvious that this deviation is not observed. We hypothesize that the dissolved FAD can only transfer electrons to the electrode via the adsorbed molecules. As only 18% of the electrode surface is covered with adsorbed FAD this will result in a sixfold lower, and therefore negligible, diffusion-controlled current. A schematic representation of this model is shown in Fig. 2.

The consequence of the model is that it should be possible to calculate the peak current at any scan rate by taking the sum of eqn. (1) and eqn. (2), using equal surface areas (A). This is however only valid when *linear* diffusion takes place. We
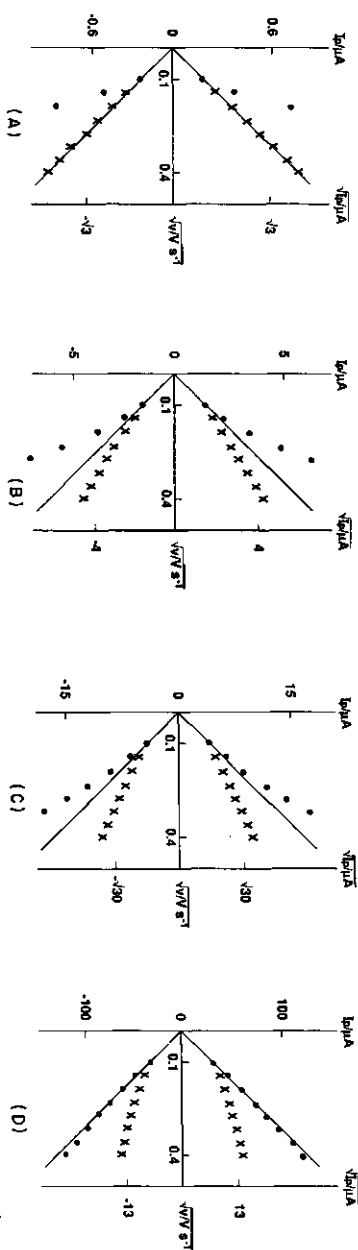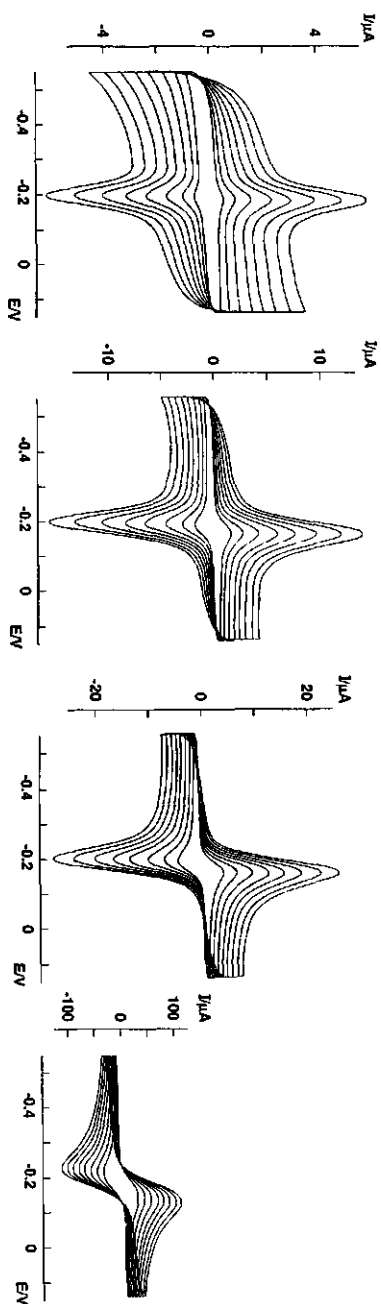
Fig. 1. Cyclic voltammograms and the associated peak current vs. scan-rate plots of FAD in 5 mM potassium phosphate buffer pH 6.6: (A) 1 μM; (B) 10 μM; (C) 100 μM (D) 1000 μM Conditions: working/counter/reference electrodes, glassy carbon/platinum/saturated calomel; temperature, 23°C. ● is the peak current; × is the square root of the peak current.
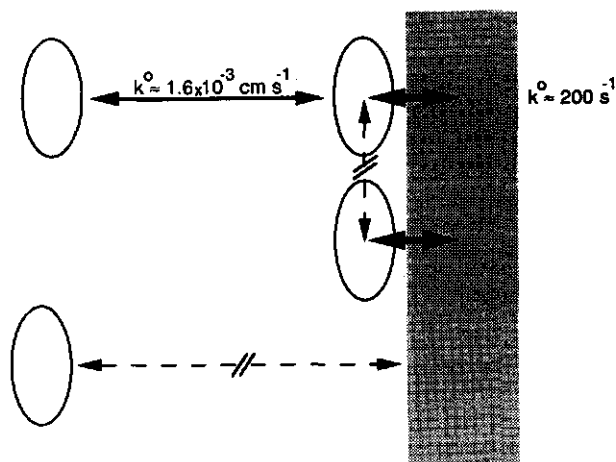
27

Fig. 2. Schematic representation of the model of 'self-mediation'. The solid arrows represent the allowed and the dashed arrows represent the non-allowed electron transfer pathways.

assume that this is a good approximation, especially when the electrode surface is almost completely covered.

The data taken at higher FAD concentrations are consistent with the model of 'self-mediation'. At a tenfold higher concentration (10 μM, Fig. 1(B)) the electrode surface is maximally covered with adsorbed FAD and available for mediated, diffusion-controlled electron transfer. Now the ratio of $I_p^{\text{diffusion}}$ over I_p^{surface} is calculated, using eqns. (1) and (2), to be 1/4 at a scan rate of 0.01 V s^{-1}. Indeed, a significant deviation from linearity is observed in the current versus scan rate plot (Fig. 1(B)).

Another tenfold increase of the concentration (100 μM, Fig. 1(C)) will not change the mediating surface further. Therefore, only the diffusion-controlled electron transfer will increase. With this concentration the ratio of $I_p^{\text{diffusion}}$ over I_p^{surface} is calculated to be 3. Figure 1(C) clearly shows that the diffusion-controlled contribution has indeed become dominant. With a concentration of 1 mM (Fig. 1(D)) the contribution of the surface redox reaction has become negligible; the peak current is diffusion controlled. From the slope of Fig. 1(D), using eqns. (1) and (2), we can recalculate the electrochemically active surface area $A = 0.17$ cm^2. This is almost identical to the previously mentioned geometrical surface area.

There is an analogy between the model of self-mediation and the model which is suggested by Armstrong et al. for electron transfer of proteins to solid electrodes [17]. In that model it is proposed that fast electron transfer occurs at isolated microscopic electroactive sites. These sites are presumably oxygen containing and generated by surface polishing. With FAD we assume that the active sites are generated by the adsorption of the cofactor. This results in a surface functionalized with FAD molecules. These adsorbed FAD molecules have the same redox
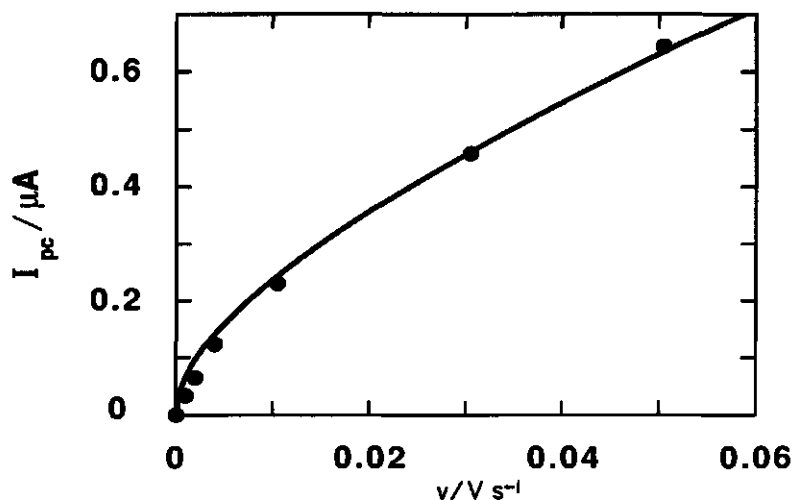
Fig. 3. Scan-rate dependence of the cathodic peak current from *M. elsdenii* ferredoxin (1 mg/ml) in 5 mM potassium phosphate, pH 7.0. The data were taken from reference 8. The solid line is the curve calculated using the model of self-mediation with a surface area of 0.016 cm^2. Conditions: working/counter/reference electrodes, glassy carbon/platinum/saturated calomel; temperature, 22°C.

potential as the FAD in solution and efficient electron transfer to the electrode can therefore occur through mediation. This has been reported earlier by Chao et al. for the electrochemistry of soluble horse heart cytochrome *c* at a ferrocenophane surface [18].

We now address the question as to whether the proposed mechanism of self-mediation can be extended to protein electrochemistry. Hagen reported a time lag of 6–8 h before the voltammograms of *Megasphaera elsdenii* rubredoxin and ferredoxin developed [12]. The development of these voltammograms consisted of a change from sigmoidal to peak-shaped. It is tempting to assume that the development of the voltammograms coincides with the formation of an adsorbed monolayer of protein. This monolayer then behaves as a mediating surface for the molecules in solution. The peak current vs. scan-rate plot of *M. elsdenii* 2 [4Fe4S]$^{(2+;1+)}$ ferredoxin shows an intermediate pattern between adsorbed and diffusion-controlled (Fig. 3). This dependence can be explained using the model of self-mediation. The data are described by taking the sum of a diffusion-controlled and an adsorbed contribution using a surface area of 0.016 cm^2. This is approximately 10% of the geometrical surface area.

Data of Armstrong et al. on ferredoxin cannot be explained with the above model [19]. They obtained well-defined cyclic voltammograms of *Desulfovibrio africanus* ferredoxin in the presence of neomycin (a promotor of protein electrochemistry) and only a small deviation from linearity in the plot of the current vs. the square root of the scan rate could be observed. Although this deviation was ascribed by the authors to a contribution of adsorbed protein, it is, in fact, too

small to be caused by a fully covered mediating surface. Data on the electrochemistry of *Megasphaera elsdenii* ferredoxin at our activated glassy carbon electrode in the presence of neomycin confirm the scan rate dependence observed by Armstrong et al. (not shown). We can therefore conclude that the difference between the data reported by Hagen [12] and the data reported by Armstrong et al. [19] is caused by the use of neomycin.

pH dependence

The pH dependence of FAD was measured using a concentration of 10 μM (Fig. 4). In the alkaline region of the pH titration an extra peak in the voltammogram was observed. The midpoint potential of this peak was -392 mV at pH = 8.90. This peak was pH dependent and increased slowly during successive scans. From earlier reports it is known that photolysis and hydrolysis of FAD can occur in alkaline solutions resulting in the formation of e.g. riboflavin and lumichrome [20,21]. It is very likely that the extra peak is caused by one of these products of the hydrolysis. In order to avoid interference of the extra peak, we determined the midpoint potential of FAD in this region of the pH titration from the first few scans.
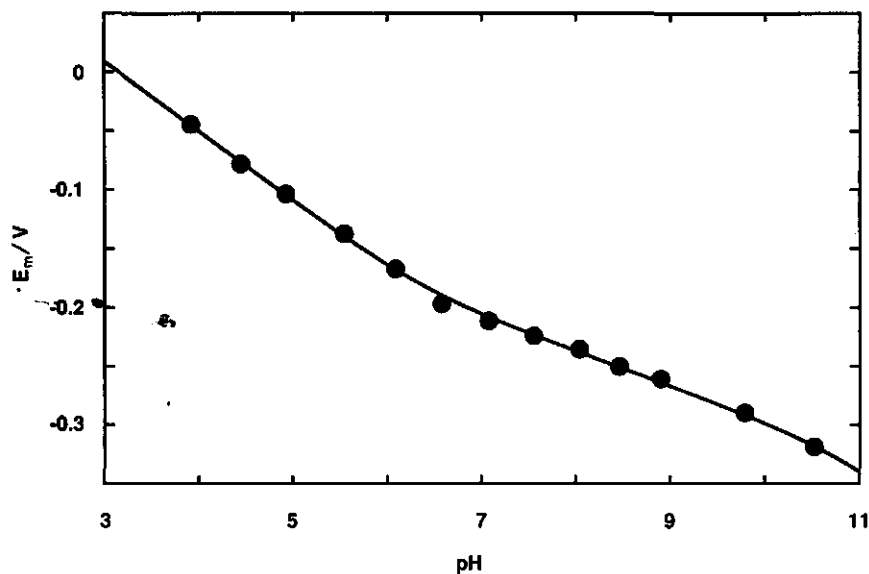

Fig. 4. pH dependence of the half-wave potential of 10 μM FAD in 100 mM buffer solutions at a glassy carbon electrode. The solid line is a least-squares fit to the data points using eqn. (3); temperature, 23°C.

30

The change of the midpoint potential as a function of the pH coincides with the results of Lowe and Clark [10]. For this system the behaviour of the pH dependence is theoretically described by:

$$E_m = E^{\text{low pH}} + (RT/nF) \ln\left\{\left([H^+]^3 + K_{\text{red}}[H^+]^2\right)/\left([H^+] + K_{\text{ox}}\right)\right\} \qquad (3)$$

K_{red} and K_{ox} are the dissociation constants for, respectively, the reduced and the oxidised species. $E^{\text{low pH}}$ is the midpoint potential at a pH of approximately 0. Equation (3) applies only when two pK values of FAD are considered. From literature data it is known that FAD has two extra pK values of ± 0 and < 0 [2]. These are however far beyond the lower limit of the applied pH interval and therefore no influence from these pK values is expected. The solid line in Fig. 4 is a least-squares fit to eqn. (3), giving p$K_{\text{red}} = 6.3$ and p$K_{\text{ox}} = 10.7$. $\Delta E/\Delta$pH was calculated to be 59 mV/pH below pH 6.3 and 32 mV/pH between pH 6.3 and 10.7. The slope of the curve above pH 10.7 could not be measured accurately. The pK values mentioned are in good agreement with the previously published pK values for the flavohydroquinone and the flavoquinone [9,10,21].

Our data contradict the results reported by Ksenzhek and Petrova [11]. They observed two peaks in their cyclic voltammograms and concluded from this that the semiquinone concentration in neutral and weak basic solutions can rise to a maximal 61%. We have not been able to reproduce these results and our cyclic voltammograms, as well as our differential pulse voltammograms (data not shown) only show one single peak ($n = 2$). Therefore, we have to conclude that FAD behaves as a two-electron transferring molecule in these electrochemical studies.

Determination of the rate constants

The rate of the surface electron transfer can be calculated from the shift in the peak potential (E) with increasing scan rate (v) using the equation [13]:

$$E_{\text{pc}} = E_c + (RT/n\alpha_c F) \times \ln\left\{RTk^{\circ}_{\text{sc}}/(n\alpha_c Fv)\right\} \qquad (4)$$

where α is the transfer coefficient and k°_{sc} is the heterogeneous rate constant for the surface electron transfer (s^{-1}). The other symbols have their usual meaning. The equation for the anodic peak potential is similar to eqn. (4) except that the shift in the peak potential will be negative. As a consequence of this relationship we expect that an increase of the scan rate will cause a shift in the anodic and cathodic peak potential. In the irreversible domain this will result in a linear dependence of peak potential vs. ln(v). This dependence can be used to extract the transfer coefficient and the heterogeneous rate constant for the electron transfer between FAD and the glassy carbon electrode.

The electron transfer reaction between FAD and the glassy carbon electrode proved to be very fast. Figure 5 shows the cyclic voltammograms of 1 μM FAD, pH 6.5, at three different scan rates. The relation between peak potential and ln(v) is plotted in Fig. 6. From the slope in the irreversible domain, and using
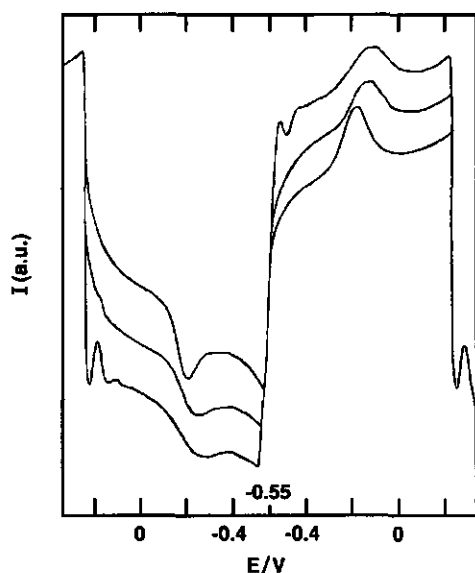
Fig. 5. Fast scan rate voltammograms replotted from transient recorder data of 1 μM FAD in 5 mM potassium phosphate pH 6.5 adsorbed on a glassy carbon electrode. Scan rate from top to bottom: 80 V s^{-1}, 40 V s^{-1}, 4 V s^{-1}. Conditions: working/counter/reference electrodes, glassy carbon/platinum/saturated calomel; temperature, 23°C.

$n = 2$, it is calculated that $\alpha_c = 0.31$ and $\alpha_a = 0.37$. Although these values deviate significantly from the theoretical value of 0.5 for a symmetrical energy barrier, they are comparable to the values reported by Lane and Hubbard for some other multi-electron transferring systems [22].

The calculated values for the heterogeneous rate constant $k_{sc}^{\circ} = 219$ s^{-1} and $k_{sa}^{\circ} = 191$ s^{-1} are very high. The surface electron transfer of FAD adsorbed at the glassy carbon electrode is considerably faster than that reported for FAD covalently attached to a glassy carbon electrode [6] or ferrocene covalently attached to a platinum surface [13]. The midpoint potential of the adsorbed species is identical to the value for the species in solution. Brown and Anson predicted a shift in peak potential when interaction between molecules occurs [23]. Since this is not observed we conclude that there is no significant intermolecular interaction between the adsorbed molecules.

The rate of the diffusion-controlled electron transfer can be calculated from the peak-to-peak separation as a function of the scan rate [24]. Using the data from the experiments with 1 mM FAD (Fig. 1(D)) it can be calculated that the heterogeneous rate constant is $k^{\circ} \approx 1.6 \times 10^{-3}$ cm s^{-1}. This value is within the range which is commonly defined as quasi-reversible [25] and comparable to the rate constant reported for small redox proteins like cytochrome c [12]. Considering the fast comproportionation reaction of FAD with a rate constant at neutral pH of
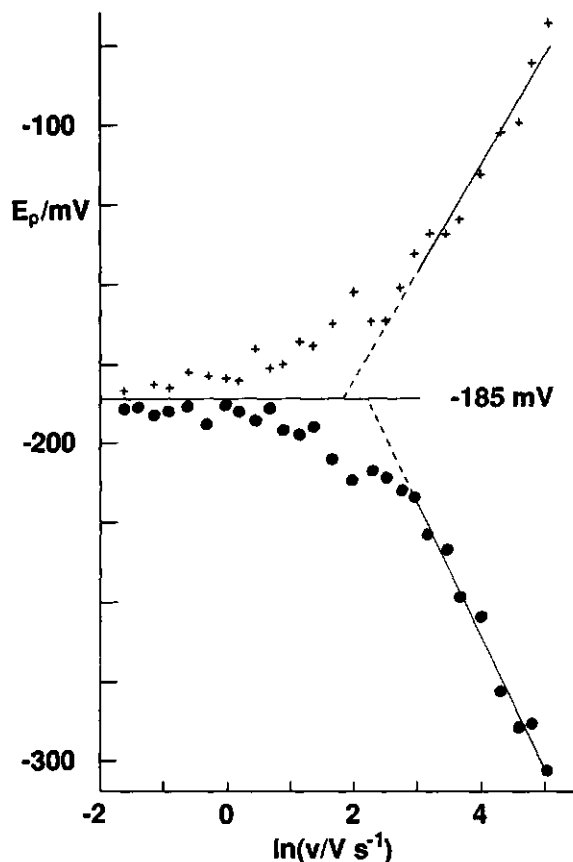
Fig. 6. Plot of the peak potential vs. ln(v) for the cyclic voltammogram of 1 μM FAD in 5 mM potassium phosphate pH 6.5 adsorbed on a glassy carbon electrode. ($\bullet$) Cathodic peak potential; ($+$) anodic peak potential; temperature, 23°C.

approximately 1×10^9 M^{-1} s^{-1} [2] we conclude that the electron transfer between adsorbed FAD and FAD in solution has been slowed down due to the adsorption.

CONCLUSIONS

The electrochemistry of FAD at the glassy carbon electrode results in sharp, well defined voltammograms. The reduction and oxidation can be regarded as two-electron transfer reactions. The rate of electron transfer between FAD and the electrode is very high in cases where the FAD is adsorbed. The adsorbed layer of FAD is necessary for efficient electron transfer from dissolved FAD to the electrode. This model of self-mediation explains some of the scan-rate dependences observed with protein electrochemistry. The pH dependence of the mid-

point potential is not affected by adsorption and is identical to the dependence obtained by chemical titrations.

REFERENCES

1 A.E.G. Cass, G. Davis, G.D. Francis, H.A.O. Hill, W.J. Aston, I.J. Higgins, E.V. Plotkin, L.D.L. Scott and A.P.F. Turner, Anal. Chem., 56 (1984) 667.
2 F. Müller, Free Radical Biology and Medicine, 3 (1987) 215.
3 M.M. Kamal, H. Elzanowska, M. Gaur, D. Kim and V.I. Birss, J. Electroanal. Chem., 318 (1991) 349.
4 H. Shinohara, M. Grätzel, N. Vlachopoulos and M. Aizawa, Bioelectrochem. Bioenerg., 26 (1991) 307.
5 O. Miyawaki and L.B. Wingard, Jr., Biotechnol. Bioeng., 26 (1984) 1364.
6 O. Miyawaki and L.B. Wingard, Jr., Biochim. Biophys. Acta, 838 (1985) 60.
7 S. Ueyama, S. Isoda and M. Maeda, J. Electroanal. Chem., 264 (1989) 149.
8 L. Gorton and G. Johansson, J. Electroanal. Chem., 113 (1980) 151.
9 B. Ke, Arch. Biochem. Biophys., 68 (1957) 330.
10 H.J. Lowe and W.M. Clark, J. Biol. Chem., 221 (1956) 983.
11 O.S. Ksenzhek and S.A. Petrova, J. Electroanal. Chem., 11 (1983) 105.
12 W.R. Hagen, Eur. J. Biochem., 182 (1989) 523.
13 M. Sharp, M. Petersson and K. Edström, J. Electroanal. Chem., 95 (1979) 123.
14 R.S. Nicholson and I. Shain, Anal. Chem., 36 (1964) 706.
15 L. Müller and W. Friedrich, Z. Chem., 17 (1977) 70.
16 A.J.W.G. Visser and A. van Hoek, Proc. SPIE-Int. Soc. Opt. Eng., 909 (1988) 61.
17 F.A. Armstrong, A.M. Bond, H.A.O. Hill, B.N. Oliver and I.S.M. Psalti, J. Am. Chem. Soc., 111 (1989) 9185.
18 S. Chao, J.L. Robbins and M.S. Wrighton, J. Am. Chem. Soc., 105 (1983) 181.
19 F.A. Armstrong, S.J. George, R. Cammack, E.C. Hatchikian, and A.J. Thomson, Biochem. J., 264 (1989) 265.
20 H. Beinert, in P.D. Boyer, H. Lardy and K. Myrbäck (Eds.), The Enzymes, Academic Press, New York, 1960, Vol. 2, p. 365.
21 E. Knobloch, in D.B. McCormick and L.D. Wright (Eds.), Methods in Enzymology, Academic Press, New York, 1971, Vol. 18, Part B, p. 305.
22 R.F. Lane and A.T. Hubbard, J. Phys. Chem., 77 (1973) 1401.
23 A.P. Brown and F.C. Anson, Anal. Chem., 49 (1977) 1589.
24 R.S. Nicholson, Anal. Chem., 37 (1965) 1351.
25 A.J. Bard and L.R. Faulkner, Electrochemical Methods, Fundamentals and Applications, Wiley, New York, 1980.

Chapter 3

Cytochrome *c* 553 from *Desulfovibrio vulgaris* (Hildenborough); Electrochemical properties and electron transfer with hydrogenase

Marc F.J.M. Verhagen, Ronnie B.G. Wolbert and Wilfred R. Hagen

Cytochrome c_{553} from *Desulfovibrio vulgaris* (Hildenborough)
Electrochemical properties and electron transfer with hydrogenase

Marc F. J. M. VERHAGEN, Ronnie B. G. WOLBERT and Wilfred R. HAGEN

Department of Biochemistry, Wageningen Agricultural University, The Netherlands

An electrochemical study of the periplasmic cytochrome c_{553} of *Desulfovibrio vulgaris* (Hildenborough) is presented. The dependence of the midpoint potential on temperature and pH was studied with cyclic voltammetry. The voltammograms obtained were reversible and revealed that this cytochrome showed fast electron transfer on a bare glassy carbon electrode. The midpoint potential at pH 7.0 and 25°C was found to be 62 mV versus the normal hydrogen electrode. It was observed that the temperature dependence was discontinuous with a transition temperature at 32°C. The standard reaction entropy at the growth temperature of the organism (37°C) was calculated to be $\Delta S^{\circ\prime} = -234$ J mol^{-1} K^{-1}. The pH dependence of the midpoint potential could be described with one pK of the oxidized form with a value of 10.6. The second-order rate constant for electron transfer between cytochrome c_{553} and the Fe-hydrogenase from *D. vulgaris* (H) was also determined with cyclic voltammetry. The equivalent rate constant for cytochrome c_3 and hydrogenase was measured for comparison. The second-order rate constants are 2×10^7 M^{-1} s^{-1} for cytochrome c_{553} and 2×10^8 M^{-1} s^{-1} for cytochrome c_3. The kinetic parameters of the hydrogenase for both cytochromes were determined using the spectrophotometric hydrogen consumption assay. With cytochrome c_{553} this resulted in a K_m of 46 µM and a maximum turnover number of 7.1×10^2 s^{-1} in the H$_2$ consumption assay. The values with cytochrome c_3 were 17 µM and 6.4×10^2 s^{-1}, respectively. The importance of the different kinetic parameters for contrasting models proposed to describe the function of the Fe-hydrogenase are discussed.

Cytochrome c_{553} is a c-type cytochrome which has been demonstrated in several sulfate reducers [1]. The protein has been purified from *Desulfovibrio vulgaris* strains Hildenborough and Miyazaki and from *Desulfovibrio desulfuricans* strain Norway [2, 3]. The cytochrome contains one covalently bound heme with histidine and methionine as axial ligands to the iron. In *D. vulgaris* (H) the ratio of cytochrome c_{553} over tetraheme cytochrome c_3 has been reported to be 1:1.5 [4]. The structural gene of *D. vulgaris* (H) cytochrome c_{553} has been cloned and sequenced [5]. The postulated localization in the periplasmic space was confirmed by the sequence data since a leader sequence, essential for transport through the cytoplasmic membrane, could be demonstrated. The physiological role for this protein is still unknown although it has been claimed that *D. vulgaris* Miyazaki cytochrome c_{553} can react *in vitro* with cytoplasmic lactate dehydrogenase [6]. Since the cytochrome and the lactate dehydrogenase are located on different sides of the cytoplasmic mem-

brane, it is not very likely that this reaction is physiological. Yagi proposed that the cytochrome from the Miyazaki strain functions as an electron acceptor for formate dehydrogenase. This conclusion was based on experiments with partially purified formate dehydrogenase preparations which were capable of reducing the cytochrome. In experiments with the periplasmic Fe-hydrogenase from the same strain he found that it was impossible to reduce the cytochrome using the hydrogenase and hydrogen [2].

The redox properties of cytochrome c_{553} have been studied using different kinds of techniques. Redox titrations monitored by EPR or optical spectroscopy and some voltammetric experiments using a gold electrode and 4,4'- bipyridine have been described [7–9]. A midpoint potential of 20 ± 10 mV versus the normal hydrogen electrode (NHE) was obtained from differential pulse voltammetry. Values of 20 ± 5 mV and 80 ± 5 mV were obtained from the EPR and optical experiments, respectively. The pH was shown to have an effect on the methionine binding to the heme iron since the characteristic absorption at 690 nm reversibly disappeared on titration of the protein. A pK of 10.9 for this titration was obtained for the *D. vulgaris* cytochrome. The effect of the pH on the midpoint potential was only described qualitatively to decrease above pH 10 [7].

Several reports have been made in the literature about the kinetics of electron transfer between electron carriers and hydrogenase. Hoogvliet et al. studied the kinetics of the reaction between three different viologens and *D. vulgaris* (H) hydrogenase [10]. In their experiments they used hydrogen-

ase as a proton-reducing enzyme and therefore the viologens functioned as electron donors. Moreno et al. repeated these experiments with *D. gigas* hydrogenase using several small electron carrier proteins, including cytochrome c_3 and ferredoxin, instead of methylviologen [11]. The reversed electron transfer was also studied using hydrogenase and tetraheme cytochrome c_3 from several *Desulfovibrio* strains in different combinations [12–14]. In these studies the hydrogenase functioned as a hydrogen-oxidizing enzyme and the cytochromes were used as electron acceptors. In all cases, except for the ferredoxin, a reasonably high rate constant was obtained between the electron carrier and the hydrogenase. The high rate constant in the experiments with cytochrome c_3 was used as supporting evidence for the previously proposed function of this cytochrome as a physiological redox partner of hydrogenase [15, 16].

There are several unanswered questions with respect to the electron transfer from or to hydrogenase. The function of the periplasmic hydrogenase has not been established yet. Since this enzyme can both reduce protons or oxidize hydrogen it is not known whether we have to look for an electron donor or acceptor. Furthermore, in only one of the aforementioned papers are data presented on the K_m and V_{max} of hydrogenase for cytochrome c_3, both from *D. gigas* [12]. In the other papers the magnitude of the rate constants is implicitly taken as evidence for physiological relevance. The present paper describes the results of an electrochemical investigation of the electron transfer between *D. vulgaris* (H) hydrogenase and cytochrome c_3 as well as cytochrome c_{553}. The enzyme and both cytochromes are found in the periplasmic space of the bacterial cell. Dependent on the physiological function of the hydrogenase there is a possibility that cytochrome c_{553} and hydrogenase will react with each other. This is, of course, only feasible when the reaction is thermodynamically and kinetically favourable.

MATERIALS AND METHODS

Cytochrome c_{553} from *Desulfovibrio vulgaris*, strain Hildenborough NCIB 8303, was purified using a modified version of the procedures described previously [2, 3]. The purification steps were all performed at $0-4°C$. The periplasmic proteins of 160 g wet cells were extracted according to the procedure described by van der Westen et al. [17]. The resulting extract was dialyzed against 10 mM Tris/HCl pH 8.0 and loaded onto a column (5×20 cm) of DEAE-Sephadex (Pharmacia) equilibrated with 10 mM Tris/HCl pH 8.0. The bright red fraction which did not bind to this anion exchanger was loaded onto an aluminum oxide column (3×6 cm; Merck), activated according to Horio and Kamen [18] and equilibrated with 10 mM Tris/HCl pH 8.0. The cytochrome fraction was eluted with 1 M potassium phosphate pH 7.0 and concentrated in an Amicon stirred cell equipped with a YM 5 membrane. The concentrated fraction was applied to a Sephadex G-75 gel-filtration column (2.6×60 cm; Pharmacia) equilibrated with 10 mM potassium phosphate and 150 mM NaCl. Three peaks eluted from this gel-filtration column: high-molecular-mass cytochrome, tetraheme cytochrome c_3 and cytochrome c_{553}. The fraction containing cytochrome c_{553} was pooled and concentrated. A rerun on the Sephadex G-75 gel-filtration was performed to obtain the final preparation with a purity index $[A_{553}(red)-A_{570}(red)/A_{280}(ox)] = 1.0$. The fraction containing cytochrome c_3 was pooled and concentrated in an Amicon cell with a YM 10

membrane. This fraction was also subjected to a rerun on the Sephadex G-75 gel-filtration column. The purity index of the final preparation was 2.6. Hydrogenase from *D. vulgaris* (H) was purified according to Van der Westen et al. [17]. The specific activity of the final preparation was 2300 U/mg protein in the manometric hydrogen production assay according to [19].

The water used in the experiments was purified with a NANOpure II system from Sybron/Barnstead, Boston. The output resistivity of this system was set at >16.7 Mohm/cm. Cyclic voltammograms were measured with either a Wenking POS 73 potentiostat (Bank Elektronik, Germany) or a BAS CV27 potentiostat (Bioanalytical systems, Indiana, USA) connected to a Philips PM 8043 x-y-t recorder (Philips). The potential axis was calibrated with a Fluka 8022-A digital multimeter. The electrochemical experiments were performed with a three-electrode microcell using the method described by Hagen [20]. The working electrode was a nitricacid-activated glassy carbon disc (Le Carbon Loraine, Rotterdam); the P1312 micro platinum (Pt) electrode (Radiometer, Copenhagen) served as the counter electrode. The potential was measured with reference to a K-401 saturated calomel electrode (SCE) (Radiometer). All reported potentials have been recalculated with respect to the NHE. During the kinetic experiments the temperature was kept constant at $25°C$ by immersing the electrochemical cell in a thermostatted water bath. The same setup was used for measurement of the temperature dependence of the midpoint potential. The pH dependence was measured in 20 mM Good's buffers (Mes, Hepes, Ches, Caps) using 20 μl cytochrome c_{553} with a final concentration of 0.5 mg/ml. Oxygen was removed from argon and hydrogen by passing both gases over a BasF catalyst prior to passage through a reduced methyl viologen solution.

The kinetic experiments with hydrogenase and hydrogen were performed using the following procedure. First the voltammograms of cytochrome c_{553} in 100 mM Hepes pH 7.0 were recorded at different scan rates. These measurements were performed after purging the cell with argon. Subsequently hydrogenase was added and, after two scans, the argon flow was replaced by a hydrogen flow. It took approximately 20 min before a stable voltammogram was obtained and the scan rate dependence could be recorded. After this measurement the hydrogen flow was replaced by an argon flow in order to check whether anything had changed during the experiment. No significant changes from the initial voltammogram were observed. Finally the hydrogenase concentration was checked by activity measurements. Either a small amount of dithionite was added to the solution in the electrochemical cell and subsequently a sample was withdrawn or the activity of the hydrogenase solution before addition to the electrochemical cell was checked. The activity was measured as hydrogen production activity in the manometric assay according to Chen and Mortenson [19]. The possible influence of hydrogen on the electrochemistry of cytochrome c_{553} was carefully checked in a separate experiment. Hydrogen did not cause any significant change of the voltammogram.

For the determination of the K_m value and the maximum turnover number, anaerobic cuvettes sealed with a screwcap and a septum were used. The hydrogenase stock solution with a concentration of 0.9 μM was preincubated with hydrogen in the presence of 0.5 mM sodium dithionite for 10 min. The cuvettes were filled with 500 μl of a cytochrome solution buffered in 100 mM Hepes pH 7.0. Subsequently the

cuvettes were made anaerobic by three alternating cycles of vacuum and hydrogen. The cuvettes remained under an overpressure of 20 kPa hydrogen after the final cycle. The absorbance at 553 nm was measured using a Zeiss M4 QIII spectrophotometer connected to a Kipp & Zonen BD 40 recorder; 0.5 μl 0.5 mM sodium dithionite was added to remove traces of oxygen. This also accounted for the initial change in absorbance due to the addition of the hydrogenase solution. After this addition the absorbance was again measured and 0.5 μl of the activated hydrogenase solution was added. The slope of the tangent drawn at the start of the recorded trace was used to calculate the hydrogen oxidation rate using an absorption coefficient of 110 mM^{-1} cm^{-1} for cytochrome c_3 [21] and 23.4 mM^{-1} cm^{-1} for cytochrome c_{553} [7].

RESULTS

pH and ionic strength dependence
of the midpoint potential of cytochrome c_{553}

The cyclic voltammetry of 1 mg/ml cytochrome c_{553} in 20 mM Hepes pH 7.0 at 23°C results in well defined voltammograms as shown in Fig. 1A. The voltammetric response is immediate and stable for a prolonged period. The peak separation (ΔE) at a potential scan rate (v) of 10 mV · s^{-1} is 55 ± 2 mV. The peak current is proportional to the square root of the potential scan rate (Fig. 1B). This is in contrast with previous work in which the voltammetry of cytochrome c_{553} generally showed slow electron-transfer kinetics with either a glassy carbon electrode [20] or a gold electrode with 4,4'-bypyridine [8]. The reported voltammograms were broad with a peak separation of at least 75 mV at low scan rates.

The midpoint potential of cytochrome c_{553} is pH-independent in the pH range 6.0–pH 10.0. Above pH 10.0 the midpoint potential decreases as shown in Fig. 2. This behaviour can be described with the equation:

$$E_m = E_{m\,(low\,pH)} + RT/nF \cdot \ln \{[H^+]/(K_{ox} + [H^+])\} .$$

A least-squares fit of this equation to the data points results in $E_{m\,(low\,pH)} = 64 \pm 5$ mV and $pK_{ox} = 10.6$. This pK is in good agreement with the results of Bianco et al. who found that the methionine ligand of the heme could be reversibly titrated with a pK of 10.9 [7]. There is virtually no effect of the pH on the height of the peak current or the shape of the voltammogram in the pH range 6.0–11.0. At pH 12.0 a response is no longer detectable. This is probably due to the fact that this pH is considerably higher than the isoelectric point. Under these circumstances it is expected that both the cytochrome and the electrode have a negative surface charge. The resulting repulsion causes a deterioration of the voltammetric response. The midpoint potential at pH 7.0 and 25°C is calculated to be 62 ± 5 mV. This is somewhat higher than the previously reported midpoint potential of 20 mV obtained by EPR titration and voltammetry experiments using a gold electrode and 4,4'-bypyridine [7, 8] but equal to the preliminary value obtained previously using cyclic voltammetry with a glassy carbon electrode [20].

Changing the ionic strength caused a decrease in midpoint potential. At an ionic strength above 1 M some extra peaks, although small, appeared in the voltammogram. The nature of these peaks is not known. The shape of the voltammogram of cytochrome c_{553} did not change significantly and the data were therefore used to calculate the midpoint potential. A linear relationship between the midpoint potential and
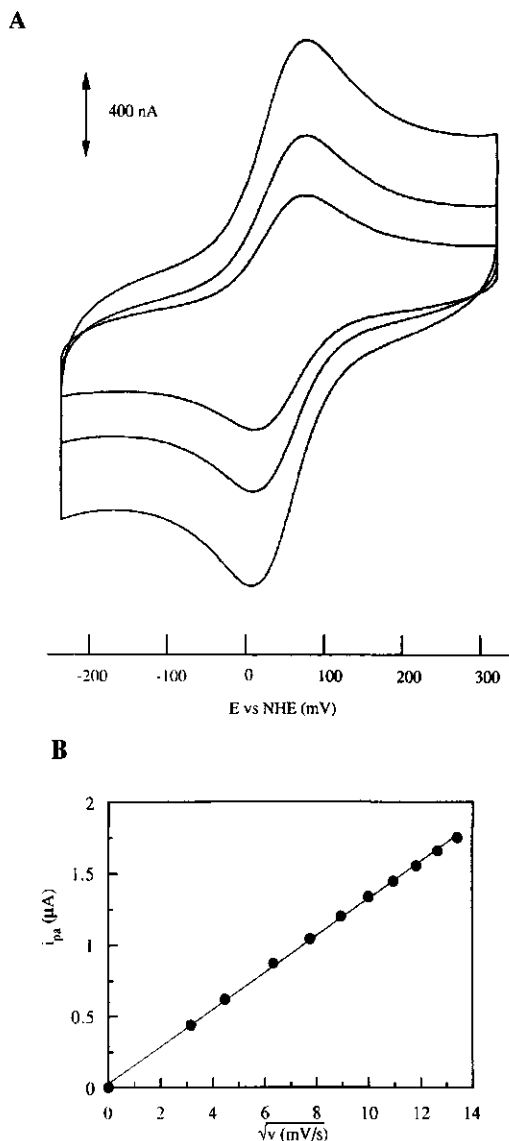
A

B

Fig. 1. (A) Cyclic voltammogram of 1 mg/ml cytochrome c_{553} in 20 mM Hepes pH 7.0. (B) Scan rate dependence of the anodic peak current. (A) Scan rates were 10, 20, and 40 mV/s. The potential axis is defined versus the normal hydrogen electrode. Temperature, 23°C; working/reference/counter electrodes, glassy carbon/SCE/Pt.

the square root of the ionic strength was obtained as shown in Fig. 3. The slope of the line was −46 mV M$^{-1/2}$.

The heterogeneous rate constant for the electron transfer was estimated from the peak separation at potential scan rates above 150 mV/s according to Nicholson [22]. The standard rate constant k_s was found to be 3×10^{-2} cm s^{-1}. The high
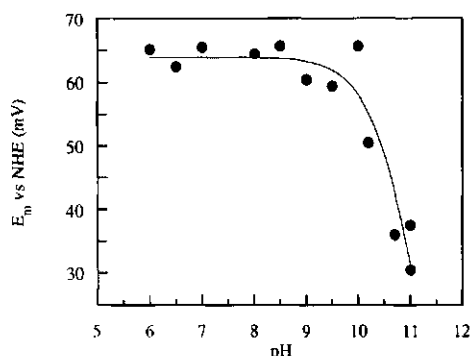
Fig. 2. pH dependence of the midpoint potential of cytochrome c_{553}. Cyclic voltammograms of 0.5 mg/ml cytochrome c_{553} in 20 mM Good's buffers of the desired pH were recorded at 23°C. Voltammograms were taken from +50 to −450 mV versus the SCE using a scan rate of 10 mV/s. The solid line is a least-squares fit using a pK_{ox} of 10.6.

Fig. 4. Temperature dependence of the midpoint potential of cytochrome c_{553}. The voltammograms of a 0.5-mg/ml solution of cytochrome c_{553} in 20 mM Hepes pH 7.0 were recorded from −500 to +100 mV versus SCE in an isothermal cell. The solid line is a least-squares fit to the data points with a temperature coefficient of −1.1 mV/K between 0−30°C and −3.1 mV/K above 32°C.
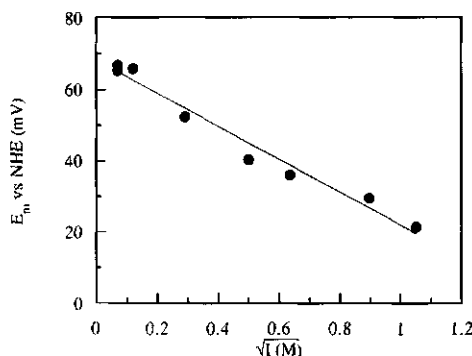

Fig. 3. Dependence of the midpoint potential of cytochrome c_{553} on the square root of the total ionic strength. The voltammograms were measured in 20 mM Hepes pH 7.0 and NaCl was added to increase the ionic strength. Voltammograms were taken at 23°C between +50 and −450 mV versus SCE with a scan rate of 10 mV/s. Glassy carbon/SCE/Pt served as the working/reference/counter electrodes. The solid line is a fit with a slope of −46 mV M$^{-1/2}$.

value for this rate constant indicates that the electron transfer is reversible [23].

Temperature dependence of the midpoint potential

The temperature dependence is shown in Fig. 4. A least-squares fit through the data points results in a temperature coefficient of −1.1 mV · K^{-1} between 0−31°C and −3.1 mV · K^{-1} above 32°C. The standard entropy change can be calculated using the equation:

$$\Delta S° = n \cdot F \cdot (dE°/dT).$$

For cytochrome c_{553} this results in $\Delta S°'$ values of −106 J · mol^{-1} · K^{-1} below 31°C and −299 J · mol^{-1} · K^{-1} above. The reaction entropy, $\Delta S°'_{rc}$ for this protein becomes −41 J · mol^{-1} · K^{-1} at temperatures below 30°C. This is comparable to the values obtained for other c-type cytochromes like horse heart cytochrome c or cytochrome c_{551} from *Pseudo-*
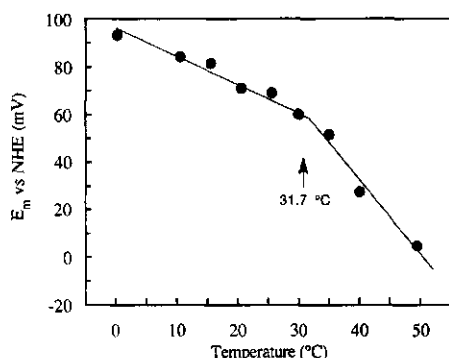
monas aeruginosa [24]. The enthalpy change $\Delta H°'$ at 25°C and pH 7.0 was calculated to be −38 kJ · mol^{-1}. At 31.7°C their is a change in the slope of the plot of temperature versus potential. This has also been described for horse heart cytochrome c and it was suggested that such a transition point represented a conformational change [25]. The reaction entropy for the reduction of the protein $\Delta S°'_{rc}$ above 32°C has a value of −234 J · mol^{-1} · K^{-1}. The enthalpy change $\Delta H°'$ at the optimal growth temperature of *D. vulgaris* (37°C) becomes −96 kJ · mol^{-1} at pH 7.0.

Determination of the K_m of cytochrome c_{553} and c_3

In order to be able to study the electron transfer between the cytochromes and the hydrogenase it is necessary to know the K_m of hydrogenase for the different cytochromes. Grande et al. reported kinetic data on the reaction between *D. vulgaris* hydrogenase and cytochrome c_3 [26]. At pH 8.0 and 37°C they found a value of 0.74 mM for the K_m of hydrogenase for this cytochrome using the hydrogen production assay. This is very high especially since cytochrome c_3 is postulated to be the physiological redox partner of hydrogenase [27, 28]. In contrast, Nivière et al. used the hydrogen consumption assay and reported a value of 7.4 μM at pH 7.6 and 25°C for the Michaelis constant of *D. gigas* hydrogenase for cytochrome c_3 of the same organism [12].

Fig. 5 shows the Michaelis Menten curves for the two cytochromes with hydrogenase. In the hydrogen consumption assay we find a Michaelis constant of 17 μM for cytochrome c_3 and 46 μM for cytochrome c_{553} at pH 7.0 and 23°C. The 50-fold difference between the value reported by Grande et al. and our value for cytochrome c_3 is unexpected. The K_m value for the reduced cytochrome does not have to be equal to the value of the oxidized cytochrome. However, this enormous difference suggests a physiological role for the oxidized form of the cytochrome rather than for the reduced form. The maximum turnover number of hydrogenase in the hydrogen consumption assay at infinite concentration of cytochrome c_3 was calculated to be 6.4×10^2 s^{-1}. At infinite concentration of cytochrome c_{553} a value of 7.1×10^2 s^{-1} was obtained.
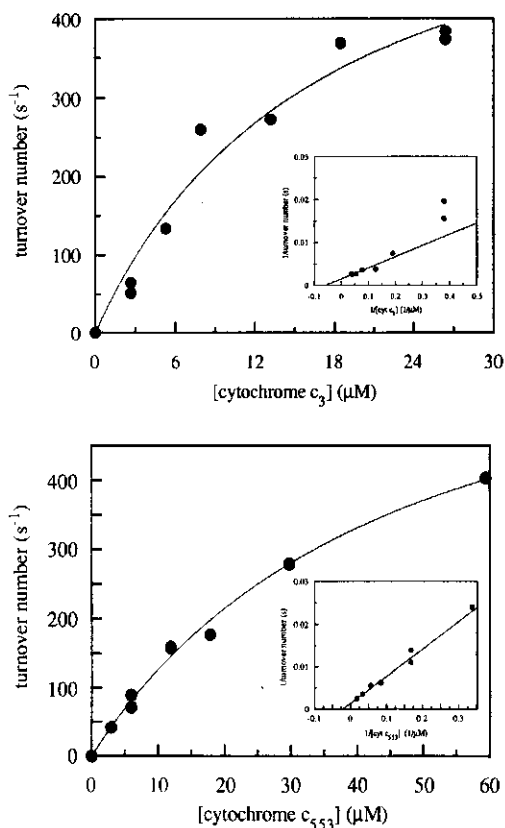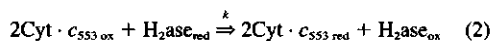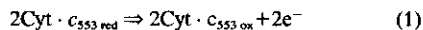
40

Fig. 5. **Michaelis-Menten curves for the reaction between cytochrome c_3 and hydrogenase (top) and cytochrome c_{553} and hydrogenase (bottom).** The reactions were measured in 100 mM Hepes pH 7.0 and the reaction rate was recalculated to turnover number from the change in absorbance at 553 nm. The inset shows the corresponding Lineweaver-Burke plot.

Electron transfer between cytochrome c_{553} and hydrogenase

Cyclic voltammetry experiments were performed as described in Materials and Methods. In these experiments the cytochrome c_{553} concentration was 110 µM and the hydrogenase concentration was varied over 0–180 nM. In the experiments with cytochrome c_3 a concentration of 52 µM was used and the hydrogenase concentration was varied over 0–84 nM. Changing the argon atmosphere into a hydrogen atmosphere caused a significant change of the voltammogram. For cytochrome c_{553} this is shown in Fig. 6 for a hydrogenase concentration of 4.5 nM. The resulting voltammogram is sigmoidal due to the significant increase of the anodic peak and the complete vanishing of the cathodic peak. These effects are caused by the continuous re-reduction of the cytochrome by hydrogenase (H_2ase). A representation of this process is shown in Fig. 7.

A scheme of the reaction sequence is indicated below. In this scheme the cytochrome is represented by Cyt; the reduced and oxidized forms are indicated by red and ox respectively.

$$2\text{Cyt} \cdot c_{553\,red} \Rightarrow 2\text{Cyt} \cdot c_{553\,ox} + 2e^- \qquad (1)$$

$$2\text{Cyt} \cdot c_{553\,ox} + H_2\text{ase}_{red} \overset{k}{\Rightarrow} 2\text{Cyt} \cdot c_{553\,red} + H_2\text{ase}_{ox} \qquad (2)$$

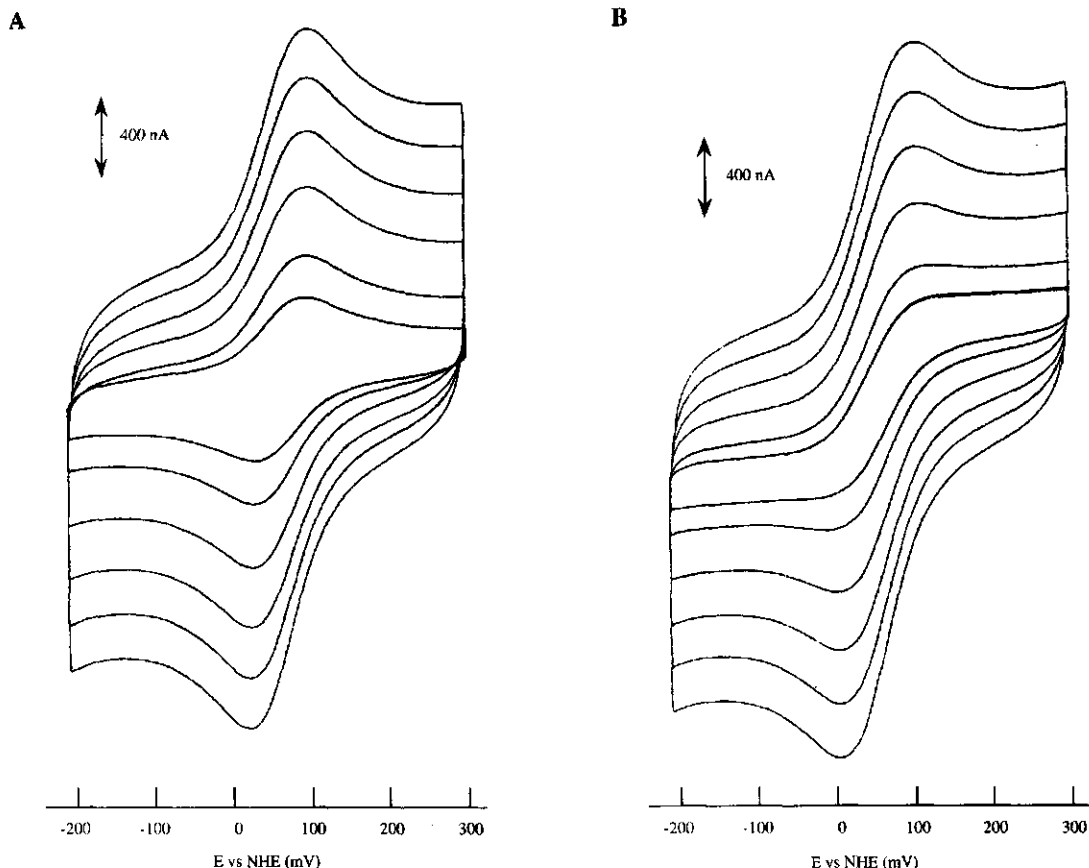$$H_2\text{ase}_{ox} + H_2 \Rightarrow H_2\text{ase}_{red} + 2\,H^+. \qquad (3)$$

Note that in this model, a single kinetic bottleneck is assumed but without specifying the molecular nature of this step, i.e. electron transfer or dissociation. In the latter case kinetic analysis would afford a value for the dissociation constant K_d rather than the K_m. The mechanism for this model has been described mathematically for linear sweep voltammetry by Savéant and Vianello [29] and by Nicholson and Shain [30]. The boundary conditions used in their description are also valid for the cytochrome c_{553} hydrogenase system. This follows from the following four arguments.

First, the heterogeneous electron transfer between the cytochrome and the electrode is a reversible reaction. Second, although hydrogenase is not present in large excess, the concentration of reduced hydrogenase can be considered constant during the reaction. This is caused by the continuous and fast reduction of hydrogenase by hydrogen. The cytochrome concentration is above its K_m and the catalytic reaction can therefore be considered as a pseudo-first-order reaction. The pseudo-first-order rate constant for this reaction is then defined by the product of the second-order rate constant and the concentration of the transient complex of H_2ase and the cytochrome: $k' = k \cdot$ [H_2ase-cytochrome]. Within the transient complex the ratio of hydrogenase over cytochrome is determined by the number of electrons needed to reduce the cytochrome and the number of electrons delivered by hydrogenase. When we want to express k' as a function of the total hydrogenase concentration we need to correct for the stoichiometry in the transient complex. The correction factor is the inverse of the earlier mentioned ratio. The pseudo-first-order rate constant k' now becomes $k' = 2 \cdot k \cdot$ [H_2ase] for monoheme cytochrome c_{553} and $k' = 0.5 \cdot k \cdot$ [H_2ase] for tetraheme cytochrome c_3 assuming that intramolecular redox interactions can be neglected (cf. [31]). Third, the homogeneous catalytic reaction (2) is essentially irreversible under the conditions employed. Due to the excess of hydrogen in solution, the equilibrium is completely shifted to the hydrogenase reduction and consequently to the cytochrome c_{553} reduction. Fourth, the diffusion coefficients of the reduced and oxidized form of cytochrome c_{553} can be considered equal but that of hydrogenase, which is important for the catalytic reaction, is only half of this. This can lead to significant errors in the interpretation of the experimental data, as discussed by Andrieux et al. [32]. However under our experimental conditions with hydrogen excess, we can expect a homogeneous distribution of the reduced hydrogenase even within the reaction layer. Therefore, it is not necessary to correct for the difference in diffusion coefficients.

The rate constant of reaction (2) can thus be measured under conditions of hydrogen excess by studying the ratio of the catalytic current over the diffusion controlled current as a function of the scan rate. With this ratio it is possible to obtain the dimensionless parameter λ using the working table given in [30]. The parameter λ is defined as:

$$\lambda = k'(RT/nF)/v$$

where k' is the pseudo-first-order rate constant (s^{-1}) and v is the scan rate (V/s). All other symbols have their usual meaning.

41

A

B

400 nA

-200 -100 0 100 200 300
E vs NHE (mV)

400 nA

-200 -100 0 100 200 300
E vs NHE (mV)

Fig. 6 b. Voltammogram of 110 μM cytochrome c_{553} in 100 mM Hepes pH 7.0 in (A) the absence of hydrogenase and (B) in the presence of 4.5 nM hydrogenase and hydrogen at scan rates of 10, 20, 40, 60, 80 and 100 mV s^{-1}. The dotted line at a scan rate of 10 mV s^{-1} is the control to check if anything changed during the measurement of the scan rate dependence. Voltammograms were taken at 25°C between +50 and −450 mV versus SCE using glassy carbon/SCE/Pt as the working/reference/counter electrodes respectively. The potential axes are defined versus the normal hydrogen electrode.
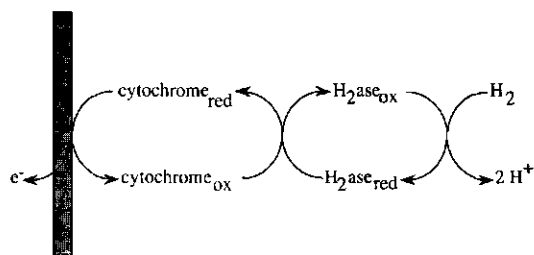
Fig. 7. Scheme of the reactions of cytochrome c_{553} in the presence of hydrogenase and H$_2$. The cytochrome is oxidized at the glassy carbon electrode and subsequently reduced by hydrogen. The reduction is catalyzed by hydrogenase. The electron transfer between the cytochrome and hydrogenase is considered to be the rate-determining step.

A plot of the parameter λ as a function of the inverse potential scan rate at a certain hydrogenase concentration (Fig. 8A) results in a slope of $\lambda \cdot v$. This slope can be used to calculate the heterogeneous electron transfer coefficient between the cytochrome and hydrogenase. In Fig. 8B the dependence of $\lambda \cdot v$ on the concentration of hydrogenase is shown for the two different cytochromes. The resulting rate constants can now be calculated to be $2 \times 10^7 \, M^{-1} \, s^{-1}$ for cytochrome c_{553} and $2 \times 10^8 \, M^{-1} \, s^{-1}$ for cytochrome c_3. The ratio of 10 between the rate constants of cytochrome c_3 and cytochrome c_{553} can be checked independently using the earlier determined K_m value and maximum turnover number. According to Nivière et al. [12] the second-order rate constant k can be expressed as:

$$k = (\text{maximum turnover number})/K_m.$$

The rate constant calculated this way has not been corrected for the number of transferred electrons. Using the pre-
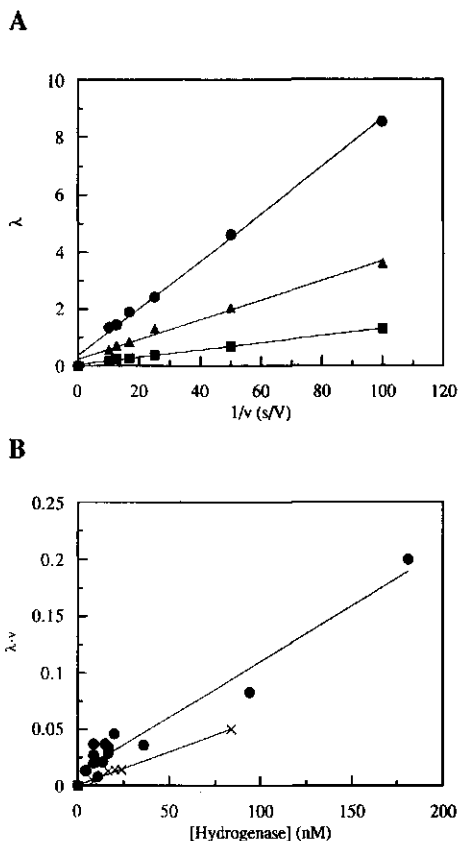
42

A

B

Fig. 8. (A) Dependence of λ on the inverse of the scan rate for cytochrome c_{553} at hydrogen concentrations of (●) 94 nM, (▲) 36 nM and (■) 4.5 nM. (B) Dependence of the kinetic parameter λ times the scan rate ($\lambda \cdot v$) on the hydrogenase concentration for cytochrome c_{553} (●) and cytochrome c_3 (×). The lines are linear fits to the data points.

viously defined correction factor for the two cytochromes, we also find a ratio of 10 for the two rate constants.

DISCUSSION

The temperature dependence of cytochrome c_{553} shows a transition point at 31.7 °C. This value differs remarkably from the value of 50 °C obtained for horse heart cytochrome c at pH 7.0 [25]. Since *D. vulgaris* is grown by us at a temperature of 37 °C we can expect that cytochrome c_{553}, in contrast to horse heart cytochrome c, functions in its second conformational state. The reaction entropy for the reduction of cytochrome c_{553} above 32 °C has a value of -234 J mol^{-1} K^{-1}. This is a rather high number, which indicates either a more rigid protein conformation or less solvent disordering upon reduction at these temperatures.

The pH dependence of the midpoint potential can be described with a pK_{ox} of 10.6. According to Bianco and co-workers this pK is associated with the loss of methionine as a ligand to the heme iron [7]. With horse heart cytochrome

c the methionine residue is replaced by a lysine residue and this results in an electroactive 'alkaline' form with a considerably decreased potential [33, 34]. The voltammograms of cytochrome c change significantly at these high pH values. An explanation for the shape of the resulting voltammograms was given by Haladjian et al. who proposed that two redox-active forms of cytochrome c with different potentials and in slow equilibrium with each other were present in solution [33]. With cytochrome c_{553} no significant change of the shape of the voltammogram is detected in the pH interval studied and this suggests that a different process takes place. From the sequence it follows that the methionine, which functions as a ligand to the heme iron is not preceded by a lysine. Therefore it can be expected that a different ligand coordinates to the iron upon raising the pH. The single pK_{ox} observed indicates an extra stabilization of the oxidized state. Due to the differences in the voltammetry of cytochrome c compared to cytochrome c_{553} we suggest that the methionine in the oxidized state above pH 10.6 is replaced by a ligand that can exchange rapidly. A likely option for such a ligand would be OH$^-$.

The results obtained by us in the electron transfer experiments between cytochrome c_{553} and the periplasmic Fe-hydrogenase contradict the conclusions of Yagi [2]. Under the circumstances applied in our experiments the cytochrome c_{553} is efficiently reduced by hydrogen and hydrogenase. The K_m value of 46 µM suggests a possible role for this cytochrome in the hydrogen metabolism of *D. vulgaris*. It has frequently been suggested that cytochrome c_3 functions as the natural electron acceptor or donor for hydrogenase. However a role as electron donor is somewhat difficult to imagine since the K_m value in the hydrogen production assay is 0.74 mM at pH 8.0 [26]. The K_m value in the hydrogen consumption assay, obtained by us in this study, is similar to the value reported by Nivière et al. for *D. gigas* NiFe-hydrogenase and cytochrome c_3 [12]. Apparently the nature of the metal centers has little effect on the interaction between the enzyme and the cytochrome.

Comparing our rate constants with the ones obtained by Hoogvliet et al. for the reaction between hydrogenase and several viologens we notice that the rate constants for the cytochromes are considerably higher [10, 35]. Hoogvliet et al. showed a relation between the magnitude of the positive charge of the viologen and the magnitude of the corresponding rate constant. Both cytochrome c_3 and c_{553} from *D. vulgaris* (H) are basic proteins with pI values of 10.0 and 9.3, respectively [20]. They both have an area with positively charged lysine residues at their surface as indicated by the crystal structures [36, 37]. Surface charge, therefore, appears crucial for efficient electron transfer in this system. The resulting rate constant for cytochrome c_3 is at first sight in good agreement with the rate constant published by Bianco et al. [14]. However they used a reaction scheme in which one cytochrome c_3 molecule reacts with one hydrogenase molecule. Since the four heme groups in *D. vulgaris* cytochrome c_3 essentially behave as independent redox centers [31] it is, in our opinion, necessary to use a correction factor in order to obtain the proper stoichiometry. If we do so the value of Bianco et al. becomes approximately 6×10^8 M^{-1} s^{-1}, which is three times higher than our value. The reason for this discrepancy is not known.

The values obtained by us for the two rate constants indicate a very efficient electron transfer between the hydrogenase and both cytochromes. This is remarkable since it means that cytochrome c_3 and cytochrome c_{553} will compete with

each other for electrons from hydrogenase. The discussion however is troubled by the fact that the function of the periplasmic Fe-hydrogenase is still controversial. Odom and Peck suggested a role for the Fe-hydrogenase in the obligate hydrogen-cycling model [28]. In this model the periplasmic Fe-hydrogenase functions as an uptake hydrogenase and delivers its electrons to cytochrome c_3. The electrons are subsequently transferred back across the membrane and used in the cytoplasm for the reduction of sulfate. The work of van den Berg et al. does not support this model. With antisense RNA techniques they reduced the cellular level of periplasmic hydrogenase which led to a decrease of the hydrogen concentration in the headspace of the cultures containing the modified bacteria [38]. They concluded from these observations that the periplasmic hydrogenase functions as a production enzyme since a decrease in its concentration resulted in a decrease of the hydrogen produced. It is possible that the function of this hydrogenase depends on the growth stage of the bacterium or the environmental conditions. Gray and Gest suggested that hydrogenase functioned as a "hydrogen valve" which could dispatch excess electrons through the reduction of protons [39]. This is supposedly necessary at the early stage of cell growth when the amount of ATP available for the activation of sulfate to form adenosine phosphosulfate is limited. The lack of this adenosine phosphosulfate might force the bacterium to get rid of its reducing equivalents in a different way using, for example, cytochrome c_3 and hydrogenase. Since this route should function as a safety valve, it is expected to be under strict kinetic control. Indeed, the K_m value of the hydrogenase for cytochrome c_3 in the hydrogen production assay is very high [26]. The hydrogen production will thus only function if a large pool of reduced cytochrome c_3 is available. Although the K_m value of this hydrogenase for hydrogen has never been measured, we can use the value of 310 μM, obtained for the related hydrogenase I of Clostridium pasteurianum, for comparison [40]. Such a high value indicates a function in hydrogen production since the expected concentration of hydrogen in solution is such that the enzyme only functions at a fraction (1/300) of its maximum turnover number. Hydrogenase is, however, present during all the different growth stages of the bacterium and this certainly implies that this enzyme has a more general role in the metabolism of Desulfovibrio vulgaris than just the initial hydrogen production.

From our studies we can conclude that the appreciable rate constant observed by us for the reduction of cytochrome c_{553} by hydrogenase and hydrogen has some consequences for the hydrogen cycling model or any other model in which the hydrogenase functions in the uptake of hydrogen. It can be expected that, besides cytochrome c_3, cytochrome c_{553} will also be reduced since both cytochromes, as well as hydrogenase, are present in the periplasmic space. A possible role for this diversion of electrons remains to be established.

REFERENCES

1. Peck, H. D. Jr & LeGall, J. (1982) Biochemistry of dissimilatory sulphate reduction, Phil. Trans. R. Soc. Lond. 298, 443−466.
2. Yagi, T. (1979) Purification and properties of cytochrome c_{553}, an electron acceptor for formate dehydrogenase of Desulfovibrio vulgaris, Miyazaki, Biochim. Biophys. Acta 548, 96−105.
3. Fauque, G., Bruschi, M. & LeGall, J. (1979) Purification and some properties of cytochrome $c_{553\,(550)}$ isolated from Desulfovibrio desulfuricans (Norway), Biochem. Biophys. Res. Commun. 86, 1020−1029.
4. Mayhew, S. G., van Dijk, C. & van der Westen, H. M. (1978) in Hydrogenases: their catalytic activity, structure and function (Schlegel, H. G. & Schneider, K., eds) pp 125−140, Verlag E. Goltze, Göttingen.
5. van Rooijen, G. J. H., Bruschi, M. & Voordouw, G. (1989) Cloning and sequencing of the gene encoding cytochrome c_{553} from Desulfovibrio vulgaris, J. Bacteriol. 171, 3575−3578.
6. Ogata, M., Arihara, K. & Yagi, T. (1981) D-Lactate dehydrogenase of Desulfovibrio vulgaris, J. Biochem. (Tokyo) 89, 1423−1431.
7. Bianco, P., Haladjian, J., Pilard, R. & Bruschi, M. (1982) Electrochemistry of c-type cytochromes; electrode reactions of cytochrome c_{553} from Desulfovibrio vulgaris Hildenborough, J. Electroanal. Chem. 136, 291−299.
8. Bertrand, P., Bruschi, M., Denis, M., Gayda, J.-P. & Manca, F. (1982) Cytochrome c_{553} from Desulfovibrio vulgaris: potentiometric characterization by optical and EPR studies, Biochem. Biophys. Res. Commun. 106, 756−760.
9. Bianco, P., Haladjian, J., Loutfi, M. & Bruschi, M. (1983) Comparative studies of monohemic bacterial c-type cytochromes. Redox and optical properties of Desulfovibrio desulfuricans Norway cytochrome $c_{553\,(550)}$ and Pseudomonas aeruginosa cytochrome c_{551}, Biochem. Biophys. Res. Commun. 113, 526−530.
10. Hoogvliet, J. C., Lievense, L. C., van Dijk, C. & Veeger, C. (1988) Electron transfer between the hydrogenase from Desulfovibrio vulgaris (Hildenborough) and viologens. 1. Investigations by cyclic voltammetry, Eur. J. Biochem. 174, 273−280.
11. Moreno, C., Franco, R., Moura, I., Le Gall, J. & Moura, J. J. G. (1993) Voltammetric studies of the catalytic electron-transfer process between the Desulfovibrio gigas hydrogenase and small proteins isolated from the same genus, Eur. J. Biochem. 217, 981−989.
12. Nivière, V., Hatchikian, E. C., Bianco, P. & Haladjian, J. (1988) Kinetic studies of electron transfer between hydrogenase and cytochrome c_3 from Desulfovibrio gigas; electrochemical properties of cytochrome c_3, Biochim. Biophys. Acta 935, 34−40.
13. Haladjian, J., Bianco, P., Guerlesquin, F. & Bruschi, M. (1987) Electrochemical study of the electron exchange between cytochrome c_3 and hydrogenase from Desulfovibrio vulgaris Norway, Biochem. Biophys. Res. Commun. 147, 1289−1294.
14. Bianco, P., Haladjian, J., Bruschi, M. & Guerlesquin, F. (1992) Reactivity of [Fe] and [Ni-Fe-Se] hydrogenases with their oxido-reduction partner: the tetraheme cytochrome c_3, Biochem. Biophys. Res. Commun. 189, 633−639.
15. Yagi, T., Honya, M. & Tamiya, N. (1968) Purifications and properties of hydrogenases from different origins, Biochim. Biophys. Acta 153, 699−705.
16. Sadana, J. C. & Morey, A. V. (1961) Purification and properties of the hydrogenase of Desulfovibrio desulfuricans, Biochim. Biophys. Acta 50, 153−163.
17. van der Westen, H. M., Mayhew, S. G. & Veeger, C. (1978) Separation of hydrogenase from intact cells of Desulfovibrio vulgaris: purification and properties, FEBS Lett. 86, 122−126.
18. Horio, T. & Kamen, M. D. (1961) Preparation and properties of three pure crystalline bacterial haem proteins, Biochim. Biophys. Acta 48, 266−286.
19. Chen, J.-S. & Mortenson, L. E. (1974) Purification and properties of hydrogenase from Clostridium pasteurianum W5, Biochim. Biophys. Acta 371, 283−289.
20. Hagen, W. R. (1989) Direct electron transfer of redoxproteins at the bare glassy carbon electrode, Eur. J. Biochem. 182, 523−530.

21. Tsuji, K. & Yagi, T. (1980) Significance of hydrogen burst from growing cultures of *Desulfovibrio vulgaris*, Miyazaki, and the role of hydrogenase and cytochrome c_3 in energy production system, *Arch. Microbiol. 125*, 35–42.

22. Nicholson, R. S. (1965) Theory and application of cyclic voltammetry for measurement of electrode reaction kinetics, *Anal. Chem. 37*, 1351–1354.

23. Bard, A. J. & Faulkner, L. (1980) *Electrochemical methods; fundamentals and applications*, J. Wiley & Sons, New York.

24. Taniguchi, T., Sailasuta-Scott, N., Anson, F. C. & Gray, H. B. (1980) Thermodynamics of metalloprotein electron transfer reactions, *Pure & Appl. Chem. 52*, 2275–2281.

25. Ikeshhoji, T., Taniguchi, I. & Hawkridge, F. M. (1989) Electrochemically distinguishable states of ferricytochrome *c* and their transition with changes in temperature and pH, *J. Electroanal. Chem. 270*, 297–308.

26. Grande, H. J., van Berkel-Arts, A., Bregh, J., van Dijk, K. & Veeger, C. (1983) Kinetic properties of hydrogenase isolated from *Desulfovibrio vulgaris* (Hildenborough), *Eur. J. Biochem. 131*, 81–88.

27. Yagi, T. (1970) Solubilization, purification and properties of particulate hydrogenase from *Desulfovibrio vulgaris*, *J. Biochem. (Tokyo) 68*, 649–657.

28. Odom, J. M. & Peck, H. D. Jr (1981) Hydrogen cycling as a general mechanism for energy coupling in the sulfate-reducing bacteria, *Desulfovibrio* sp., *FEMS Microbiol. Lett. 12*, 47–50.

29. Savéant, J. M. & Vianello, E. (1965) Potential sweep chronoamperometry: kinetic currents for first-order chemical reaction parallel to electron-transfer process (catalytic currents), *Electrochim. Acta. 10*, 905–920.

30. Nicholson, R. S. & Shain, I. (1964) Theory of stationary electrode polarography: single scan and cyclic methods applied to reversible, irreversible, and kinetic systems, *Anal. Chem. 36*, 706–723.

31. Benosman, H., Asso, M., Bertrand, P., Yagi, T. & Gayda, J.-P. (1989) EPR study of the redox interactions in cytochrome c_3 from *D. vulgaris* Miyazaki, *Eur. J. Biochem. 182*, 51–55.

32. Andrieux, C. P., Hapiot, P. & Savéant, J. M. (1985) Electron transfer coupling of diffusional pathways; homogeneous redox catalysis of dioxygen reduction by the methylviologen cation radical in acidic dimethylsulfoxide, *J. Electroanal. Chem. 189*, 121–133.

33. Haladjian, J., Pilard, R., Bianco, P. & Serre, P.-A. (1982) Effect of pH on the electroactivity of horse heart cytochrome *c*, *Bioelectrochem. Bioenerg. 9*, 91–101.

34. Ferrer, J. C., Guillemette, J. G., Bogumil, R., Inglis, S., Smith, M. & Mauk, A. G. (1993) Lys79 replaces Met80 as an iron ligand in one form of alkaline yeast ferricytochrome *c*, *J. Inorg. Biochem. 51*, 95.

35. Hoogvliet, J. C., Lievense, L. C., van Dijk, C. & Veeger, C. (1988) Electron transfer between the hydrogenase from *Desulfovibrio vulgaris* (Hildenborough) and viologens. 2. Investigations by chronoamperometry, *Eur. J. Biochem. 174*, 281–285.

36. Nakagawa, A., Higuchi, Y., Yasuoka, N., Katsube, Y. & Yagi, T. (1990) S-class cytochromes *c* have a variety of folding patterns: structure of cytochrome c_{553} from *Desulfovibrio vulgaris* determined by the multi-wavelength anomalous dispersion method, *J. Biochem. (Tokyo) 108*, 701–703.

37. Morimoto, Y., Tani, T., Okumura, H., Higuchi, Y. & Yasuoka, N. (1991) Effects of amino acid substitution on three-dimensional structure: an X-ray analysis of cytochrome c_3 from *Desulfovibrio vulgaris* Hildenborough at 2 Å resolution, *J. Biochem. (Tokyo) 110*, 532–540.

38. van den Berg, W. A. M., van Dongen, W. M. A. M. & Veeger, C. (1991) Reduction of the amount of periplasmic hydrogenase in *Desulfovibrio vulgaris* (Hildenborough) with antisense RNA: direct evidence for an important role of this hydrogenase in lactate metabolism, *J. Bacteriol. 173*, 3688–3694.

39. Gray, C. T. & Gest, H. (1965) Biological formation of molecular hydrogen, *Science 148*, 186–192.

40. Adams, M. W. W. & Mortenson, L. E. (1984) The physical and catalytical properties of hydrogenase II of *Clostridium Pasteurianum*; a comparison with hydrogenase I, *J. Biol. Chem. 259*, 7045–7055.

Chapter 4

On the two iron centers of desulfoferrodoxin

Marc F.J.M. Verhagen, Wilfried, G.B. Voorhorst, Joost A. Kolkman, Ronnie B.G. Wolbert,
Wilfred R. Hagen

On the two iron centers of desulfoferrodoxin

Marc F.J.M. Verhagen, Wilfried G.B. Voorhorst, Joost A. Kolkman, Ronnie B.G. Wolbert, Wilfred R. Hagen*

Department of Biochemistry, Agricultural University, Dreijenlaan 3, NL-6703 HA Wageningen, The Netherlands

Desulfoferrodoxin from *Desulfovibrio vulgaris*, strain Hildenborough, is a homodimer of 28 kDa; it contains two Fe atoms per 14.0 kDa subunit. The N-terminal amino-acid sequence is homogeneous and corresponds to the previously described *Rbo* gene, which encodes a highly charged 14 kDa polypeptide without a leader sequence. Although one of the two iron centers, Fe_A, has previously been described as a 'strained rubredoxin-like' site, EPR of the ferric form proves very similar to that of the pentagonal bipyramidally coordinated iron in ferric complexes of DTPA, diethylenetriaminepentaacetic acid: both systems have spin $S = 5/2$ and rhombicity $E/D = 0.08$. Unlike the Fe site in rubredoxin the Fe_A site in desulfoferrodoxin has a pH dependent midpoint potential with $pK_{ox} = 9.2$ and $pK_{red} = 5.3$. Upon reduction ($E_{m,7.5} = +2$ mV) Fe_A exhibits an unusually sharp $S = 2$ resonance in parallel-mode EPR. The second iron, Fe_B, has $S = 5/2$ and $E/D = 0.33$; upon reduction ($E_{m,7.5} = +90$ mV) Fe_B turns EPR-silent.

Bioelectrochemistry; EPR; Rubredoxin; Redox; *Desulfovibrio vulgaris* (H)

1. INTRODUCTION

Rubredoxin is a small, monomeric, mononuclear iron protein. It is generally present in fermentative and in sulfate reducing anaerobic bacteria, where it probably functions in secondary electron transport. There is refined structural data on several rubredoxins to 1.2–1.5 Å resolution. The mononuclear iron is coordinated by four cysteinate ligands forming a highly distorted tetrahedron. The reduction potential at neutral pH is close to 0 mV ([1] and refs quoted therein).

Three different, and mutually quite distinct classes of iron proteins have been described in sulfate reducers as intriguing variants to the rubredoxin system: (1) rubrerythrin/nigerythrin, (2) desulforedoxin, and (3) desulfoferrodoxin. The reddish rubrerythrin and the similar, blackish protein nigerythrin appear to contain a regular $Fe(Cys)_4$ rubredoxin site, however, with an unusually high reduction potential; they also contain a high-potential dinuclear iron cluster presumably with His/Glu coordination [2,3]. Both desulforedoxin and desulfoferrodoxin have been proposed to contain an $Fe(Cys)_4$ site that is more 'strained' compared to the site in rubredoxin because two of the Cys residues are adjacent in the primary sequence [4,5]. Furthermore, desulfoferrodoxin contains a second iron site presumably with octahedral N/O coordination [5]. Acid-labile sulfide is not found in any of these proteins. No biological function has been established or even indicated.

There are several unsolved questions related to the so-called strained rubredoxin-like center in desulfore-

doxin and desulfoferrodoxin. The proposed coordination is based on a questionable analogy with rubredoxin; redox potentials at unspecified pH have been reported in preliminary reports [6,7]; the proposed subunit composition is puzzling: homodimeric for desulforedoxin [4] and monomeric for desulfoferrodoxin [5]; desulfoferrodoxin from *D. vulgaris* has been reported to be a mixture of two proteins with distinct primary sequence [5]. These questions are addressed in what follows.

2. MATERIALS AND METHODS

Desulfovibrio vulgaris, strain Hildenborough, NCIB 8303, was maintained, grown in 300 liter batch cultures, and harvested as previously described [8]. The purification scheme of desulfoferrodoxin was similar to the original one described by Moura et al. [5] with minor modifications:

After the first DEAE column the ionic strength of the sample was adjusted by dilution with 1 mM potassium phosphate buffer and the sample was loaded onto a hydroxylapatite column (Bio-Rad) (2.6 × 7 cm) equilibrated with 1 mM potassium phosphate pH 7.0. A linear phosphate gradient (1–200 mM) with a total volume of 350 ml was applied and the pooled fractions were concentrated in an Amicon cell with a YM 10 membrane. The sample was subsequently loaded onto a Superdex G-75 gelfiltration column (2.6 × 60 cm) (Pharmacia) equilibrated with 50 mM potassium phospate pH 7.0 and 150 mM NaCl. The fractions containing desulfoferrodoxin were collected using polyclonal antibodies and, after concentration and dilution, applied onto a MonoQ HR 5/5 column (Pharmacia) equilibrated with 10 mM HEPES pH 7.0. A shallow linear gradient (0–1 M NaCL) was applied and two closely spaced purple peaks were eluted from the MonoQ column and analyzed separately (see below).

2.1. *Analytical determinations*

Iron was determined colorimetrically according to the procedure described in [9] using 3-(2-pyridyl)-5,6-bis(5-sulfo-2-furyl)-1,2,4-triaz-

*Corresponding author. Fax: (31) (8370) 848 01.

ine, disodium salt trihydrate (ferene, Aldrich) as the chelator. Protein was determined using either the microbiuret method [10] with trichloroacetic acid/deoxycholate precipitation [11] or the method described by Bradford [12]. The reagent used for the Bradford protein determination was obtained from Bio-Rad. Bovine serum albumine was used as a standard.

Electrophoresis was performed with a Midget system (Pharmacia) using 17.5% and 20% gels, or with a Phastsystem (Pharmacia) using 8–25% gradient gels. The SDS-polyacrylamide gels were according to Laemmli [13]. The gels were calibrated with Pharmacia low molecular weight markers. For Isoelectric focussing 3–9 precoated gels were used with a Phastsystem. The calibration was performed with the broad pI calibration kit (Pharmacia). The native molecular mass of the protein was determined with a superdex G-75 gelfiltration column equilibrated with 50 mM potassium phosphate pH 7.0 and 150 mM NaCl using a flow rate of 1.5 ml/min. BSA (67 kDa), ovalbumine (43 kDa), myoglobin (18.8 kDa), cytochrome c_3 (14.1 kDa) and cytochrome c_{553} (9.2 kDa) were used as the markers for the calibration. The void volume was determined with Blue dextran.

2.2. Spectroscopy

UV/VIS spectra were recorded on a Aminco DW 2000 spectrophotometer using 1 cm quartz cuvettes. EPR measurements and mediated redox titrations were as previously described [8].

2.3. N-terminal sequencing

4 µg quantities of the purified protein were freeze dried. Gas-phase sequencing of these samples was carried out at the sequencing facility of the Netherlands Foundation for Chemical Research (SON) (Dr R. Amons, University of Leiden, NL).

2.4. Antibodies

The purified desulfoferrodoxin was applied to a Laemmli gel (300 × 150 × 1.5 mm) and the protein was electroeluted after excision of the 14.0 kDa band. Antibodies were induced in mice by subcutaneous injection of a 35 µg quantity mixed with Freund's complete adjuvant. Boosts of equal amounts of antigen mixed with Freund's incomplete adjuvant were administered twice at three-weekly intervals. The serum was used without further purification. Proteins were blotted onto a nitrocellulose support after separation on denaturing SDS gels [14]. Goat anti-mouse IgG alkaline phosphatase conjugate (Boehringer, Germany) was used for immunostaining.

2.5. Electrochemistry

The electrochemical measurements were performed as described by Hagen [15] with the following modifications: The working electrode was treated with nitric acid and washed with 0.1 M dipotassiumhydrogenphosphate and water. Instead of polishing, the electrode was held in a methane flame until it became red-hot. After cooling down, 20 µl of a 20 mM neomycine solution was applied onto the electrode. Subsequently the electrode was dried with a tissue and mounted in the electrochemical cell. The sample was applied and the cyclic voltammetry was started using a BAS CV 27 potentiostat (BioAnalytical Systems Indiana, USA) connected to an X-Y recorder (Kipp & Zonen, NL). After one scan neomycin was added to the sample in a final concentration of 2 mM. The pH dependence was measured using sodium acetate, MES, HEPES, TAPS, CHES and CAPS all at a final concentration of 50 mM. Temperature dependence was measured as described by Link et al. [16].

3. RESULTS

3.1. Primary structure

A mixture of two different amino-acid sequences has

Fig. 1. (A) SDS-PAGE of purified *D. vulgaris* (Hildenborough) desulfoferrodoxin. Lane 1, molecular mass marker mixture; lane 2, 5 µg desulfoferrodoxin. The band at 28 kDa is the dimeric form of the protein. (B) Calibration of the native molecular mass of Desulfoferrodoxin with a Superdex G-75 gelfiltration column. The gelfiltration was performed as described in section 2. K_{av} is the ratio of the elution volume V_e minus the void volume V_o over the total volume V_t minus the void volume V_o.

been reported for *D. vulgaris* desulfoferrodoxin by Moura et al. one corresponding to the sequence of the protein from *D. desulfuricans* ATCC 27774 and the second corresponding to the *Rbo* gene from *D. vulgaris* except for the first two residues [5,17]. Since in our hands the protein always eluted in two separate peaks from the final MonoQ column, samples from both peaks were freeze dried and mailed for separate analysis in the gas-phase sequenator at the University of Leiden. The two samples had identical N-terminal sequences, which fully corresponded to that of the *D. vulgaris Rbo* gene including the leading residues:

```
          1            5              10             15
protein:  Met-Pro-Yyy-Gln-Tyr-Glu-Ile-Tyr-Lys-Xxx-Ile-Yyy-Xxx-Gly-Asn-Ile
Rbo gene: Met-Pro-Asn-Gln-Tyr-Glu-Ile-Tyr-Lys-Cys-Ile-His-Cys-Gly-Asn-Ile
```
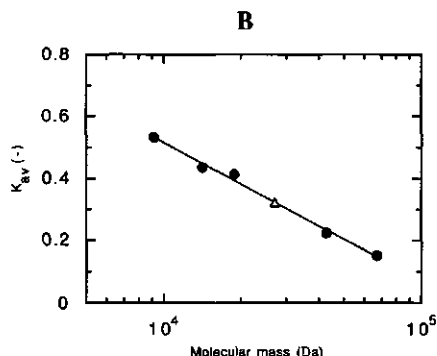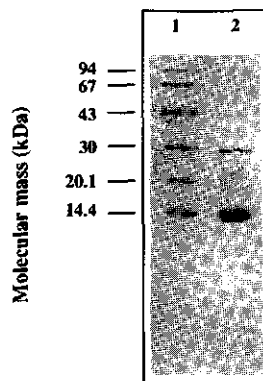
No indication whatsoever was found for a sequence corresponding to the *D. desulfuricans* protein. Since both samples were also found to be indistinguishable on SDS-PAGE, in isoelectric focussing, and in spectroscopy (not shown) their distinction is ignored from now on.

3.2. *Subunits and antibodies*

The purified protein exhibited a two-band pattern on SDS-PAGE corresponding to molecular masses of approximately 14 and 28 kDa (see Fig. 1A). The 14 kDa band was excised and used to raise polyclonal antibodies in mouse. When these antibodies were used in a Western blot of the purified protein both the 14 kDa and the 28 kDa proved to exhibit comparable reactivity suggesting that the 28 kDa band is a dimeric aggregate of the 14 kDa band (data not shown). It was subsequently found that the dimerization in the SDS gel was dependent on the lapse time after boiling of the protein in SDS, but was independent of the boiling time and of the excess amount of SDS. Application of the sample onto the gel directly after boiling and running the gel immediately afforded mainly a 14 kDa band pattern. When the sample was left for 1 h after boiling and/or

Fig. 3. Redoxtitration of purified desulfoferrodoxin from *D. vulgaris* (H). The protein was mixed with mediators in 100 mM HEPES pH 7.5. The reduction was performed with sodium dithionite, the oxidation with ferricyanide. Samples were withdrawn at different potentials and frozen in liquid nitrogen. The reduction of Fe_A was followed at $g = 7.7$. The reduction of Fe_B was followed at $g = 4.3$ after correction for the $g = 4.1$ feature in the spectrum. The data points were fitted with two different Nernst curves with $n = 1$ and $E_m = +2$ and $+90$ mV respectively.

when the gel was run on low voltage overnight a 14 + 28 kDa two-band pattern would evolve.

The *D. desulfuricans* desulfoferrodoxin has previously been reported to be a monomer based on analytical gel filtration [5]. In view of its unusually strong tendency to dimerize under denaturing conditions we repeated the gel-filtration experiment for the *D. vulgaris* protein. On the Superdex G-75 hiload column the native protein ran with an apparent molecular mass of 27.1 kDa (Fig. 1B). We conclude that *D. vulgaris* desulfoferrodoxin is a homodimer.

The antibodies were used to explore the expression of desulfoferrodoxin protein as a function of growth phase. Cells were harvested from a 1 liter culture of *D. vulgaris* from 16 to 64 h after inoculation. Cell-free extracts were prepared and samples (with a volume corrected for the 600 nm optical density of the culture at the time of harvesting) were used for Western blotting. No significant variation in expression was found (not shown) suggesting that expression of the protein is not dependent on the growth phase.

3.3. *Optical and analytical data*

The optical spectrum of the protein as isolated was virtually identical to that reported for the *D. desulfuricans* protein [5]: there are peaks at 279, 367, 502 nm and shoulders at 317 and 567 nm. The purity index of the *D. vulgaris* protein, $A_{279}/A_{502} = 6.7$, is also comparable to that reported for the *D. desulfuricans* protein, $A_{297}/A_{495} = 7.8$ [5]. When the protein concentration is determined with the Biuret method the extinction coefficient at 279 nm is $\varepsilon = 57.3$ mM^{-1}·cm^{-1} for the 28 kDa dimer. The Bradford method (Coomassie brilliant blue colouring) of protein determination gives a 10% overestima-
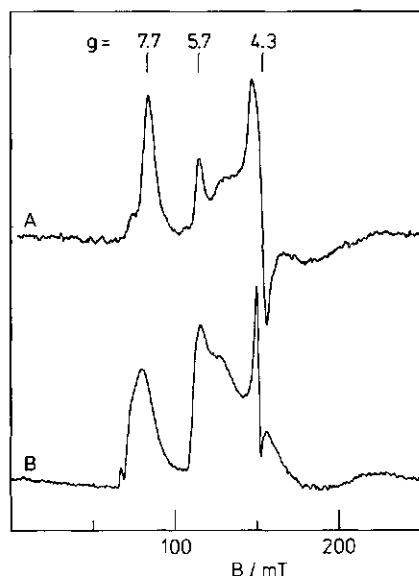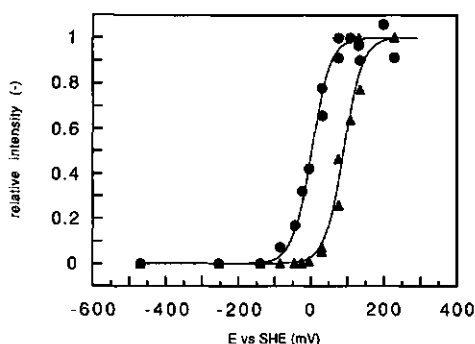
Fig. 2. Comparison of the EPR spectral shapes from desulfoferrodoxin (trace A) and ferric DTPA (trace B). The 'as isolated' desulfoferrodoxin from *D. vulgaris* (H) was 2.4 mg/ml in 10 mM Tris/HCl pH 8.0. Ferric DTPA was 1 mM FeCl₃ plus 10 mM DTPA with the pH adjusted to 5.0. EPR conditions: microwave frequency, 9.14 GHz; microwave power, 200 mW; modulation frequency, 100 KHz; modulation amplitude, 1.25 and 1.6 mT; temperature, 10 and 16 K. The microwave power level is somewhat saturating for the middle part of the FeDTPA spectrum resulting in an emphasized peak at $g = 5.7$.

tion compared to the Biuret method. The ferene coloring method quantitates to 2.2 iron atoms per 14.0 kDa subunit ($n = 2$). This number is not significantly reduced upon overnight dialysis against 25 mM HEPES pH 7.0 with 1 mM EDTA. In iso-electric focussing the protein (i.e. both forms from the MonoQ column) consistently exhibited two well resolved bands with pI = 5.3 and 5.5.

3.4. EPR of ferric sites

The low-temperature EPR spectrum of ferric DTPA (diethylenetriaminepentaacetic acid) at neutral pH is presented in trace B of Fig. 2. This spectrum is essentially independent of the pH in the range 1.9 to 10.0. At elevated pH > 11.0 the spectrum is converted into the familiar $g = 4.3$ type signal. The spectra of ferric TTHA (triethylenetetraaminehexaacetic acid) are essentially identical to those of the DTPA complexes (not shown). The Fe-DTPA spectra have been published before because of their qualitative similarity with pH-dependent spectra from the ferric ion in soybean lipoxygenase [18]. The EPR was not analyzed, however, the crystal structure of [FeHDTPA]$^{1-}$ and [FeDTPA]$^{2-}$ was determined (ibidem).

In trace A of Fig. 2 the spectrum is given of desulfoferrodoxin as it is isolated. Its similarity with the Fe-DTPA spectrum is striking, and is much stronger than that between lipoxygenase and Fe-DTPA. In fact, the only significant difference between the two spectra is one of line width. The effective g-values of both spectra can be understood in terms of the $S = 5/2$ spin Hamiltonian

$$H = D(S_z^2 - 35/12) + E(S_x^2 - S_y^2) + 2.00\beta B \cdot S$$

in the weak-field regime and with rhombicity $E/D = 0.08$ [19]. This description predicts $g \approx 7.7, 4.1, 1.8$ for the $| \pm 1/2 >$ doublet and $g = 5.7$ for the $| \pm 3/2 >$ doublet.

From a Mössbauer study Moura et al. concluded that the second iron site in $D.$ $desulfuricans$ desulfoferrodoxin was ferrous, however, in recent preliminary reports the isolation has been announced of fully oxidized protein; those preparations exhibit extra EPR features at $g = 9.74$ and 4.3 from high-spin ferric ion [6,7]. The $D.$ $vulgaris$ desulfoferrodoxin spectrum exhibits a weak feature at $g = 4.3$. When the protein is incubated with redox mediators and carefully (see below) reduced with sodium dithionite this feature decreases in intensity. We identify this signal with the second iron site, Fe$_B$.

3.5. EPR redox titration

The protein was incubated with a mixture of 13 redox mediators [8] and then stepwise reduced with additions of sodium dithionite or oxidized with potassium ferricyanide. EPR samples were drawn at redox equilibrium, and the oxidation state of the two iron centers was
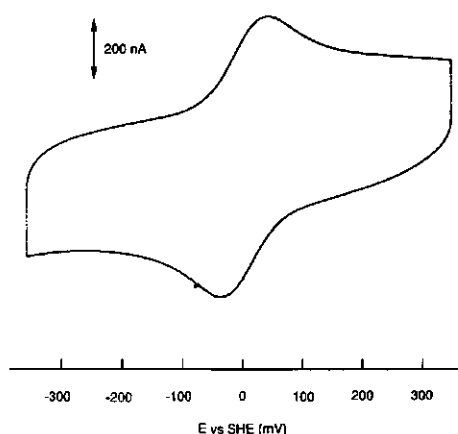
determined from the amplitude of the $g = 7.7$ peak (Fe$_A$) or the $g = 4.3$ derivative feature (Fe$_B$). The result is presented in Fig. 3 with the potential axis relative to the standard hydrogen electrode. Both iron centers behave as independent one-electron transferring entities; the potentials are $E_{m,7.5} = +2$ mV for Fe$_A$ and +90 mV for Fe$_B$. When the potential is raised with ferricyanide to values greater than approximately 250 mV erratic results are obtained: the signal from Fe$_A$ decreases and the Fe$_B$ signal is replaced by a sharp, intense signal at $g = 4.3$. We have recently reported a similar effect for the ferricyanide-oxidation of the nitrogenase MoFe-protein beyond some +245 mV [20].

3.6. Electrochemistry

The electrochemistry of desulfoferrodoxin results in well defined cyclic voltammograms (Fig. 4) between pH 5.0 and pH 9.5. Beyond pH 9.5 the voltammograms become less defined. The low potential iron (Fe$_A$) gives rise to a quasi reversible diffusion controlled electron transfer. The potential is pH dependent as shown in Fig. 5 and can be described by the equation:

$$E_m = E_{low\ pH} + RT/nF \cdot \ln\{(K_{red} \cdot [H^+] + [H^+]^2)/(K_{ox} + [H^+])\}$$

A least squares fit of this equation to the data points results in a $E_{low\ pH}$ of 307 mV, a pK_{ox} of 9.21 and a pK_{red} of 5.25. The temperature coefficient is -1.4 mV·°C^{-1} in the range between 10 and 40°C. The midpoint potential at 25°C and pH 7.0 is calculated to be -4 ± 5 mV versus SHE. The high potential iron (Fe$_B$) is not detected in the cyclic voltammograms. Since this site can be reduced in a chemical titration using dithionite and mediators we
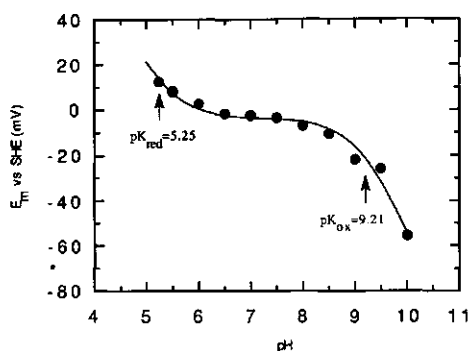
Fig. 5. pH dependence of the midpoint potential of desulfoferrodoxin. Voltammograms were taken from −600 to +100 versus SCE at a scan rate of 10 mV/s. The concentration of desulfoferrodoxin was 3 mg/ml in 50 mM buffer of the appropiate pH and 2 mM neomycin.

suggest that Fe_B is buried within the protein. Together with the high potential of Fe_B and the destruction of the protein upon oxidation beyond 250 mV this might indicate that Fe_B has a structural or a coordination function rather than a redox function.

3.7. Ferrous EPR

A very broad EPR feature with zero crossing at $g_{eff} \approx 10.9$, indicative of an integer spin system, was found by Moura et al. with D. desulfuricans desulfoferrodoxin after reduction with excess dithionite [5]. Integer spin systems are usually more readily studied in parallel-mode EPR [21]. Therefore, dithionite-reduced D. vulgaris desulfoferrodoxin was studied in the dual-mode cavity, which allows to do both experiments sequentially under identical conditions. The two spectra are given in Fig. 6. Not only the position of the observed line at $g_{eff} = 11.6$ but also the narrow line width and the considerable intensity difference of the signal between parallel-mode and normal-mode are unusual for ferrous $S = 2$ [21]. The latter two properties are reminiscent of the EPR from a putative $S = 2$ system in O_2-pulsed cytochrome oxidase [22], from a putative $S = 3$ system in nitrogenase [20] and from a putative $S = 4$ system in the prismane protein [23]. This pattern is indicative of a system with a very narrow distribution in zero-field splitting parameters; it is a fingerprint for Fe_A as it sets it apart from other ferrous $S = 2$ systems.

4. DISCUSSION

4.1. Structural aspects

Desulfoferrodoxin from D. vulgaris has been reported to be a mixture of two proteins with different primary sequence [5]. We find only a single homogeneous sequence corresponding to the Rbo gene [17]. We suggest that the previously described preparation has been iso-

lated from a mixed culture of D. vulgaris and D. desulfuricans. Also, in contrast to previous work [5] we find desulfoferrodoxin to be a 2 × 14 kDa dimer under non-denaturing conditions. The protein carries two iron sites with putatively novel coordination. Particularly, a strained coordination by four cysteines has been proposed for the Fe_A site [5]. This idea is based on an unsubstantiated inference from the well-known rubre-doxin structure. However, the midpoint potential of desulfoferrodoxin shows a complicated dependence on the pH. This is completely unlike rubredoxin that has a pH independent midpoint potential between pH 5.5 and 9.0 (our unpublished results). From a sequence comparison with desulforedoxin it follows that two of the putatively coordinating Cys are adjacent residues. From our present EPR spectral comparison with iron complexes it would appear that a higher coordination number is not excluded. In the DTPA complex the iron is seven-coordinated in a pentagonal bipyramide. Just recently, the crystal structure of soybean lipoxygenase L-1, for which this DTPA complex functioned as a model compound, was solved at a resolution of 2.5 Å. The iron was found to be coordinated by three histidines, the C-terminal isoleucine and possibly an asparagine. With asparagine as a ligand the coordination was described as approximate octahedral with one vacant position [24]. Without the coordination of asparagine the iron atom was described to be at the center of a highly distorted octahedron with two adjacent, unoccupied positions [25]. From this we conclude that, despite
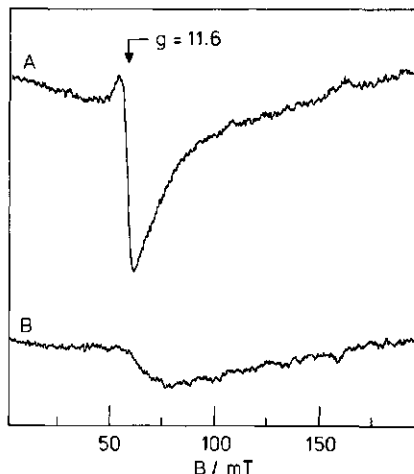
Fig. 6. Parallel-mode (trace A) and perpendicular mode (trace B) EPR spectrum of dithionite-reduced desulfoferrodoxin from D. vulgaris (H). The protein concentration was 2.4 mg/ml in 10 mM Tris-HCl pH 8.0. Dithionite was added to a final concentration of 2 mM. EPR conditions: microwave frequency, 9085 MHz (parallel mode) and 9138 MHz (perpendicular mode); microwave power, 200 mW; modulation frequency, 100 kHz; modulation amplitude, 1.25 mT; temperature 9K.

the ultimate differences, the spectral properties of FeDTPA initially gave a reasonable indication of the symmetry around the iron atom in lipoxygenase . We therefore believe that the similarity between the spectral properties of FeDTPA and desulfoferrodoxin is also indicative for a novel type of coordination of the iron atom in this protein. Comparison of the primary sequences of *D. gigas* desulforedoxin, *D. desulfuricans* desulfoferrodoxin, and *D. vulgaris* desulfoferrodoxin [5] shows several conserved residues with potential metal binding capacity near the Cys cluster: Tyr-8, Cys-10, Cys-13, Cys-29, Cys-30, Glu-32, Met-34. Thus, even for a full oxygen/sulfur seven coordination the involvement of both Cys-29 and Cys-30 is not a mandatory condition.

4.2. *Functional aspects*

The biological function of desulfoferrodoxin is unknown. A function in secondary electron transfer is not likely in view of its strong tendency to dimerize. A function in the biosynthesis of other proteins (e.g. iron insertion) is less likely as expression of desulfoferrodoxin is not dependent on the bacterial growth phase. Brumlik and Voordouw named the gene encoding *D. vulgaris* desulfoferrodoxin the *Rbo*, or rubredoxin oxidoreductase encoding gene because it forms a transcriptional unit with the gene encoding rubredoxin [17]. This suggests that rubredoxin may be a natural redox partner of desulfoferrodoxin, however, it does not really suggest a function, as rubredoxin oxidoreductase is not a self-evident biological activity. The name Rbo does suggest that desulfoferrodoxin is a redox enzyme. Our determination of the iron redox potentials puts a thermodynamic limit on this suggestion. The E_m's are at +2 and +90 mV, and oxidation beyond 250 mV is irreversible. The substrate would have to be one or two electron accepting with a reduction potential of the order of +0.1 V.

REFERENCES

[1] Adman, E.T., Sieker, L.C. and Jensen, L.H. (1991) J. Mol. Biol. 217, 337–352.

[2] LeGall, J., Prickril, B.C., Moura, I., Xavier, A.V., Moura, J.J.G. and Huynh, B.-H. (1988) Biochemistry 27, 1636–1642.

[3] Pierik, A.J., Wolbert, R.B.G., Portier, G.L., Verhagen, M.F.J.M. and Hagen, W.R. (1993) Eur. J. Biochem., 212, 237–245.

[4] Moura, I., Huynh, B.-H., Hausinger, R.P., Le Gall, J., Xavier, A.V. and Münck, E. (1980) J. Biol. Chem. 255, 2493–2498.

[5] Moura, I., Tavares, P., Moura, J.J.G., Ravi, N., Huynh, B.-H., Liu, M.-Y. and LeGall, J. (1990) J. Biol. Chem. 265, 21596–21602.

[6] Tavares, P., Ravi, N., Liu, M.Y., LeGall, J., Huynh, B.H., Moura, J.J.G. and Moura, I. (1991) J. Inorg. Biochem. 43, 264.

[7] Tavares, P., Moura, J.J.G., Ravi, N., Huynh, B.H., LeGall, J. and Moura, I. (1993) J. Inorg. Biochem. 51, 478.

[8] Pierik, A.J., Hagen, W.R., Redeker, J.S., Wolbert, R.B.G., Boersma, M., Verhagen, M.F.J.M., Grande, H.J., Veeger, C., Mutsaers, P.H.A., Sands, R.H. and Dunham, W.R. (1992) Eur. J. Biochem. 209, 63–72.

[9] Pierik, A.J., Wolbert, R.B.G., Mutsaers, P.H.A., Hagen, W.R. and Veeger, C. (1992) Eur. J. Biochem. 206, 697–704.

[10] Goa, J. (1953) Scand. J. Clin. Lab. Invest. 5, 218–222.

[11] Bensadoun, A. and Weinstein, D. (1976) Anal. Biochem. 70, 241–250.

[12] Bradford, M.M. (1976) Anal. Biochem. 72, 248–254.

[13] Laemmli, U.K. (1970) Nature 227, 680–685.

[14] Towbin, H., Staehelin, T. and Gordon, J. (1979) Proc. Natl. Acad. Sci. USA 76, 4350–4354.

[15] Hagen, W.R. (1989) Eur. J. Biochem. 182, 523–530.

[16] Link, T.A., Hagen, W.R., Pierik, A.J., Assmann, C. and von Jagow, G. (1992) Eur. J. Biochem. 208, 685–691.

[17] Brumlik, M.J. and Voordouw, G. (1989) J. Bacteriol. 171, 4996–5004.

[18] Finnen, D.C., Pinkerton, A.A., Dunham, W.R., Sands, R.H. and Funk, M.O., Jr. (1991) Inorg. Chem. 30, 3960–3964.

[19] Hagen, W.R. (1992) in: Advances in Inorganic Chemistry, Vol. 38: Iron-Sulfur Proteins, (Cammack, R. and Sykes, A. G., Eds.) Academic Press, San Diego, pp. 165–222.

[20] Pierik, A.J., Wassink, H., Haaker, H. and Hagen, W.R. (1993) Eur. J. Biochem. 212, 51–61.

[21] Hagen, W.R. (1982) Biochim. Biophys. Acta 708, 82–98.

[22] Hagen, W.R., Dunham, W.R., Sands, R.H., Shaw, R.W. and Beinert, H. (1984) Biochim. Biophys. Acta 765, 399–402.

[23] Pierik, A.J., Hagen, W.R., Dunham, W.R. and Sands, R.H. (1992) Eur. J. Biochem. 206, 705–719.

[24] Minor, W., Steczko, J., Bolin, J.T., Otwinowski, Z. and Axelrod, B. (1993) Biochemistry 32, 6320–6323.

[25] Boyington, J.C., Gaffney, B.J. and Amzel, L.M. (1993) Science 260, 1482–1486.

Chapter 5

Redox characteristics of cytochrome P-450 from *Pseudomonas putida* studied by direct electrochemistry

Marc F.J.M. Verhagen, Bart E. van de Beek and Wilfred R. Hagen

Redox characteristics of cytochrome P-450 from *Pseudomonas putida* studied by direct electrochemistry

Marc F.J.M. Verhagen, Bart E. van de Beek and Wilfred R. Hagen

Abstract

The redox properties of cytochrome $P\text{-}450_{cam}$ from *Pseudomonas putida* were determined with cyclic voltammetry using a bare glassy carbon electrode, and were compared with results from EPR monitored redox titrations in homogeneous solutions. The use of cyclic voltammetry with either the substrate-bound or the substrate-free enzyme resulted in identical, well defined voltammograms. The scan rate dependence of the peak current indicated that the enzyme was adsorbed onto the electrode surface. A value of -85 mV vs. SHE at pH 7.5 and 25 °C was obtained for the midpoint potential of both enzyme forms. The midpoint potentials determined from an EPR monitored redox titration were -127 and -175 mV vs. SHE at pH 7.5 and 23°C for the camphor-bound and camphor-free enzyme, respectively. The pH dependence of the midpoint potential, measured with cyclic voltammetry in the range between pH 5.5 and 10.5, indicates the presence of two pK-values. A model is proposed in which one of these values is assigned to the oxidized form of the protein (pK_{ox}=8.4), and the other one to the reduced form (pK_{red}=7.3). The midpoint potential is temperature dependent with a distinct breakpoint at 20 °C. The slope of the curve is -0.5 $mV \cdot K^{-1}$ below this breakpoint and -1.1 $mV \cdot K^{-1}$ above this value. The associated standard entropy changes are calculated to be $\Delta S^{o'}$ = -46 $J \cdot mol^{-1} \cdot K^{-1}$ and -101 $J \cdot mol^{-1} \cdot K^{-1}$, respectively. The midpoint potential of *Pseudomonas putida* ferredoxin has also been determined with cyclic voltammetry using a neomycin modified electrode. A value of -170 mV vs. SHE at 25 °C and pH 7.5 was obtained for this protein. This value is linearly dependent on the temperature with a slope of -1.9 $mV \cdot K^{-1}$ and is not dependent on the pH in the interval between pH 5.5 and 9.

Cytochrome P-450 from camphor grown *Pseudomonas putida* is one of the best studied monooxygenase systems. The enzyme is the terminus of a three component electron transfer chain also consisting of an NADH dependent reductase and a [2Fe-2S] ferredoxin. Cytochrome P-450 catalyzes the hydroxylation of the camphor molecule at the 5-*exo* position. This is the first step in a series of reactions which make it possible for the bacterium to use the relatively inert monoterpene as the sole carbon source. Since camphor is the physiological substrate the enzyme is called cytochrome P-450$_{cam}$. The structural genes for the three proteins from the bacterial cytochrome P-450 electron transfer chain have all been cloned and sequenced ([1] and refs. therein). The cytochrome P-450$_{cam}$ has been crystallized in the presence and absence of substrate and the crystal structure has been solved to 1.6 Å and 2.2 Å resolution respectively [2]. P-450$_{cam}$ is an enzyme of 45 kDa containing one single heme. The ferric iron in the substrate bound protein is mainly in the high spin state, S=5/2. From the crystal structure it appeared that the iron in this state is pentacoordinate with one axial ligand. Upon release of camphor a sixth ligand, probably a water molecule or a hydroxide ion, coordinates to the iron. The spin state of the ferric iron in this substrate free enzyme consequently becomes low-spin, S=1/2 [2].

The reduction potential of the iron in cytochrome P-450 has been found to be dependent on binding of the substrate. For the camphor-bound enzyme a value of -170 mV vs. SHE was determined photochemically using a mediator to calibrate the potential axis and with anaerobic stopped flow spectrophotometry using *Pseudomonas putida* ferredoxin as the reductant [3,4] . The latter technique was also used to determine the midpoint potential of the camphor-free enzyme at a value of -303 mV vs. SHE [4]. Contrasting results were reported by Huang et al., who used a spectroelectrochemical cell to determine the potential of the substrate bound P-450$_{cam}$ enzyme. They reported a midpoint potential of -128 mV vs. SHE at 25 °C and pH 7.5. However, this potential appeared to be dependent on the concentration of the redox dye indigo carmine, which was added to the solution in order to calibrate the potential axis. At ratios of dye over enzyme below 0.4 the potential decreased linearly. Extrapolation to zero concentration of the dye resulted in a value of -168 mV vs. SHE [5]. Finally, a value of -138 mV was reported, recently, for the substrate bound P-450$_{cam}$ enzyme at pH 7.4 [6]. Unfortunately, the authors did not describe the exact procedure, which they used to determine this value.

The properties of the [2Fe-2S] ferredoxin from *Pseudomonas putida* , which is the current IUBMB nomenclature for the formerly called putidaredoxin [7], have also been studied extensively. The redox potential of this ferredoxin was reported to be in the range between -233 and -241 mV vs. SHE [3,8,9] and was found to shift upon binding to the cytochrome P-450 to a value of -196 mV vs. SHE [3]. The potential was found to be pH dependent with two pK's in the oxidized and one pK in the reduced form. Exchange of the acid labile sulfur in the iron

sulfur cluster for selenium only caused a small change in the redox potential [8]. No data on the temperature dependence were reported for this protein.

In this paper we describe a re-investigation of the redox properties of cytochrome P-450$_{cam}$ and *Pseudomonas putida* ferredoxin. Instead of the hitherto used optical methods here we employ for the first time direct electrochemistry as well as EPR-monitored equilibrium redox titrations on these proteins. The nature of the enzyme-electrode interaction will be discussed on the basis of the results obtained with the camphor-bound and the camphor-free enzyme.

2. Materials and Methods

Pseudomonas putida strain ATCC 17453 was obtained from the ATCC (USA). D-(+) camphor was obtained from Sigma. Maintenance and growth of the bacterium and purification of both the cytochrome P-450$_{cam}$ and the *Pseudomonas putida* ferredoxin were performed according to Gunsalus and Wagner with some minor modifications with respect to the column material used [10]. DEAE sepharose Fast-Flow (Pharmacia) was used as the anion exchange column and a MonoQ column (Pharmacia) was added to the purification scheme. The purity index (OD$_{392}$/OD$_{280}$) of the final preparation of the cytochrome was 0.84. The enzyme was made camphor-free according to the procedure described in [10]. Optical spectra of both forms of the enzyme were recorded with an Aminco DW-2000 spectrophotometer interfaced with an IBM PC. The spectra obtained for the two forms were similar to the spectra reported in [11].

Cyclic voltammetry was performed as described by Hagen using a BAS CV-27 potentiostat (BioAnalytical Systems, USA) connected to a X-Y recorder (Kipp & Zonen, NL) [12]. The preparation of the glassy carbon electrode for the electrochemistry with cytochrome P-450 followed the procedure described in [12]. The electrode used for the voltammetry of the ferredoxin was pretreated as described in [13]. Neomycin was added to the solution in a final concentration of 1 mM. All potentials were recalculated to the SHE. Temperature dependence of the midpoint potential was measured in an isothermal setup as described in [14]. The pH dependence of the midpoint potential was determined in 250 mM of a Goods' buffer of the appropriate pH. The buffers used were Mes, Bis-Tris, Mops, Tes, Taps, Ches, and Caps. Only the effect of the ionic strength on the potential was determined by addition of different amounts of KCl to the solution. In the other experiments no potassium was used since this cation has been reported to be a potent modulator of the spin state of the camphor-bound enzyme ([15] and refs. therein).

Redox titrations were performed as described by Pierik and Hagen in an anaerobic stirred cell with the bulk potential measured at a Radiometer P-1312 platinum electrode with respect to the potential of a Radiometer K-401 saturated calomel electrode [16]. EPR spectra

were taken using a Bruker ER-200 D spectrometer equipped with data acquisition facilities and cryogenics as described in [16]. The reductive titration was performed by adding small aliquots of dithionite buffered in 0.5 M Hepes pH 7.5. For the camphor-bound protein the degree of reduction was monitored on the decrease of the relative intensity of the S=5/2 peak at g=7.78 in the ferric EPR spectrum. For the camphor-free enzyme the intensity of the g=2.41 feature (S=1/2) was used. Reversibility of the titration was checked by reoxidation of the reduced protein with ferricyanide and air. During the titration the ratio of the low spin signal over the high spin signal remained constant indicating that the spin equilibrium of the heme iron did not change.

3. Results and Discussion

3.1. Cyclic voltammetry

The cyclic voltammetry of camphor-free as well as camphor-bound cytochrome P-450 results in well defined voltammograms as shown in fig. 1.
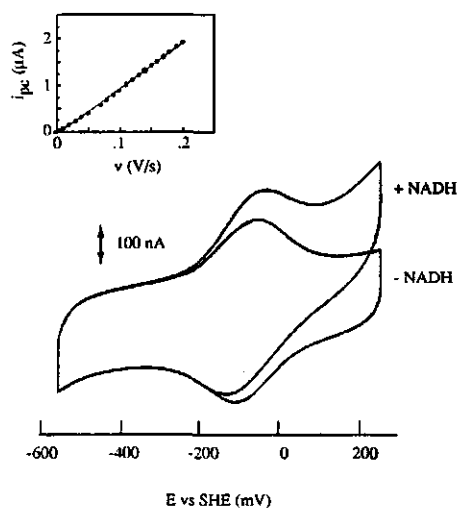
Figure 1: Cyclic voltammogram of 0.8 mg/ml camphor-free cytochrome P-450 from *Pseudomonas putida* in the absence (lower trace) and presence (upper trace) of NADH and cell-free extract. Voltammograms were taken after 15 minutes cycling at a scan rate of 20 mV/s. Conditions: working/ counter/ reference electrodes, glassy carbon/ platinum/ saturated calomel; scan rate 20 mV/s; temperature 23 °C. The potential axis is defined versus the saturated hydrogen electrode. The inset shows the scan rate dependence of the cathodic peak current (i_{pc}) between 2 and 200 mV/s.

The shape of the voltammograms for the two forms of the enzyme is identical. The only difference is the rate at which the peaks in the voltammogram develop. The peak current in the voltammogram for the camphor-free protein develops to maximal value in approximately 15 minutes compared to 30 minutes needed for the camphor-bound protein. The scan rate dependence of the peak current for this voltammogram is also shown in fig 1. The linearity between the scan rate and the peak current clearly indicates that the cytochrome is adsorbed onto the electrode surface. Apparently the adsorption of the enzyme did not cause inactivation as was obvious from the effect of adding a small amount of cell-free extract and NADH. In the presence of these components an increase of the anodic peak current was observed indicating a catalytic re-reduction of the cytochrome (fig. 1). The addition of camphor in a separate experiment did not cause any change of the voltammogram.

The peak to peak distance ΔE, as obtained from the voltammogram in fig. 1, is 41 mV. This is considerably higher than the theoretically value of 0 mV expected for an adsorbed species [17]. No significant change of ΔE is observed in the potential scan range between 2 and 200 mV/s. This indicates that the deviation of ΔE is not caused by changes in the coordination of the redox center upon reduction [18,19].

The similar results obtained for the camphor-bound and the camphor-free enzyme suggest that the heme in both forms is in a comparable environment during the electrochemical experiment. It has previously been reported that the redox potential of this cytochrome is very sensitive to the ligand field of the heme iron. Differences of 130 mV between the redox potentials of the enzyme in the absence and presence of substrate were observed [4]. The different rates of adsorption and the equal redox potential suggest that the electrode competes with the substrate and that the enzyme can only adsorb onto the electrode in its camphor-free form.

The midpoint potential of the enzyme as obtained from the voltammogram is -85 mV vs. SHE at pH 7.5. This value is considerably more positive than the value of -303 mV vs. SHE reported for the substrate-free enzyme [4] and also more positive than the value of -170 mV reported for the substrate-bound enzyme [3,4]. These substantial differences might be a consequence of the adsorption of the enzyme onto the electrode. In order to check this we performed EPR monitored redox titrations of cytochrome P-450 in homogeneous solution in both the substrate-bound as well as the substrate-free form.

3.2. EPR redoxtitration

The EPR spectrum of cytochrome P-450 plus camphor (fig. 2A) is essentially identical to that previously reported [20]. The ferric heme in the camphor-bound enzyme is high spin and has an effective g-tensor 7.78;3.97;1.78, which corresponds well with the predicted tensor of

7.79;3.97;1.78 for the $|\pm 1/2>$ doublet of an S = 5/2 system with real g-value 2.00 and rhombicity E/D 0.085. The ferric heme in the camphor-free enzyme is low-spin, S = 1/2, and has a g-tensor 2.41;2.23;1.91. As previously reported by Tsai et al. [20] we also observe a sharp, negative feature at g = 1.97 of unknown origin.
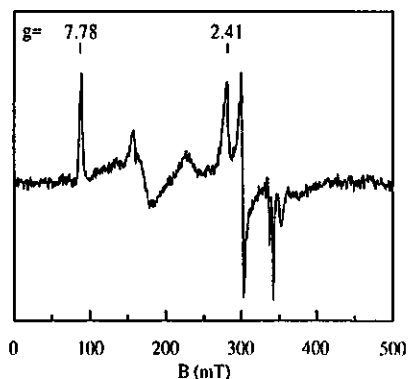
A   B

Figure 2: (A) EPR spectrum of 0.8 mg/ml camphor-bound cytochrome P-450$_{cam}$ from *Pseudomonas putida* . EPR conditions: microwave frequency, 9311.2 MHz; microwave power, 5 mW; modulation amplitude, 1.25 mT, modulation frequency, 100 kHz; temperature, 17 K. (B) EPR-monitored redox titration of camphor-free (o) and camphor-bound ($\bullet$) cytochrome P-450$_{cam}$. The camphor-free enzyme was monito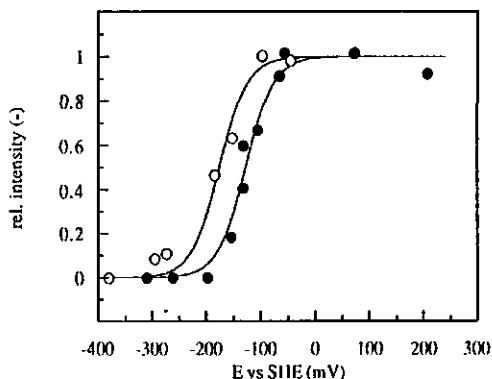red at g= 2.41 with a microwave power of 4.8 mW at a temperature of 23 K. The camphor-bound enzyme was monitored at g= 7.78 with a microwave power of 200 mW; at a temperature of 12 K. The solid lines are fits of the data points to the Nernst equation (n=1).

The result of an EPR monitored redox titration of cytochrome P-450 is presented in fig. 2B. The solid lines in the figure are Nernst curves (n=1) fitted to the data points. From these fits we obtain a value of -127 mV vs. SHE for the camphor-bound and -173 mV vs. SHE for the camphor-free protein. The reversibility of the reduction was checked with ferricyanide but the intensity of the g=7.78 signal after reoxidation indicated that only 40% of the original intensity was recovered. It proved necessary to leave the sample overnight at 0 °C in air in order to recover 80 % of the original intensity of the high spin signal. The value obtained from our redox titration for the substrate-bound enzyme is similar to the potential of -128 mV vs. SHE determined by Huang et al. from a dye-mediated optical titration [5]. However, these authors mentioned that this value was affected by the mediating dye. They postulated that the dye potential had changed upon non-specific binding to the protein with a subsequent effect on the

calibration of the potential axis. This explanation certainly does not hold for the results obtained by us, since in our experiments the solution potential was measured with two electrodes as described in the Materials and Methods section.

3.3. pH dependence

The pH dependence of the midpoint potential of cytochrome P-450, studied with cyclic voltammetry, resulted in a close-to linear dependence of the potential on the pH between pH 5.5 and 10.5 as shown in fig. 3A. However, a linear dependence is not likely since the slope of the line would become -44 mV/pH unit. The theoretically expected value for such a slope in an one-electron transfer process is a multiple of 58.8 mV/pH (=2.3RT/F) dependent on the number of protons involved. From the crystal structure of the camphor-free protein it is known that both a cysteine and a water molecule are coordinated to the heme iron. These ligands can be involved in the redox process. Therefore, the data were fitted with two pK values using the equation:

$$E_m = E_s + (RT/F) \cdot \ln\{([H^+]^2 + K_{red} \cdot [H^+])/(K_{red} \cdot K_{ox} + K_{red} \cdot [H^+])\}$$

E_s is the potential at $[H^+] = \sqrt{(K_{ox} \cdot K_{red})}$, the other symbols have their usual meaning. In this equation it is assumed that one of the pK values is associated with the oxidized form (K_{ox}) and one with the reduced form (K_{red}) of the protein. The solid line in fig. 3A is a least squares fit of this equation to the data points, resulting in an E_s of -121.8 mV, pK_{ox} = 8.40 and pK_{red} = 7.31. These values can be explained in terms of deprotonation of the ligands to the heme iron. The pK_{ox} is presumably caused by a water molecule coordinated to the oxidized heme iron. The pK_{red} can be assigned to the cysteine in the reduced protein. A similar pK value was obtained from the MCD studies on hemoprotein H-450 from rat liver. The active site of this protein, like cytochrome P-450, consists of a heme in which the iron is coordinated by a cysteinate sulfur. In the ferrous, but not in the ferric form of the protein this ligand can be titrated with a pK of approximately 7 [21].

3.4. Temperature and ionic strength dependence of the midpoint potential

The temperature dependence of the midpoint potential of cytochrome P-450 is shown in fig. 3B. The curve has a breakpoint at a temperature of 20.2 °C. This transition temperature indicates a change in the entropy value of the redox reaction and probably represents a conformational change [22]. The slope of the curve is -0.48 mV·K^{-1} below the transition temperature and -1.05 mV·K^{-1} above this value. With these parameters we can determine the

standard entropy change of the reduction $\Delta S^{\circ\prime}$ to be -46 J·mol^{-1}·K^{-1} and -101 J·mol^{-1}·K^{-1}, respectively. Some data on the temperature dependence of the redox potential of substrate bound cytochrome P-450 have been reported before by Huang et al. [5]. These authors also observed a biphasic dependence of the midpoint potential on the temperature with slopes comparable to the results described here. However, their transition temperature is shifted approximately 10 °C. Unfortunately, it is not clear whether or not these data can be used for comparison since our results are obtained with substrate free enzyme.
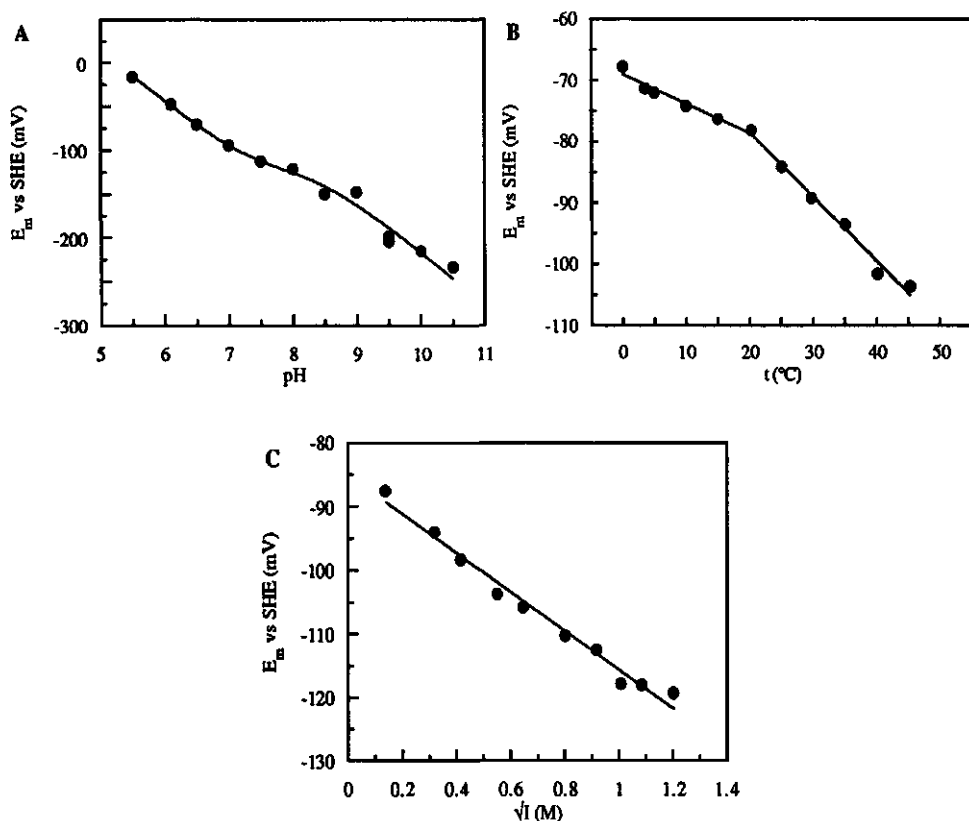
Figure 3: (A) pH dependence of the midpoint potential of cytochrome P-450$_{cam}$. Data were recorded using 200 mM buffer of the appropriate pH. The curve is a least squares fit to the data points using pK$_{ox}$ = 8.40 and pK$_{red}$ = 7.31. (B) Temperature dependence of the midpoint potential of cytochrome P-450$_{cam}$. The electrochemical cell was immersed in a water bath and voltammograms were recorded at different temperatures. Mops (50 mM, pH 7.5) was used as the buffer. (C) Ionic strength dependence of the midpoint potential of cytochrome P-450$_{cam}$. Increasing amounts of KCl were added to the protein in 50 mM Mops pH 7.5. The protein concentration in the experiments was 0.8 mg/ml. Cyclic voltammograms were taken at t = 23 °C between 0 and -800 mV versus the SCE at a scan rate of 20 mV/s.

The differences in the observed redox potentials from the cyclic voltammetry experiments and the equilibrium redox titrations remain puzzling. The potential shift may well be due to a difference in the ionic strength of the buffer used in the two studies. In order to quantitate such an effect we measured the ionic strength dependence of the redox potential. The midpoint potential of cytochrome P-450 is linearly dependent on the square root of the ionic strength as is shown in fig 3C. The solid line is a linear fit to the data points resulting in a slope of -30.6 mV$\cdot$M$^{-1/2}$. This relationship enables us to recalculate our data and compare them to the values obtained from the EPR-monitored redox titration. Doing so we find a value for the midpoint potential of -95 mV vs. SHE at pH 7.5, 25 °C and I= 0.1 M. This potential is approximately 30 mV more positive than the value obtained for the camphor-bound enzyme in the EPR monitored redox titration and 80 mV more positive than the value for the camphor-free enzyme.

3.5. Cyclic voltammetry of the ferredoxin

The voltammetry of the *Pseudomonas putida* ferredoxin was studied using a glassy carbon electrode modified with neomycin. In this way it is possible to obtain reversible voltammograms as shown in fig. 4.
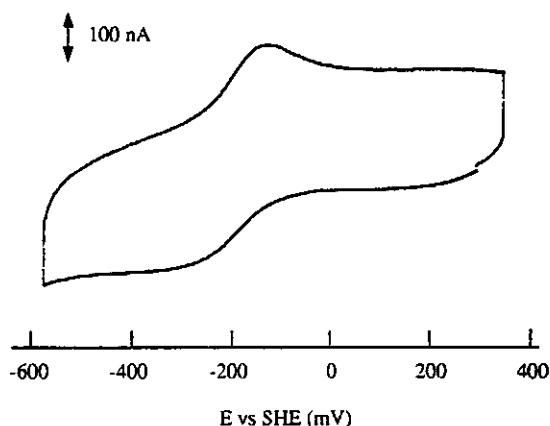
Figure 4: Cyclic voltammogram of 3.4 mg/ml *Pseudomonas putida* ferredoxin in 50 mM Tris HCl pH 7.4 and 100 mM KCl. After one scan neomycin was added to the solution in a final concentration of 1 mM. Cyclic voltammograms were taken at t = 23 °C between 0 and -800 mV versus the SCE at a scan rate of 20 mV/s. Conditions: working/ counter/ reference electrodes, glassy carbon/ platinum/ saturated calomel.

65

The intensity of the cathodic peak decreases upon continuous cycling. The intensity of the anodic peak remains constant. Determination of the midpoint potential at pH 7.5 and 25 °C resulted in a value of -170 mV vs. SHE. This potential is considerably higher than the reported values of -241 mV [8], -233 mV [9], and -239 mV vs. SHE [3]. These latter potentials were all determined with optical titrations. There is no obvious explanation for this difference of 70 mV between our value and the reported ones. An effect caused by adsorption does not seem to be very likely since the voltammograms are diffusion controlled. This rules out the possibility that the potential is shifted in a similar way as was reported to occur upon binding of this ferredoxin to cytochrome P-450$_{cam}$ [3]. The midpoint potential studied by us with cyclic voltammetry is temperature dependent with a slope of -1.86 mV$\cdot$K^{-1}.

The midpoint potential of *P. putida* ferredoxin has been reported previously, to be pH dependent in the range from pH 6.5 to pH 10.0. Two pK's were assigned to the oxidized and one pK to the reduced form [8]. In our hands, however, the midpoint potential remains unchanged from pH 5.5 to pH 9.0. This pH independence is not surprising since *P. putida* ferredoxin has been classified as a 'plant type' ferredoxin in which the [2Fe-2S] cluster is coordinated by 4 cysteines [1]. So far, only the midpoint potential of Rieske type [2Fe-2S] clusters have been reported to be affected by the pH due to deprotonation of one of the putative histidine ligands of the cluster [14]. An all cysteine coordinated [2Fe-2S] cluster, like the one in spinach ferredoxin, does not show any pH dependence in the range between pH 5.5 and 10 (our unpublished results). Considering the similarities between the spinach ferredoxin and the *P. putida* ferredoxin the latter is also not expected to have a pH dependent midpoint potential.

4. Conclusions

This work indicates the possibility to study a medium sized enzyme like cytochrome P-450$_{cam}$ with electrochemical techniques using a bare glassy carbon electrode. With these techniques it is possible to obtain detailed information about pH dependence, temperature dependence and ionic strength dependence of the reduction process. The interpretation of these data for substrate-free cytochrome P-450$_{cam}$ is, however, not completely straightforward. The temperature dependence of the midpoint potential obtained by us for this enzyme is different from the previously reported data for the substrate-bound enzyme [5]. Furthermore, the pH dependence indicates that two ionizable groups are linked to the redox state of the heme iron. We hypothesized that this pH dependence was caused by protonation and deprotonation of a cysteine and a water molecule, both ligands to the heme iron in the substrate-free enzyme. From the crystal structure it is known that the water ligand disappears upon binding of camphor [2]. Our assignment of one of the pK values to a water molecule indicates that adsorption of the enzyme to the electrode does not displace the water ligand. Therefore, it is expected that the

adsorbed enzyme resembles the substrate-free cytochrome. However, the electrochemically determined redox potential is significantly more positive than the value obtained for the substrate free enzyme in the EPR monitored redox titration. It seems unlikely that this difference is caused by a change of the spin state of the iron due to the adsorption of the enzyme to the electrode. Although a change from low spin to high spin has been reported to raise the redox potential of the cytochrome, it is expected that the value of -127 mV vs. SHE, obtained for the substrate bound, high spin form of the enzyme, serves as an upper limit [4]. The value determined with cyclic voltammetry is above this limit and, therefore, we suggest that the shift in the redox potential is not a consequence of spin state changes but rather due to intermolecular interactions between the adsorbed molecules as has been reported earlier [23].

The adsorption of the protein onto the electrode, as observed in the cyclic voltammetry experiments, apparently does not cause denaturation of the protein. Upon addition of NADH and cell-free extract a catalytic current develops, which indicates that the enzyme is still capable of accepting electrons from its ferredoxin. Unfortunately, it is not possible to monitor the physiological hydroxylation of camphor in the electrochemical cell since this reaction requires oxygen. The presence of oxygen will give rise to a strong reduction current thus disturbing the electrochemical measurements. The uncertainties about the state of the adsorbed cytochrome might be elucidated using a spectroelectrochemical cell. Such a cell enables the synchronous monitoring of redox properties and e.g. the spin state of the heme iron. In this way it will be possible to study the exact nature of the interactions between the enzyme and the electrode.

The values for the midpoint potential obtained by us for the substrate bound cytochrome and the ferredoxin are positively shifted by equal amounts with respect to the literature values. The difference in potential between the two proteins and, therefore, the driving force in their physiological reaction remain unchanged. Even the hypothesized mechanistic significance of the spin state change between substrate-bound and substrate-free enzyme remains valid. It was suggested that the decrease of potential upon change of the spin state served to avoid reduction by the ferredoxin ([2] and refs. therein). Judged from the midpoint potential obtained by us for the substrate-free enzyme we can conclude that the reduction of this protein by the ferredoxin remains unfavourable.

References

1. Romeo, C., Gunsalus, I.C. & Yasunobo, K.T. (1991) in New Trends in Biological Chemistry, (Ozawa, T., ed.), Japan Sci. Soc. Press/Springer-Verlag, Tokyo/Berlin, pp 363-371.

2. Poulos, T.L., Finzel, B.C. & Howard, A.J. (1986), Biochemistry, 25, 5314-5322.

3. Sligar, S.G. & Gunsalus, I.C. (1976), Proc. Natl. Acad. Sci. U.S.A., 73, 1078-1082.

4. Fisher, M.T. & Sligar, S.G. (1985), J. Am. Chem. Soc., 107, 5018-5019.

5. Huang, Y-Y., Hara, T., Sligar, S., Coon, M. & Kimura, T. (1986), Biochemistry, 25, 1390-1394.

6. Koga, H., Sagara, Y., Yaoi, T., Tsujimura, M., Nakamura, K., Sekimizu, K., Makino, R., Shimada, H., Ishimura, Y., Yura, K., Go, M., Ikeguchi, M. & Horiuchi, T. (1993), FEBS Lett., 331, 109-113.

7. Nomenclature Committee. (1991), Eur. J. Biochem., 200, 599-611.

8. Wilson, G.S., Tsibris, J.C.M. & Gunsalus, I.C. (1973), J. Biol. Chem., 218, 6059-6061.

9. Davies, M.D., Qin, L., Beck, J.L., Suslick, K.S., Koga, H., Horiuchi, T. & Sligar, S.G. (1990), J. Am. Chem. Soc., 112, 7396-7398.

10. Gunsalus, I.C. & Wagner, G.C. (1978) in Methods in enzymology Vol. 52, (Fleischer, S. & Packer, L., eds.), Academic Press, New York, pp 166-188.

11. Sligar, S.G. (1976), Biochemistry, 15, 5399-5406.

12. Hagen, W.R. (1989), Eur. J. Biochem., 182, 523-530.

13. Verhagen, M.F.J.M., Voorhorst, W.G.B., Kolkman, J.A., Wolbert, R.B.G. & Hagen, W.R. (1993) FEBS Lett., 336, 13-18.

14. Link, T.A., Hagen, W.R., Pierik, A.J., Assmann, C. & von Jagow, G. (1992), Eur. J. Biochem., 208, 685-691.

15. Hui Bon Hoa, G., Di Primo, C., Geze, M., Douzou, P., Kornblatt, J.A. & Sligar, S.G. (1990), Biochemistry, 29, 6810-6815.

16. Pierik, A.J. & Hagen, W.R. (1991), Eur. J. Biochem., 195, 505-516.

17. Bard, A.J. & Faulkner, L. (1980) in Electrochemical methods; fundamentals and applications., J. Wiley & Sons, New York, pp 521-523.

18. Armstrong, F.A. (1992) in Advances in Inorganic Chemistry; vol. 38: Iron sulfur proteins, (Cammack, R. & Sykes, A. G., eds.), Academic Press, San Diego, pp 117-163.

19. Butt, J.N., Sucheta, A., Armstrong, F.A., Breton, J., Thomson, A.J. & Hatchikian, E.C. (1993), J. Am. Chem. Soc., 115, 1413-1421.

20. Tsai, R., Yu, C.A., Gunsalus, I.C., Peisach, J., Blumberg, W., Orme-Johnson, W.H. & Beinert, H. (1970), Proc. Nat. Acad. Sci. USA, 66, 1157-1163.

21. Svastits, E.W., Alberta, J.A., Kim, I.-C. & Dawson, J.H. (1989), Biochem. Biophys. Res. Commun., 165, 1170-1176.

22. Ikeshhoji, T., Taniguchi, I. & Hawkridge, F.M. (1989), J. Electroanal. Chem., 270, 297-308.

23. Brown, A.P. & Anson, F.C. (1977), Anal. Chem., 49, 1589-1595.

Chapter 6

On the reduction potentials of Fe and Cu-Zn containing Superoxide dismutases

Marc F.J.M. Verhagen, Elise T.M. Meussen and Wilfred R. Hagen

On the reduction potentials of Fe and Cu-Zn containing Superoxide dismutases.

Marc F.J.M. Verhagen, Elise T.M. Meussen, Wilfred R. Hagen

Abstract

The reduction potentials of bovine erythrocyte copper-zinc superoxide dismutase and *Escherichia coli* iron superoxide dismutase were determined in EPR monitored redox titrations in homogeneous solution. The copper zinc enzyme is reduced and reoxidized with a midpoint potential of +120 mV versus SHE at pH 7.5. The iron enzyme can be reduced with an apparent midpoint potential of -67 mV versus SHE at pH 7.5. However, reaction with ferricyanide affords only slow, partial re-oxidation. Cyclic voltammetry of the copper-zinc enzyme in the presence of 50 mM Sc^{3+} at pH 4.0 using a glassy carbon electrode results in asymmetric voltammograms. The midpoint potential of the enzyme at this pH value, calculated as the average of the anodic and cathodic peak potentials, is +400 mV versus SHE. The physiological relevance of this value is limited since EPR experiments indicated that reduction of the copper-zinc enzyme at pH 4.0 is not reversible. Consequences of the irreversible behavior of the two dismutases for the previously reported studies on their redox properties will be discussed.

Introduction

Superoxide dismutase is a metalloenzyme capable of catalyzing the disproportionation of two superoxide radicals. In this process one superoxide ion is oxidized to form oxygen while the other one is reduced and simultaneously takes up two protons to form hydrogen peroxide. The enzyme has been demonstrated to be present in both eukaryotes and prokaryotes and is believed to decrease the toxicity of reduced oxygen species ([1] and refs. therein). The presence of the enzyme is not restricted to aerobic organisms as is obvious from the purification of a superoxide dismutase from the strict anaerobic organism *Desulfovibrio desulfuricans* [2]. Based on the metal ion present in the active site of the enzyme three different types can be distinguished. Superoxide dismutases from prokaryotes contain either iron or manganese in their active site. The enzymes from eukaryotes either contain copper and zinc or manganese [1].

Conflicting reports have been published about the redox potential of the bovine erythrocyte copper-zinc superoxide dismutase. Values of +403 mV [3], +350 mV [4], +280 mV [4] and + 400 mV [5] versus SHE at pH 7.0 were determined using either coulometric titrations or visible spectroelectrochemical techniques. Cyclic voltammetry experiments with the copper-zinc enzyme at an unmodified gold disk electrode were performed by Iyer and Schmidt. They obtained an anodic peak in their voltammograms located at + 512 mV versus SHE at pH 4.0. The cathodic counter peak could not be observed and the response disappeared upon raising the pH to 5.0 [6]. Borsari and Azab used a gold electrode modified with 1,2-bis(4-pyridyl)-ethene in their cyclic voltammetry experiments and determined a midpoint potential of +320 mV versus SHE [7]. The voltammetric response was reported to be quasi reversible and to increase linearly with the square root of the scan rate and this lead to the conclusion that the electrode reaction was diffusion controlled. However, it proved necessary to use a rather large scan rate of 200 mV/s to obtain a reasonable response. Furthermore, the peak shape is significantly different from the theoretically expected one for a diffusion controlled process, which suggests that some adsorption has taken place. In a subsequent paper Azab et al. used cyclic voltammetry to measure the apparent midpoint potentials of different mutants of human superoxide dismutase and study the pH dependence of these potentials [8]. The midpoint potential of wild type human SOD was found to have a pK of 8.9. This pK value, which was assigned to a histidine residue, was corroborated in NMR experiments and, therefore, the authors concluded that it was possible to study the redox properties of Cu-Zn SOD with cyclic voltammetry. The authors emphasize, however, that the determined midpoint potentials have relative value; absoluteness is explicitly disclaimed [8].

From the different reports on the reduction potentials of superoxide dismutase it is often not possible to determine where the differences in these values originate. With some of the techniques used it is doubtful whether equilibrium conditions have been met. In some other experiments, especially the ones at low pH, it is uncertain if the enzyme is not denatured. In this paper we describe the results of EPR monitored redox titrations of Bovine erythrocyte CuZn

SOD and *E. coli* FeSOD. The use of EPR spectroscopy enabled us to monitor both the redox state and the coordination of the metal in the enzyme. In this way it was also possible to check the reversibility of the redox reaction. Activity measurements were performed during the titrations to monitor if the enzyme remained active. The results obtained from the EPR monitored redox titrations will be compared to the results obtained from cyclic voltammetry experiments with a glassy carbon electrode.

Materials and Methods

Bovine erythrocyte Cu-Zn SOD was obtained from Boehringer. The preparation showed one single band on SDS-PAGE. The purification of *Escherichia coli* Fe-SOD from *E coli* TG-2 cells essentially followed the procedure described in [9]. A MonoQ HR 5/5 column (Pharmacia) was added to the purification scheme. The protein was judged to be pure by SDS-PAGE. Activity measurements were performed according to the method of McCord and Fridovich using horse heart cytochrome *c* (Sigma, grade VI), xanthine (Merck) and xanthine oxidase (Boehringer) [10]. The reduction of the cytochrome was followed at 553 nm with a Zeiss M4 QIII spectrophotometer connected to a y-t recorder. Cyclic voltammetry was performed as described in [11] using a BAS CV 27 potentiostat (Bioanalytical systems, USA) connected to a x-y recorder (Kipp & Zonen, NL). Redox titrations were performed in 50 mM Hepes in the presence of thirteen mediators at 22 °C as described by Pierik and Hagen [12]. A K-401 saturated calomel electrode (Radiometer) and a P-1312 platinum wire electrode (Radiometer) were used in combination with a digital Voltmeter (Fluke) to calibrate the potential axis. All potentials were recalculated with respect to the saturated hydrogen electrode(SHE) by using a potential of +243 mV vs. SHE for the calomel electrode at 22 °C [13]. EPR spectra were taken using a Bruker ER-200 D spectrometer equipped with data acquisition facilities and cryogenics as described in [12].The reductive titration was performed by adding small aliquots of freshly prepared dithionite buffered in 0.5 M Hepes pH 7.5. Reversibility of the titration was checked by oxidation of the reduced protein with ferricyanide or oxygen.

Results and discussion

Redox titration of bovine erythrocyte CuZn SOD

The result of the equilibrium redox titration of CuZn SOD in homogeneous solution is presented in fig. 1. The reduction of the copper ion bounded to the protein was monitored using the EPR intensity of the low-field copper hyperfine line. This reduction was reversible since the reoxidation of the protein with ferricyanide resulted in the reappearance of the EPR spectrum.

No changes in this spectrum could be observed indicating that the coordination of the copper in the active site had not changed. The obtained data points were fitted with a Nernst curve (n=1) and this resulted in a midpoint potential of +120 mV versus SHE.
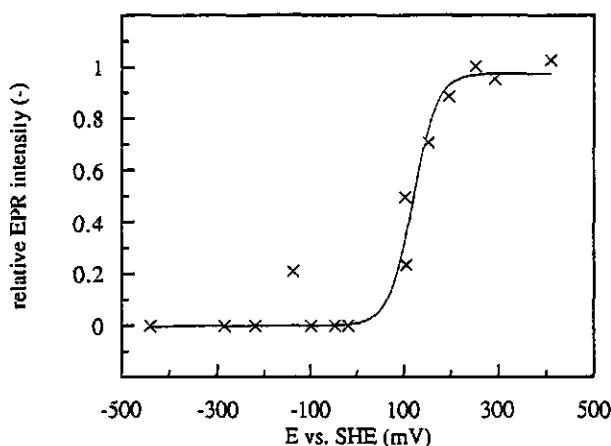
Figure 1: Redox titration of bovine erythrocyte Cu-Zn SOD. The reduction state of the enzyme was monitored from the intensity of the low-field copper hyperfine line with a microwave power of 32 mW and a temperature of 119 K. The solid line is a least squares fit of the Nernst equation (n=1) to the data points.

The midpoint potential calculated from the redox titration is considerably lower than the values of +280 to +400 mV versus SHE reported so far for this enzyme. A possible origin for this discrepancy might be that in a number of previous studies ferricyanide and ferrocyanide were used without mediators to titrate the enzyme. It has been reported, however, that this redox couple is in slow equilibrium with proteins [3]. Therefore, the criterion of reversibility should be checked carefully in order to detect problems with the equilibrium. Fee and Dicorletto used ferrocyanide to reduce Cu-Zn SOD, and only the reduction reaction was reported [5]. The measurements were performed in the presence of oxygen and although the authors mention that the SOD is not autooxidizable, the ferrocyanide certainly is. This might cause a problem since the ferro/ferricyanide couple is used to calibrate the potential axis. When the equilibrium between the enzyme and the ferri/ferrocyanide couple is slow compared to the oxidation rate of the ferrocyanide by oxygen the potential axis will apparently shift to more positive values.

Another example is the spectroelectrochemical titration of bovine erythrocyte Cu-Zn SOD reported by Strong St. Clair et al. These authors used ferricyanide as the mediator and poised the potential of the solution with a potentiostat using a gold electrode. Only a reductive titration was presented and again no reoxidation was performed to show the reversibility of the

76

reaction. However, it was mentioned that Cu-Zn SOD could be reduced with $Ru(NH_3)_5(py)$ which has a midpoint potential of +260 mV versus SHE. The reduction of the enzyme by this compound is of course only possible when the midpoint potential of the protein is above the value of the ruthenium compound. In view of the midpoint potential of Cu-Zn SOD obtained by us it should have been impossible to reduce the protein with this compound. Remarkably, more than 4 hours were necessary to reduce the Cu-Zn SOD with the Ru(II) compound. Checks on the stability of the compounds over these long-time periods were not reported [3].

Electrochemistry of bovine erythrocyte CuZn SOD

Cyclic voltammetry of Cu-Zn SOD at a bare glassy carbon electrode did not result in any detectable voltammograms. Several ions were, therefore, checked to find out if they could function as promotors for SOD electrochemistry. The function of such a promotor has been postulated to be one of charge compensation ([14] and refs. therein). Scandium, Calcium, Terbium and Magnesium constitute a set of ions with different properties with respect to charge and complex formation. Ca^{2+} and Tb^{3+} have flexible coordination (*i.e.* variable bond length and angle); typical coordination numbers are 7 and 9, respectively. Mg^{2+} and Sc^{3+} both have a rigid coordination and an invariable coordination number of 6 but they differ in their valence. The use of these elements in several concentrations at different pH values allows for a quick screening of conditions possibly favourable for protein electrochemistry. Cyclic voltammograms of CuZn SOD could only be obtained in the presence of 50 mM Sc^{3+}. An additional prerequisite for the development of a voltammogram was a solution pH of about 4.0. Under these conditions a voltammogram develops in approximately fifty minutes continuous cycling. The result is shown in fig 2A. The voltammogram is always asymmetric and the anodic peak current, after full development of the voltammogram, does not show linear dependence with either the scan rate or the square root of this value (fig. 2B). The deviation from linearity with the scan rate suggests that the voltammetry is diffusion controlled. However, the non-linear dependence of the anodic peak current on the square root of the scan rate indicates that there are some kinetic limitations in the electron transfer between the enzyme and the electrode [13].

The requirement of a low pH to make electron transfer between the enzyme and an electrode possible was reported earlier by Iyer and Schmidt [6]. As mentioned before their voltammograms only showed a pronounced anodic peak while the cathodic peak was absent. The voltammograms obtained by us are also asymmetric, however, the cathodic peak is now detectable. The asymmetry of the peaks and the non-linear dependence of the peak current on the square root of the scan rate, as observed in these voltammograms, might be due to extreme values for the transfer coefficient (cf. [15]). The uncertainty about this value makes it difficult to

interpret the rather large peak to peak distance of 150 mV, however, this distance does not reflect irreversibility because it is independent of the potential scan rate.
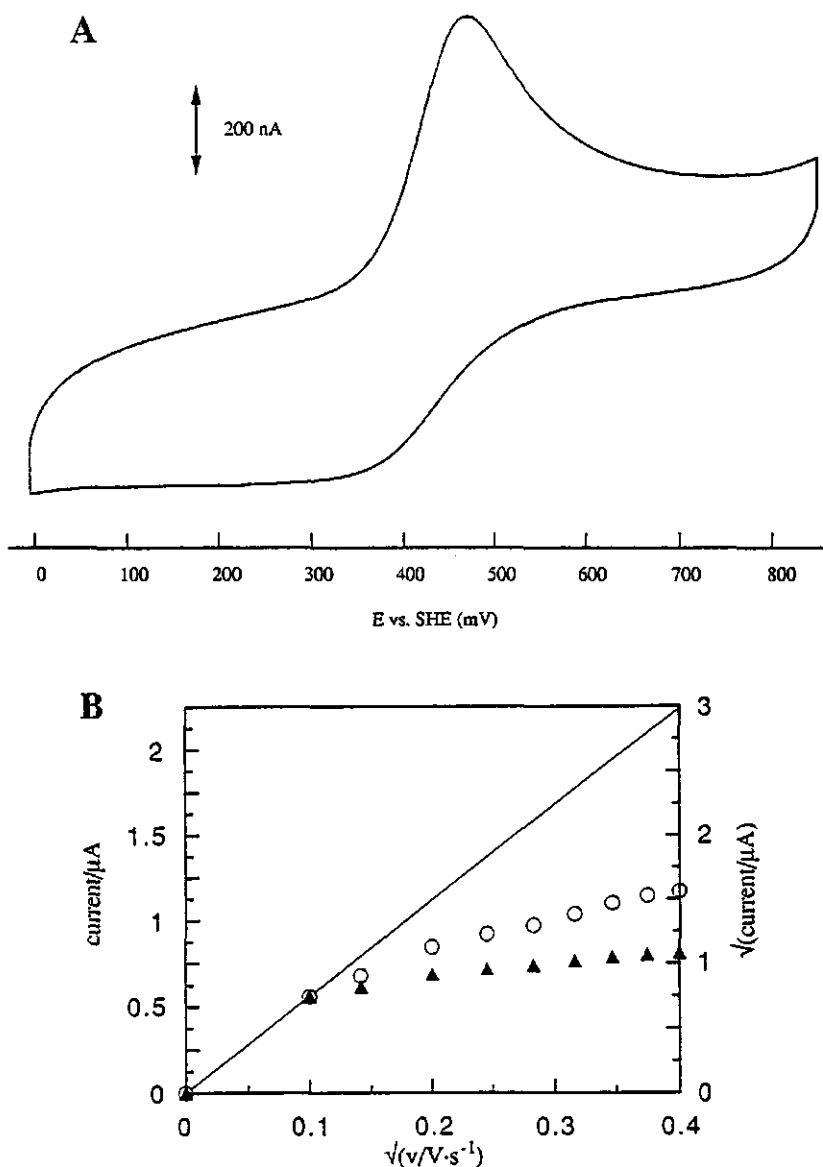
Figure 2: (A) Cyclic voltammogram of 2 mg/ml CuZn SOD in 50 mM NaAc buffer pH 4.0 containing 50 mM Sc^{3+}. Voltammograms were recorded at a scan rate of 10 mV/s. Conditions: working/counter/reference electrodes, glassy carbon/ platinum/ saturated calomel. The area of working electrode is 0.2 cm^2. (B) Scan rate dependence of the anodic peak current. ▲ – i/μA, ○ – $\sqrt{(i/μA)}$. Linear dependence is for both data sets represented by the solid line.

An estimate of the midpoint potential was made by taking the average of the anodic and cathodic peak potentials. This resulted in a value of +400 mV vs. SHE at pH 4.0. It is obvious that this pH value, necessary to study the enzyme using a solid electrode, is rather extreme. Since it has been argued that the protein can lose its metals at pH values below 4.0 the question is raised if the result has any physiological significance [1]. Both activity measurements as well as an EPR monitored redox titration at pH 4.0 were used to answer this question. The activity of the enzyme after the electrochemical experiment, measured at pH 7.5 in the cytochrome *c* reduction assay, was identical to the activity of the enzyme before the experiment. The effect of scandium on the activity measurements, determined in a separate experiment, was found to be nil. Contrarily, the redox titration of the protein in 50 mM NaAc pH 4.0 indicated that the reduction was non-reversible. Reduction of the protein took place with an apparent potential of +304 mV versus SHE (data not shown). Reoxidation did not result in a reappearance of the copper EPR spectrum and this indicates that the protein does not remain in its native conformation. From the shift of 180 mV over 3.5 pH units a slope of 51 mV/pH can be calculated. This value is somewhat smaller than the value of 59 mV/pH expected when the transfer of one electron coincides with the transfer of one proton. It is, however, comparable to the value reported by Azab et al. for the slope of the redox potential of bovine erythrocyte Cu-Zn SOD in the range between pH 5.0 and 7.5.

The absence of reversible behavior in homogeneous redox titrations at pH 4.0 provides a reason to question the physiological significance of the results obtained with cyclic voltammetry at the same pH. Therefore, the detailed interpretation of the electrochemical results by Iyer and Schmidt in terms of coordination of the enzyme to the electrode is, in our opinion, premature [6].

Redox titration of E. coli Fe-SOD

The purified Fe-SOD from *Escherichia coli* had a specific activity of 8300 U/mg and its EPR spectrum integrated to 0.8 Fe per monomer. The protein was titrated at pH 7.5 in a similar way as the CuZn SOD. The result of this EPR-monitored titration is presented in fig. 3. From this figure it is obvious that several problems are encountered when performing a redox titration of Fe-SOD. First of all it was not possible to fit the data with a Nernst curve with n=1. A least squares fit of the data points using an adjustable n-value results in n=0.3. Such a value for the number of electrons can be due to co-operation between redox centers (SOD is a homodimer). The reduction of the first iron center then affects the potential of the second iron. However, redox interaction has not been reported for Fe-SOD. Slow equilibrium between the reductant and the protein is not an alternative explanation. During the titration, samples were only drawn after the potential drift was levelled off. A stable potential, indicating equilibrium, was obtained typically five to ten minutes after addition of the titrant. Furthermore, the time intervals between addition of the titrant and drawing of the sample were varied in three successive titrations. The

identical behaviour of the protein in these different titrations also indicates that the conditions for redox equilibrium were met.

A second problem was encountered with the reoxidation of the enzyme. Both ferricyanide and oxygen were used but the EPR signal only reappeared for approximately 30 %. This did not improve during overnight incubation at 0 °C with ferricyanide in air. The reason for this is not clear. Denaturation of the protein does not seem very likely. Activity measurements of the EPR samples indicated no loss of activity during the titration. Furthermore, if the reduced iron is no longer coordinated in the active site it will loose its specific EPR properties and upon oxidation an isotropic g=4.3 signal will appear in the EPR spectrum due to the aspecifically bound iron. Since this is not observed we conclude that approximately 70 % of the iron in *E. coli* Fe-SOD remains reduced during the oxidative titration.
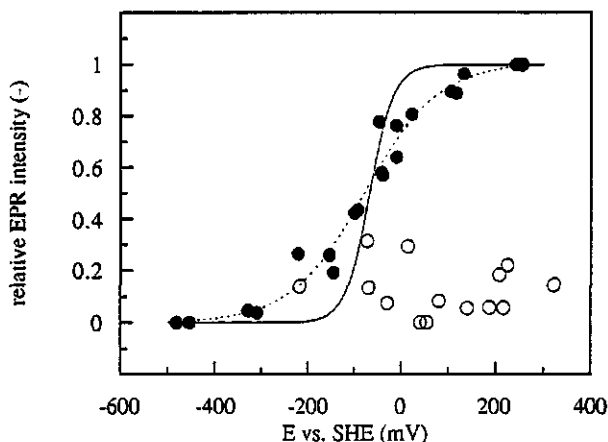
Figure 3: Redox titration of *E. coli* Fe SOD. The reduction was monitored from the intensity of the peak at g = 4.85 with a microwave power of 80 mW and a temperature of 17 K. ● reductive titration points; ○ oxidative titration points. The solid line is a least squares fit of a Nernst curve (n=1) to the data points. The dashed line is a fit of the Nernst equation using n=0.3.

Application of the Nernst equation with n=1 results in an apparent potential of -67 mV versus SHE. This is considerably lower than the average value of +255 mV vs. SHE reported by Barrette et al. for this enzyme [16]. In their paper these authors also determined the midpoint potentials of the Fe superoxide dismutases from two other bacteria including *Azotobacter vinelandii* . The enzymes were all found to have comparable potentials with an average value of +270 mV versus SHE. The high potential value raised the question how it was possible to

monitor the EPR signals of both the oxidised Fe-SOD and the reduced Iron Molybdenum (FeMo) cofactor in nitrogenase in whole cells of *Azotobacter vinelandii* [16,17]. For component I of *A. vinelandii* nitrogenase a midpoint potential of -42 mV vs. SHE has been reported for the FeMo cofactor [18]. The simultaneous detection of the FeSOD and the nitrogenase cofactor, therefore, suggests that the reduction potential of FeSOD is restricted to a potential value below -40 mV vs. SHE.

Conclusions

The equilibrium reduction potential for the Cu (II)/ Cu (I) transition in bovine erythrocyte Cu-Zn SOD is +0.12 V (pH 7.5; temperature, 22°C; ionic strength, ≈ 0.2 M). The potential for the Fe (III) / Fe (II) couple in *E. coli* SOD has not been established; the redox reaction is not reversible. The apparent reduction potential is -0.07 V.

In all previously reported determinations of "reduction potentials" for superoxide dismutases equilibrium conditions have not been met and/or established. Our work on Fe SOD indicates that this enzyme is not in equilibrium with the often used mediators. The literature values on the reduction potential of this enzyme are, therefore, not reliable.

The characterization of the redox properties of small, electron-transferring proteins (e.g., cytochromes, ferredoxins) with electrochemical techniques has become a well-established, reliable method (e.g. [19]). Contrarily, direct electrochemistry of enzymes has generally proved elusive. The present work on Cu-Zn SOD illustrates that electrochemical measurements may not give the same information as homogeneous equilibrium titrations and, therefore, should never be interpreted without comparison to independent data.

Acknowledgements

References

1. Cass, A.E.G. (1985) in Metalloproteins. Part 1: Metal proteins with redox roles (Harrison, P. M., ed.), Verlag Chemie, Weinheim; Basel, pp 121-156.
2. Hatchikian, E.C. & Henry, Y.A. (1977), Biochimie, 59, 153-161.
3. Strong St. Clair, C., Gray, H.B. & Selverstone Valentine, J. (1992), Inorg. Chem., 31, 925-927.
4. Lawrence, G.D. & Sawyer, D.T. (1979), Biochemistry, 18, 3045-3050.
5. Fee , J.A. & DiCorletto. (1973), Biochemistry, 12, 4893-4899.
6. Iyer, R.N. & Schmidt, W.E. (1992), Bioelectrochem. Bioenerg., 27, 393-404.
7. Borsari, M. & Azab, H.A. (1992), Bioelectrochem. Bioenerg., 27, 229-233.
8. Azab, H.A., Banci, L., Borsari, M., Luchinat, C., Sola, M. & Viezzoli, M.S. (1992), Inorg. Chem., 31, 4649-4655.
9. Slykhouse, T.O. & Fee, J.A. (1976), J. Biol. Chem., 251, 5472-5477.
10. McCord, J.M. & Fridovich, I. (1969), J. Biol. Chem., 244, 6049-6055.
11. Hagen, W.R. (1989), Eur. J. Biochem., 182, 523-530.
12. Pierik, A.J. & Hagen, W.R. (1991), Eur. J. Biochem., 195, 505-516.
13. Bard, A.J. & Faulkner, L. (1980) Electrochemical methods; fundamentals and applications., J. Wiley & Sons, New York.
14. Datta, D., Hill, H.A.O. & Nakayama, H. (1992), J. Electroanal. Chem., 324, 307-323.
15. Lasia, A. (1989), J. Electroanal. Chem., 260, 221-226.
16. Barrette, W.C., Jr, Sawyer, D.T., Fee, J.A. & Asada, K. (1983), Biochemistry, 22, 624-627.
17. Shah, V.K., Davis, L.C., Gordon, J.K., Orme-Johnson, W.H. & Brill, W.J. (1973), Biochim. Biophys. Acta, 292, 246-.
18. Pierik, A.J., Wassink, H., Haaker, H. & Hagen, W.R. (1993), Eur. J. Biochem., 212, 51-61.
19. Armstrong, F.A. (1990), Structure and Bonding, 72, 137-221.

Chapter 7

Redox properties of rubredoxin from *Megasphaera elsdenii* studied at a glassy carbon electrode in the presence of Europium

Marc F.J.M. Verhagen and Wilfred R. Hagen

Redox properties of rubredoxin from *Megasphaera elsdenii* studied at a glassy carbon electrode in the presence of europium.

Marc F.J.M. Verhagen and Wilfred R. Hagen

Abstract

The redox properties of rubredoxin from *Megasphaera elsdenii* were studied with cyclic voltammetry using a glassy carbon electrode. Quasi reversible voltammograms were obtained in the presence of 1 mM $Eu(Cl)_3$ although other lanthanides also served as promotors of rubredoxin electrochemistry. The midpoint potential for rubredoxin as determined from the voltammograms was found to be +37 mV vs. SHE and independent of the pH between pH 5.5 and 9.5. The electrochemistry of europium was studied in separate experiments. Cyclic voltammetry of the aqueous ion resulted in well defined voltammograms at the bare glassy carbon electrode. The midpoint potential of the Eu (III/II) redoxcouple was found to be -398 mV vs. SHE and independent of the pH. However, the peak current of the voltammograms was pH dependent indicating a pK value of 7. It is proposed that this pK value is associated with the hydrolysis of one of the water ligands of the first coordination shell. Although the europium ion does not show an electrochemical response at pH values above this pK it still functions as a promotor, judged from the unaltered peak current of rubredoxin in the pH interval studied. The implications of these results on the commonly used models for the promotor function of cations, e.g. charge compensation and complex formation, will be discussed.

Introduction

Rubredoxins are small iron-sulfur proteins containing one redox active iron atom and no acid-labile sulfur. Rubredoxins are found in anaerobic bacteria in which they are believed to be involved in electron transfer. However, their precise role in the metabolism of these bacteria remains to be established. The amino acid composition and the gene sequence of several rubredoxins has been determined [1-5] . Furthermore, the crystal structure from e.g. *D. vulgaris* rubredoxin has been solved to a resolution of 1.5 Å [6]. The structure indicates that the iron atom is in the center of a distorted tetrahedron and is directly coordinated to four thiolate ligands from cysteine residues. The coordination of the iron changes only slightly upon reduction or oxidation. Redox potentials have been determined for this protein from several species. The potential of rubredoxin from e.g. *Clostridium pasteurianum* was determined with optical spectroscopy and a value of -60 mV vs. SHE was obtained at pH 7.0 [7]. The potential of *Desulfovibrio gigas* rubredoxin was found to be +6 mV vs. SHE at pH 8.4 in an EPR monitored redox titration [8].

Some reports were presented on the electrochemistry of rubredoxins on solid state electrodes. Moreno et al. used the protein from *D. gigas* to study the *in vitro* electron transfer with hydrogenase from the same organism. However their voltammograms were broad and it was concluded that the rubredoxin showed an irreversible electrochemical behavior. By square wave voltammetry a potential of -40 mV vs. SHE was obtained [9]. Hagen studied rubredoxin from *Megasphaera elsdenii* by cyclic voltammetry using a bare glassy carbon electrode [10]. He found that it was necessary to scan continuously for 4-8 hours before a well developed voltammogram could be obtained. The peak current was linearly dependent on the square root of the scan rate below 10 mV/s indicating a diffusion controlled though kinetically hampered electrode reaction. The midpoint potential was 42 mV vs. SHE [10]. Finally, some data were reported on the electrochemistry of *Clostridium pasteurianum* rubredoxin. This protein was studied using an edge-oriented graphite electrode in the presence of 0.34 mM $Cr(NH_3)_6^{3+}$. No voltammograms were shown, but the midpoint potential and the heterogeneous rate constant were reported to be -69 mV vs. SHE and $17*10^{-3}$ cm/s respectively [11].

Numerous promotors for the electrochemistry of proteins have been tested and described. Among them is neomycin, which is frequently used in combination with carbon electrodes to enable the electrochemistry of ferredoxins. The promotor function of this positively charged molecule has been explained in terms of charge compensation. In this model the formation of a favourable protein electrode complex is only possible when neomycin is sandwiched between the protein and the electrode, which are both negatively charged, and between adjacent protein molecules [12]. Electron transfer can subsequently occur within the protein-electrode complex. Another extensively studied example is 4,4'-bipyridyl adsorbed on a gold electrode. Well defined voltammograms of horse heart cytochrome *c* can be obtained with a gold electrode functionalized with this compound. From the characterization of the

86

electrode surface with SERS and ellipsometry it was concluded that bipyridyl was bridged between the electrode and the protein with one side bound to the metal surface and the other side pointing into the solution. This is an example in which the promotor alters the properties of the electrode, thus making protein electrochemistry possible ([12] and refs. therein). Recently, a more quantitative description of the effect of a promotor was presented by Datta et al. who used two dissociation constants to describe the equilibria between a ferredoxin, various redox inert cations and a negatively charged graphite electrode [13].

We found that it was possible to use the lanthanide europium as a promotor for the electrochemistry of *Megasphaera elsdenii* rubredoxin. The redox potential of the Eu^{3+}/Eu^{2+} couple is approximately 400 mV lower than the midpoint potential of the rubredoxin and therefore both potentials can be monitored simultaneously. This enables the detection of possible interactions of the promotor with either the protein or the electrode since this is expected to cause a shift of its redox potential compared to its aqueous form. The result of such a study will be described in what follows.

Materials and Methods

$EuCl_3$ was obtained from Fluka (99.9%). Rubredoxin from *Megasphaera elsdenii*, strain LC 1 (grown on Fe-rich medium) was prepared and isolated as described in ([14] and refs. therein). Cyclic voltammetry and the preparation of the glassy carbon electrodes were performed as described by Hagen. A BAS CV 27 potentiostat (BioAnalytical Systems, USA) connected to a X-Y recorder (Kipp & Zonen, NL) was used to record the voltammograms [13]. Potentials were recalculated to the SHE scale. The pH dependence was studied using Good buffers of the appropriate pH. The buffers used were Mes, Hepes, Taps, Ches, and Caps. For pH values below pH 5.5 acetate was used as the buffer. For the electrochemistry of the europium ion a concentration of 100 µM was used in 50 mM buffer. The ionic strength of this solution was kept constant at I=0.18 M by addition of various amounts of NaCl. The electrochemistry of rubredoxin was studied at a protein concentration of 0.6 mg/ml in the presence of 1 mM Eu^{3+} in 50 mM buffer.

Results and Discussion

Electrochemistry of europium

Cyclic voltammograms at different scan rates of 1 mM europium ion in 5 mM Mes pH 5.5 at a bare glassy carbon electrode are shown in fig. 1
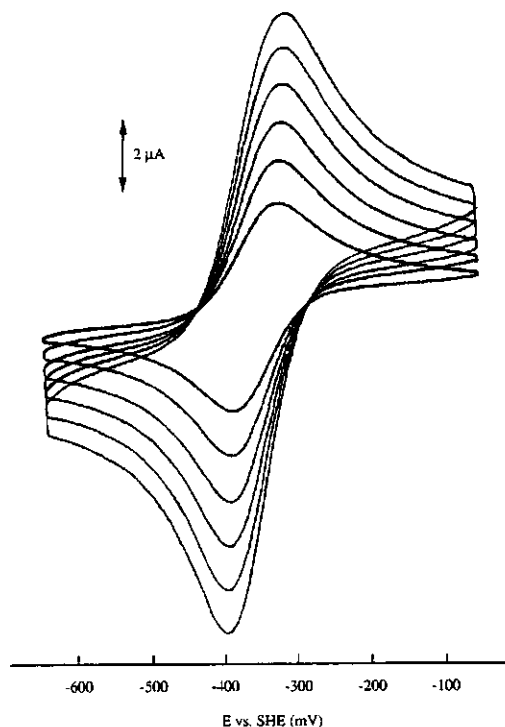
Figure 1: Voltammograms of 1 mM Eu(Cl)$_3$ in 5 mM Mes pH 5.5 obtained at different scan rates. The potential was varied between -900 and -320 mV vs. SCE at scan rates of 10, 20, 33, 49, 68, and 90 mV/s. Conditions: working/counter/reference electrodes, glassy carbon/platinum/saturated calomel.

The voltammograms are well defined and reversible. From the scan rate dependence it is obvious that europium is not adsorbed to the surface but gives rise to a diffusion controlled electrochemical response (data not shown). The voltammogram indicates a midpoint potential of -398 ±5 mV vs. SHE, which is in between the value of -350 mV vs. SHE reported for the Eu^{2+}/Eu^{3+} redoxcouple in 1M perchlorate at pH 2.08 [15] and the value of -429 mV vs. SHE reported for the couple in the presence of formate as the supporting electrolyte [16,17]. However, this latter value was believed to be influenced by the formation of a complex between europium (III) and formate ion resulting in a shift of the potential to more negative values [18].

The pH dependence of the europium ion was studied in the interval between 5.5 and 8. No precipitation was observed in this pH interval. Changing the pH does not show any effect on the midpoint potential (cf. fig. 5). Below pH 5.5 a shift of -90 mV is observed but this seems an effect of the use of acetate as the buffer rather than a pH effect [19]. The pH independence is in agreement with that previously reported in [17]. An interesting effect is observed when the relative peak current is plotted versus the pH (fig 2).
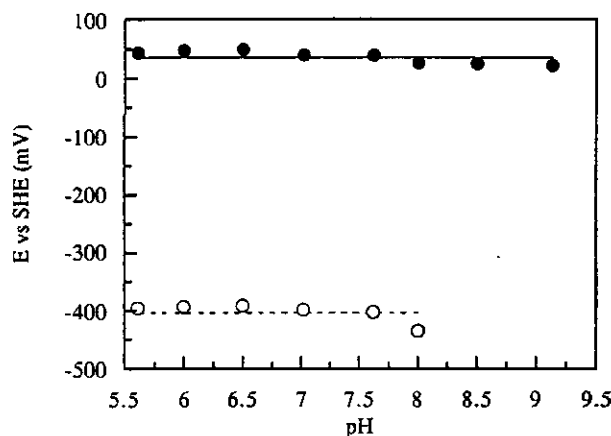
Figure 2: pH dependence of the anodic peak current of $Eu(Cl)_3$. Voltammograms of 100 μM $Eu(Cl)_3$ were recorded in 50 mM buffer at different pH at a temperature of 23 °C. The potential was varied between -900 and -300 mV vs. SCE with a scan rate of 10 mV/s. The pH dependence of Eu^{3+} was determined in the absence (●) and in the presence (△) of rubredoxin.

The anodic peak current is dependent on the pH and can be described with a single pK of 6.9. This pK value is comparable to the value of 8.0 reported for the hydrolysis of one of the nine water molecules of the first coordination shell [20]. The hydrolysis apparently alters the charge of the europium ion thus preventing the formation of a favourable complex between this ion and the electrode. From the values of $10^{-21.5}$ [17] and $10^{-25.6}$ [21] reported for the solubility product of Eu^{3+} and OH^- we can calculate that the Eu^{3+} concentration will drop below 100 μM (which is the concentration used in the experiments) above a pH value of 8.2 or 6.8 respectively. Below this value precipitation is not expected to occur and, therefore, we conclude that the decrease of the peak current in this pH interval is not due to the formation of an insoluble hydroxide complex but rather caused by the hydrolysis.

Electrochemistry of rubredoxin

The use of europium in combination with rubredoxin in an electrochemical experiment evolved from our search for cations capable of promoting protein electrochemistry. It has been proposed that both the charge of a cation and its possibility to form complexes are important for its function as a promotor [11]. The lanthanides constitute a number of relatively highly charged cations with coordination numbers up to 9 [22]. In comparison the commonly used

89

promotors like magnesium and chromiumhexamine are generally octahedrally coordinated with a coordination number of 6. Typical complexing ligands for the lanthanides are hydroxo or amino carboxylic acids. Because of these different properties these lanthanides might function as more effective promotors or might promote protein electrochemistry in situations where the commonly used promotors do not show an effect. Indeed we found that europium functions as an effective promotor for the electrochemistry of *M. elsdenii* rubredoxin. A voltammogram of this protein in the presence of 1 mM Eu(Cl)3 is shown in fig. 3.
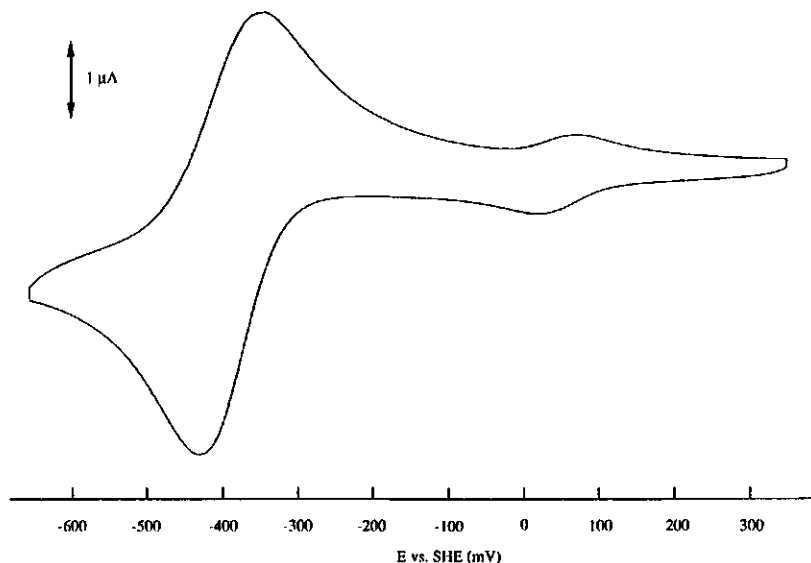
Figure 3: Wide scan voltammogram of 100 μM *Megasphaera elsdenii* rubredoxin in the presence of 1 mM EuCl3 in 50 mM Mes pH 6.0. The voltammogram was recorded from -900 to +100 mV vs. SCE with a scan rate of 10 mV/s. Conditions: working/counter/reference electrodes, glassy carbon/platinum/saturated calomel.

The voltammetric response of rubredoxin under these circumstances develops rapidly and is stable for a prolonged period. In order for the rubredoxin voltammogram to appear it was not necessary to cycle beyond the redox potential of the europium couple indicating that europium (III) is capable of promoting the electrochemistry. However, an europium ion concentration of at least 1 mM is required for the development of a reversible voltammogram (fig. 4). Stepwise addition of small amounts of europium ion causes the voltammogram to change from sigmoidal to peak-shaped. This is indicative of a change from the radial diffusion limit to the linear diffusion limit [23,24]. At europium ion concentrations of 1 mM the electrochemistry of the protein is diffusion controlled as is indicated by the linear dependence of the anodic peak current on the square root of the scan rate (data not shown).
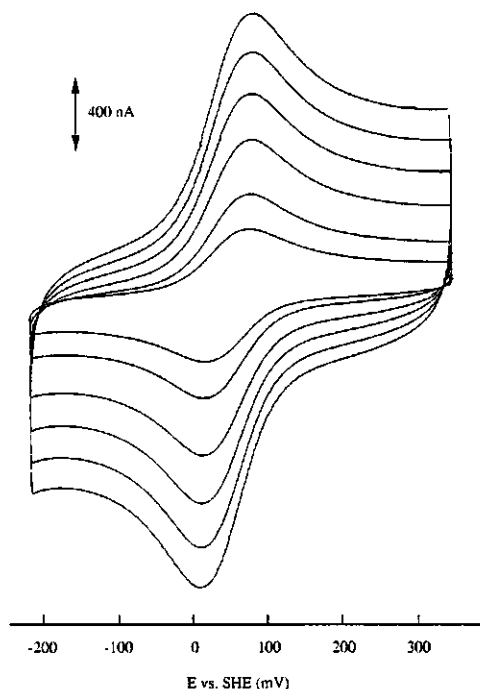
Figure 4: Voltammograms of 100 μM *M. elsdenii* rubredoxin in the presence of 1 mM Eu(Cl)$_3$ in 50 mM Mes pH 6.0. Applied potentials were varied between -450 to +100 mV vs. SCE at scan rates of 10, 20 40, 60, 80 and 100 mV·s^{-1}. The other conditions are the same as in fig. 3.

The midpoint potential of rubredoxin was calculated as the average of the anodic and cathodic peak potential and was found to be 37 ± 5 mV vs. SHE. This value is in good agreement with the one reported previously for this protein in [10]. The diffusion coefficient of 2.5·10^{-6} cm^2/s calculated for *M. elsdenii* rubredoxin from fig. 4 is identical to the value reported by Armstrong et al. for rubredoxin from *Clostridium pasteurianum* [11]. The heterogeneous rate constant for electron transfer estimated from the peak to peak separation using the calculated diffusion coefficient is 10·10^{-2} cm/s. This value is tenfold higher than the value of 17·10^{-3} cm/s reported in [11] and indicates that the europium ion serves as an efficient promotor, which enables fast electron transfer between the electrode and the protein. The pH dependence of rubredoxin in the interval between pH 6.0 and pH 9.5 in the presence of Eu(Cl)$_3$ indicates that the midpoint potential of this protein is essentially pH independent (fig. 5). The thiolate ligands can not be titrated in the applied pH interval neither in the oxidized nor in the reduced form of the protein. Up till now this is the first report on the pH dependence of the midpoint potential of rubredoxin and reference material is therefore not available.
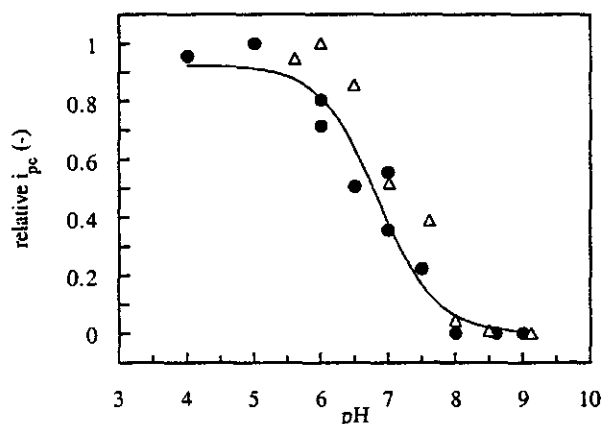
Figure 5: pH dependence of the redox potentials of rubredoxin (●) and europium (O). The midpoint potential was determined from voltammograms recorded of 100 μM rubredoxin in the presence of 1 mM Eu(Cl)$_3$ in 50 mM buffer of the appropriate pH. The midpoint potential of the Eu^{3+}/Eu^{2+} couple above pH 8.0 could not be determined due to the absence of an electrochemical response at these pH values.

The voltammograms of rubredoxin in the presence of EuCl$_3$ obtained at different pH values show an apparent inconsistency. At pH values above 8.0 the Eu^{3+}/Eu^{2+} couple cannot be detected anymore, however, the voltammograms of rubredoxin remain well defined and their intensity is essentially unaltered. As mentioned previously it appears that at these high pH values europium ion does not have any contact with the electrode anymore. It is, therefore, remarkable that europium is still capable of promoting the electrochemistry of rubredoxin. The pK value for the disappearance of the europium response in the presence of rubredoxin is very similar to the value in the absence of the protein, suggesting that the lanthanide is not bonded to the protein (cf. fig. 2). Complex formation is expected to change the first coordination shell and, consequently, alter the pK's of the associated water molecules. Furthermore, complex formation is also expected to cause a shift in the potential of the Eu(III)/Eu(II) couple. The redox potential of this lanthanide in the presence of EDTA at pH 7.0 and an ionic strength (I) of 1.0 M is reported to shift -460 mV relative to the value of the aquo ion [25,26]. Unfortunately, it appeared not possible to measure the potential of the europium-EDTA complex at the glassy carbon electrode. Therefore the inability to observe extra peaks in the voltammograms of rubredoxin in the presence of europium in the range between -1250 and +300 mV vs. SHE does not necessarily indicate the absence of complex formation. In the presence of Bis-Tris we obtained a value of -463 mV vs. SHE for the redox potential of the Eu(III)/Eu(II) couple. This negative shift in potential indicates complex formation between europium and the buffer. Thus,

the absence of a peak around this potential value in the voltammograms of rubredoxin suggests that europium is not bound to the protein.

In the pH interval studied we can expect to have three different forms of europium in solution: $Eu(H_2O)_9$, $Eu(H_2O)_8(OH^-)$, and $Eu(OH)_3$. When we make a comparison with neomycin, a molecule capable of promoting the electrochemistry of some ferredoxins, we note the following: At pH values above the pK of neomycin the electrochemical response of the protein under study decreases. Addition of extra neomycin results in an enhancement of the voltammogram. Apparently, the protonated form of neomycin is essential for its function as a promotor. For europium such a pH dependent effect has not been observed and this suggests that all the species present in solution are capable of promoting the voltammetry of rubredoxin. It is evident that this observation is not in agreement with the model of charge compensation.

Conclusions

The observation that the lanthanide europium is capable of promoting the electrochemistry of *M. elsdenii* rubredoxin in a broad pH interval challenges the proposal that an essential function of a promotor is to provide charge compensation [11,13],. This proposal in which the protein-cation complexes are regarded as the electroactive components in solution cannot be used to explain the europium promoted electrochemistry of this rubredoxin. The influence of the cations on the double layer near the electrode may offer an alternative explanation. It is expected that such an effect is not so much dependent on the type of cation used but rather on the valence of the ion in combination with its concentration. Adsorption of europium onto the electrode is not an explanation. In the experiments with 100 μM $Eu(Cl)_3$ the scan rate dependence of the peak current did not give any indication that europium ions were adsorbed onto the electrode.

The use of a redox active cation like europium as a promotor provides new insights in the working mechanism of these compounds. A thorough understanding of the exact principles of promotion of protein electrochemistry will make it possible to design electrodes for a specific purpose. At the moment it is not usually possible to rationalize the absence of an electrochemical response of a specific protein. Knowledge about the exact role of promotors during electrochemical experiments will hopefully enable the prediction and establishment of optimal electrode modification conditions for a specific protein.

Finally, this study of rubredoxin is the first to present data on the pH dependence of its midpoint potential. The absence of a pK in the pH interval between pH 5.5 and 9.5 indicates that none of the ligands to the iron can be protonated. Future studies of other rubredoxins and rubredoxin-type iron centers will be necessary to establish if this pH independence is a general property of cysteine coordinated iron atoms.

Acknowledgements:

References

1. Hormel, S., Walsh, K.A., Prickril, B.C., Titani, K., LeGall, J. & Sieker, L.C. (1986), FEBS lett., 201, 147-150.
2. Bruschi, M. (1976), Biochem. Biophys. Res. Commun., 70, 615-621.
3. Bruschi, M. (1976), Biochim. Biophys. Acta, 434, 4-17.
4. Bachmayer, H., Yasunobo, K.T., Peel, J.L. & Mayhew, S. (1968), J. Biol. Chem., 243, 1022-1030.
5. Voordouw, G. (1988), Gene, 69, 75-83.
6. Adman, E.T., Sieker, L.C. & Jensen, L.H. (1991), J. Mol. Biol., 217, 337-352.
7. Lovenberg, W. & Sobel, B.E. (1965), Biochemistry, 54, 193-199.
8. Moura, I., Moura, J.J.G., Santos, M.H., Xavier, A.V. & LeGall, J. (1979), FEBS Lett., 107, 419-421.
9. Moreno, C., Franco, R., Moura, I., Le Gall, J. & Moura, J.J.G. (1993), Eur. J. Biochem., 217, 981-989.
10. Hagen, W.R. (1989), Eur. J. Biochem., 182, 523-530.
11. Armstrong, F.A., Cox, P.A., Hill, H.A.O., Lowe, V.J. & Oliver, B.N. (1987), J. Electroanal. Chem., 217, 331-366.
12. Armstrong, F.A. (1990), Structure and Bonding, 72, 137-221.
13. Datta, D., Hill, H.A.O. & Nakayama, H. (1992), J. Electroanal. Chem., 324, 307-323.
14. Gillard, R.D., McKenzie, E.D., Mason, R., Mayhew, S.G., Peel, J.L. & Stangroom, J.E. (1965), Nature, 208, 769-771.
15. Anderson, L.B. & Macero, D.J. (1963), J. Phys. Chem., 67, 1942.
16. McCoy, H.N. (1936), J. Am. Chem. Soc., 58, 1577-1580.
17. de Zoubov, N. & van Muylder, J. (1963) in Atlas d'equilibres électrochimiques a 25°C, (Pourbaix, M., eds.), Gauthier-Villars & Cie, Paris, pp 183-197.
18. Macero, D.J., Anderson, L.B. & Malachesky, P. (1965), J. Electroanal. Chem., 10, 76-81.
19. Kolat, R.S. & Powell, J.E. (1962), Inorganic Chemistry, 1, 293-296.
20. Burgess, J. (1978) in Metal ions in solution, Ellis Horwood Ltd., Chichester, pp 267.
21. Smith, R.M. & Martell, A.E. (1976) in Critical stability constants Vol. 4: Inorganic complexes, Plenum press, New York and London.
22. Kanno, H. & Hiraishi, J. (1982), J. Phys. Chem., 86, 1488-1490.
23. Armstrong, F.A., A.M., Bond., Hill, H.A.O., Oliver, B.N. & Psalti, I.S.M. (1989), J. Am. Chem. Soc., 111, 9185-9189.
24. Armstrong, F.A., Bond, A.M., Hill, H.A.O., Psalti, I.S.M. & Zoski, C.G. (1989), J. Phys. Chem., 93, 6485-6493.
25. Tananaeva, N.N. & Kostromina, N.A. (1969), Russ. J. Inorg. Chem., 14, 631-635.

26.   Onstott, E.I. (1952), J. Am. Chem. Soc., 74, 3773-3776.

Chapter 8

Electrochemical study of the redox properties of [2Fe-2S] ferredoxins; evidence for superreduction of the Rieske [2Fe-2S] cluster

Marc F.J.M. Verhagen, Thomas A. Link and Wilfred R. Hagen

Electrochemical study of the redox properties of [2Fe-2S] ferredoxins; evidence for superreduction of the Rieske [2Fe-2S] cluster

Marc F.J.M. Verhagen, Thomas A. Link[+] and Wilfred R. Hagen

Abstract

Direct, unmediated electrochemistry has been used to compare the redox properties of [2Fe-2S] clusters in spinach ferredoxin, *Spirulina platensis* ferredoxin and the water soluble fragment of the Rieske protein. The use of electrochemistry enabled, for the first time, the observation of the second reduction step, [Fe(III),Fe(II)] to [Fe(II),Fe(II)], in a biological [2Fe-2S] system. A water-soluble fragment of the Rieske protein from bovine heart bc_1 complex exhibits two subsequent quasi-reversible responses in cyclic voltammetry on activated glassy carbon. In contrast the ferredoxins from spinach and *Spirulina platensis* only show one single reduction potential. These results support a seniority scheme for biological iron-sulfur clusters relating cluster size to electron transfer versatility. Electrochemical reduction of spinach ferredoxin in the presence of $NADP^+$ and ferredoxin:$NADP^+$ oxidoreductase results in the generation of NADPH. The second order rate constant for the reaction between the ferredoxin and the reductase was estimated from cyclic voltammetry experiments to be $> 3 \cdot 10^5$ $M^{-1}.s^{-1}$.

Introduction

Direct unmediated electrochemistry has evolved in the last decade in a valuable technique for the study of redox properties of predominantly small redox proteins. Not only is it possible to study redox potentials and their dependence on parameters like temperature and pH, but also kinetic data in the form of rate constants can be obtained [1]. An important advantage of the use electrochemistry is the possibility to extend the potential window beyond the values which can be obtained in solution with chemical reductants or oxidants. This advantage has already led to the discovery of a presumably superreduced state in [3Fe-4S] clusters [2]. The "superreduction" in this case is, however, associated with an adsorbed species and it is uncertain if this state can also be obtained in solution.

One of the major assets of iron as a bio-inorganic element is the fact that its ferric/ferrous transition is conveniently fine-tuned through its coordination chemistry over the better part of the redox potential range available to life [3]. This property is frequently used in iron-sulfur proteins, which act in electron transfer, Lewis-acid catalysis, redox catalysis, and (redox linked) regulation [4]. It is at present still poorly understood what determines the reduction potential(s) of these proteins, and what determines whether their functioning is associated with the transfer of no, one ,one pair, or multiple pairs of electrons.

By a fortunate coincidence of circumstances we have found it possible to study the complete redox behaviour of a biological [2Fe-2S] system: i) the Rieske protein can be purified as a water-soluble fragment with no observable change in its iron-sulfur cluster [5]; ii) the fragment exhibits a direct, unmediated electrochemical response on glassy carbon [6]; iii) the first reduction potential of the Rieske cluster is unusually high, namely $E_{m,7} \approx +0.3$ V [7]; iv) carbon electrodes have a high overpotential for H_2 evolution, therefore, their use allows for aqueous-solution bio-electrochemistry down to $E \approx -1$ V [8]. The voltammetric characterization of the Rieske cluster and the comparison of its properties with other (*i.e.* low-potential) biological [2Fe-2S] clusters are the subject of this study.

Materials and methods

The water-soluble fragment of the Rieske protein of bovine heart bc_1 complex was isolated and purified as described previously [5,6]. Ferredoxin:NADP$^+$ oxidoreductase from spinach leaves and [2Fe-2S] ferredoxin from *Spirulina platensis* were obtained from Sigma Chemie (Bornem, Belgium) as the salt-free lyophilizate. The redissolved ferredoxin was found to be homogeneous in SDS-PAGE and isoelectric focusing, and was used without further purification. Spinach ferredoxin was a gift from Drs M. Hirasawa and D.B. Knaff (Texas Tech at Lubbock). Both the ferredoxin from *Spirulina platensis* and from spinach were measured in

the presence of 2 mM neomycin. Direct cyclic voltammetry in 15 μl volume was performed at the nitric acid activated glassy carbon electrode with the electrochemical cell described in [9] The electrode preparation for the spinach ferredoxin was slightly modified from this procedure. After treatment of the working electrode with nitric acid and washing with 0.1 M dipotassiumhydrogenphosphate and water, the electrode was held in a methane flame until it became red-hot. After cooling down 20 μl of a 20 mM neomycin solution was applied onto the electrode. Subsequently the electrode was dried with a tissue and mounted in the electrochemical cell. The sample was applied and the cyclic voltammetry was started using a BAS CV 27 potentiostat (BioAnalytical Systems Indiana, USA) connected to a X-Y recorder (Kipp & Zonen, NL). After one scan neomycin was added to the sample in a final concentration of 2 mM. Potentials were measured with reference to the saturated calomel electrode (E = +244.4 mV at 25 °C) and re-calculated with reference to the standard hydrogen electrode (E = 0 mV). The pH dependence of the different proteins was studied using Mes, Hepes, Ches, Caps buffers of the appropriate pH all in a final concentration of 50 mM.

Results

Spinach ferredoxin

Spinach ferredoxin on a nitric acid activated glassy carbon electrode gives rise to completely irreversible voltammograms even in the presence of promotor, i.e. 2 mM neomycin. Only the electrode treatment in which the electrode has been heated in a flame and neomycin has been applied to the electrode after cooling down makes it possible to obtain quasi reversible voltammograms as shown in fig 1. Estimation of the heterogeneous rate constant from the voltammogram, using the procedure of Nicholson [10] results in a value of $2.2 \cdot 10^{-3}$ $cm^{-1}s^{-1}$. This value, which remains unchanged in the range of scan rates between 10 and 100 mV s^{-1}, is ten times higher than the value reported by Crawley and Hawkridge using viologen modified gold electrodes [11]. This is remarkable since the viologen is expected to facilitate the electron transfer between the electrode and the protein. The redox potential of spinach ferredoxin, estimated from the voltammogram as the average of the anodic and cathodic peak potentials, is found to be -405 mV versus SHE. This is slightly less negative than the potentials between -428 and -420 mV, obtained from earlier reported mediated voltammetry studies, redox titrations and equilibration studies with H_2 and hydrogenase [12,13]. The pH independence of the redox potential in the range pH 6.0 and 10.5 is consistent with previous determinations [14,15].
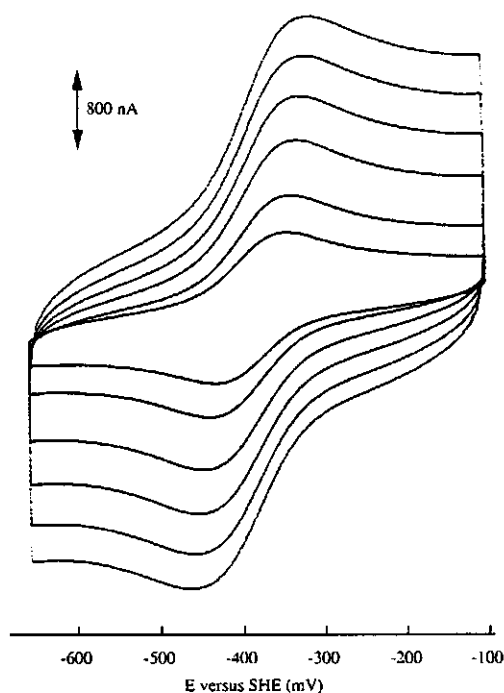
Figure 1: Cyclic voltammograms of spinach ferredoxin in the presence of 2 mM neomycin at scan rates of 10, 20, 40, 60, 80 and 100 mV/s. Ferredoxin concentration was 280 µM in 50 mM Hepes pH 7.0. Working electrode/counter electrode/reference electrode; glassy carbon/platinum/saturated calomel.

In the presence of ferredoxin:NADP$^+$ oxidoreductase and NADP$^+$ a catalytic reduction current develops due to the continuous oxidation of the ferredoxin by NADP$^+$. This is shown in fig. 2. The shape of the voltammogram, however, indicates that the electron transfer between the ferredoxin and the electrode is the rate limiting step. Therefore, it is only possible to determine the minimum value for the second order rate constant between the ferredoxin and the reductase. The value for the second order rate constant calculated as described in [16] was found to be $> 3 \cdot 10^5 \, \mathrm{M^{-1} s^{-1}}$. This value is similar to the values reported by Dasgupta and Ryan for the electron transfer between spinach ferredoxin and reductants like Eu-DTPA and Fe-EDTA, which gave the highest values in the series of reductants tested [17]. This indicates that the electron transfer between the enzyme and the ferredoxin indeed is very efficient.

102
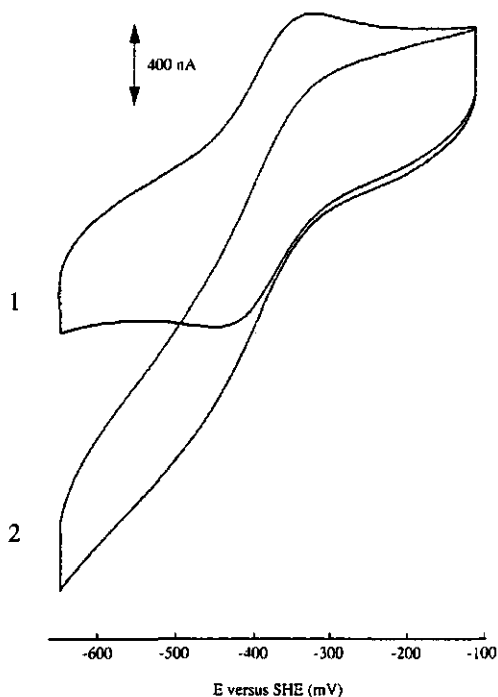
Figure 2: Cyclic voltammograms of spinach ferredoxin in 50 mM hepes pH 7.0 in the presence of 2 mM neomycin (1). The sigmoidal shaped voltammogram (2) develops after addition of 1 mM $NADP^+$ and 2.7 μM ferredoxin:$NADP^+$ oxidoreductase.

Electrochemical superreduction of the Rieske protein

Cyclic voltammetry of the water soluble fragment of the Rieske protein in the range of -100 mV to 700 mV versus SHE results in well defined voltammograms as described in ref [6]. Upon extension of the scan range to lower potentials a second redox transition was observed at - 840 mV vs. SHE. This second redox transition appears to be unique for the Rieske type cluster since this cannot be observed with either the ferredoxin from *Spirulina platensis* or spinach. Fig 3 shows the cyclic voltammograms of the Rieske fragment, the ferredoxin of *Spirulina platensis*, and a baseline.

In contrast with the first reduction the second reduction of the Rieske fragment is not pH dependent (data not shown). The independence of pH is consistent with the postulated coordination of these type of clusters. As described in earlier work the pH dependence of the

first transition can be explained by the protonation of histidines coordinated to the one of the iron atoms in the cluster [6]. However the other Fe-atom is coordinated by cysteines. Such a coordination is not likely to give rise to pH dependence as is obvious from results with the all cysteine coordinated [2Fe-2S] cluster in spinach ferredoxin [14,15].
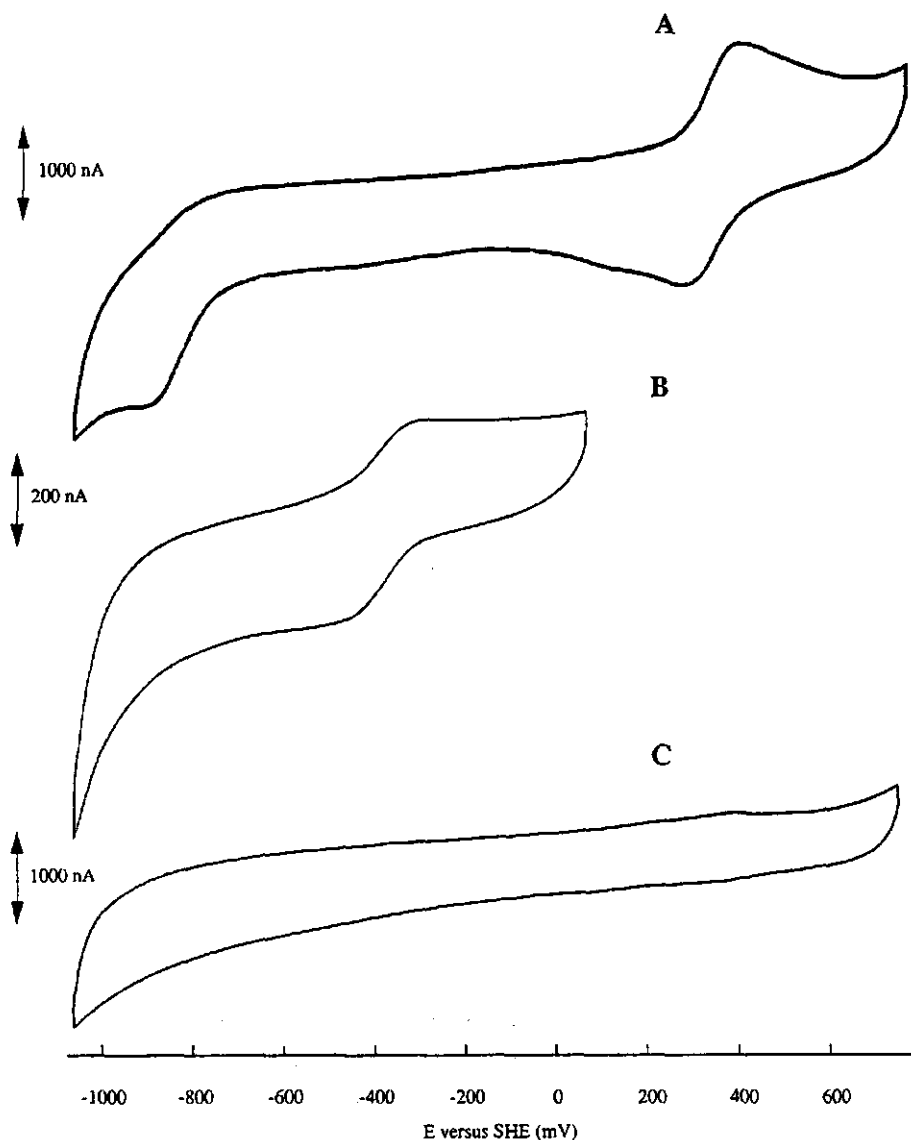
Figure 3: Cyclic voltammogram of (A) Rieske fragment (3 mg/ml), (B) *Spirulina platensis* ferredoxin (2 mg/ml) in the presence of 2 mM neomycin, and (C) baseline. The voltammograms were recorded in 50 mM Hepes pH 7.0 at a scan rate of 10 mV s^{-1}. Working electrode/counter electrode/reference electrode; glassy carbon/platinum/saturated calomel.

Discussion

In order to interpret the observation of superreduction in the Rieske fragment but not in spinach or *Spirulina platensis* ferredoxin it is necessary to consider the properties of iron sulfur clusters in proteins The biological function of iron-sulfur proteins is not limited to mediation of redox reaction through single-electron transfer. In recent times three other functions have been identified, namely, non-redox catalysis [18,19], regulation of gene expression [20,21], and (multi) electron pair associated redox catalysis. Evidence for the latter function is limited, *e.g.*, by the lack of high-resolution structural data on the complex proteins involved. The electron-pair associated hydrogenase reaction is a case in point. The active center of Fe-only hydrogenase probably encompasses a single iron-sulfur cluster [22,23]. This cluster appears to contain some six iron atoms [24]. Spectroscopic, sequence data, and X-ray structural evidence points to the possibility of similar 'superclusters' in other iron-sulfur redox enzymes, *viz* sulfite reductase [25], CO dehydrogenase [26,27], and nitrogenase [28,29]. This information combined with what is known on the redox properties of small, electron transfer iron-sulfur proteins [4] has led us to hypothesize the following seniority scheme for the redox properties of biological iron-sulfur clusters [30-32].

The size of an iron-sulfur cluster is directly related to its electron transfer versatility; 'superclusters' (*i.e.* >4 Fe) are required for multiple electron transfer. This seniority scheme follows from three theses: 1) a biological iron-sulfur cluster of n iron atoms can -in principle - go through n subsequent redox transitions (formally n ferric/ferrous transitions), *i.e.* the cluster has n reduction potentials; 2) with increasing value of n each individual reduction potential can be tuned (by protein coordination) over an increasingly wide potential range; 3) with increasing n the difference between subsequent reduction potentials decreases.

The first thesis is self-evident, when valence states other than ferric and ferrous are excluded. The second thesis reflects the range of observed reduction potentials for rubredoxins, [2Fe-2S] proteins, and [4Fe-4S] proteins [2]. The third thesis is based on the two different transitions, 3+/2+ and 2+/1+, observed in [4Fe-4S] proteins (*i.e.* high-potential iron proteins *versus* ferredoxins), and on the multiple transitions observed in the putative [6Fe-6S] protein [33] and in the P-cluster of nitrogenase [34].

Thus far, the lack of information on the second reduction potential of [2Fe-2S] proteins has been a serious weakness in the experimental support for the seniority scheme. In fact, the available cyclic voltammetry data on iron-sulfur model clusters in DMF are at variance with the scheme: the potential difference between two subsequent E_m's is small, namely ≈ 0.3 V, for $Fe_2S_2L_2$ clusters and larger, namely ≈ 0.7 V, for $Fe_4S_4L_4$ [35]. Also, the potential difference for other (*i.e.* non sulfur) biological 2Fe clusters is maximally 0.2 V [36], and is in other cases even negative [37,38]. We have now found that the Rieske [2Fe-2S] cluster can go through two subsequent reduction steps, that both these steps are not anomalous thermodynamically and kinetically, and that the potential difference is ≈ 1.1 V. We conclude from these results that

the redox data on iron-sulfur models and on non-sulfur biological 2Fe clusters is not relevant to biological [2Fe-2S] systems, and that the redox properties of the latter do support the scheme.

References

1. Verhagen, M.F.J.M., Wolbert, R.B.G. & Hagen, W.R. (1993), Eur. J. Biochem, 221, 821-829.
2. Armstrong, F.A. (1992) in: Advances in Inorganic Chemistry, Vol 38: Iron-Sulfur Proteins, (Cammack, R. and Sykes, A.G., Eds.) Academic Press, San Diego, pp 117-163.
3. Fraústo da Silva, J.J.R. & Williams, R.J.P. (1991) in The Biological Chemistry of the Elements, Oxford University Press, Oxford, pp 346.
4. Cammack, R.C. (1992) in: Advances in Inorganic Chemistry, Vol 38: Iron-Sulfur Proteins, (Cammack, R. and Sykes, A.G., Eds.) Academic Press, San Diego, pp 281-322.
5. Link, T.A. (1988), PhD thesis, Ludwig-Maximilians-Universität, München
6. Link, T.A., Hagen, W.R., Pierik, A.J., Assmann, C. & von Jagow, G. (1992), Eur. J. Biochem., 208, 685-691.
7. Leigh, J.S. & Erecínska, M. (1975), Biochim. Biophys. Acta, 387, 95-106.
8. Armstrong, F.A., George, S.J., Thomson, A.J. & Yates, M.G. (1988), FEBS Lett., 234, 107-110.
9. Hagen, W.R. (1989), Eur. J. Biochem., 182, 523-530.
10. Nicholson, R.S. (1965), Anal. Chem., 37, 1351-1354.
11. Crawley, C.D. & Hawkridge, F.M. (1983), J. Electroanal. Chem., 159, 313-324.
12. Stombaugh, N.A., Sundquist, J.E., Burris, R.H. & Orme-Johnson, W.H. (1976), Biochemistry, 15, 2633-2641.
13. Rickard, L.H., Landrum, H.L. & Hawkridge, F.M. (1978), Bioelectrochemistry and Bioenergetics, 5, 686-696.
14. Tagawa, K & Arnon, D.I. (1968), Biochim. Biophys. Acta, 153, 602-613.
15. Ke, B., Bulen, W.A., Shaw, E.R. & Breeze, R.H. (1974), Arch. Biochem. Biophys., 162, 301-309.
16. Nicholson, R.S. & Shain, I. (1964), Anal. Chem., 36, 706-723.
17. Dasgupta, S.R. & Ryan, M.D. (1982), Biochim. Biophys. Acta, 680, 242-249.
18. Beinert, H. & Kennedy, M.C. (1989), Eur. J. Biochem., 186, 5-15.
19. Switzer, R.L. (1989), Biofactors, 2, 77-86.
20. Thomson, A.J. (1991), J. Inorg. Biochem., 43, 513.
21. Rouault, T.A., Stout, C.D., Kaptain, S., Harford, J.B. & Klausner, R.D. (1990), Cell, 64, 881-883.
22. Hagen, W.R., van Berkel-Arts, A., Krüse-Wolters, K.M., Dunham, W.R. & Veeger, C. (1986), FEBS Lett., 201, 158-162.
23. Voordouw, G., Hagen, W.R., Krüse-Wolters, K.M., van Berkel-Arts, A. & Veeger, C. (1987), Eur. J. Biochem., 162, 31-36.

24. Hagen, W.R., van Berkel-Arts, A., Krüse-Wolters, K.M., Voordouw, G. & Veeger, C. (1986), FEBS Lett., 203, 59-63.

25. Pierik, A.J. & Hagen, W.R. (1991), Eur. J. Biochem., 195, 505-516.

26. Stokkermans, J.P.W.G., van den Berg, W.A.M., van Dongen, W.M.A.M. & Veeger, C. (1992), Biochim. Biophys. Acta, 1132, 83-87.

27. Jetten, M.S.M., Pierik, A.J. & Hagen, W.R. (1991), Eur. J. Biochem., 202, 1291-1297.

28. Chan, M.K., Kim, J-S. & Rees, D.C. (1993), Science, 260, 792-794.

29. Kim, J-S. & Rees, D.C. (1992), Science, 257, 1677-1682.

30. van den Berg, W.A.M., Stevens, A.A.M., Verhagen, M.F.J.M., van Dongen, W.M.A.M. & Hagen, W.R. (1994), Biochim. Biophys. Acta, 1206, 240-246.

31. Hagen, W.R. (1992) in: Advances in Inorganic Chemistry, Vol 38: Iron-Sulfur Proteins, (Cammack, R. and Sykes, A.G., Eds.) Academic Press, San Diego, pp 165-222.

32. Hagen, W.R., Pierik, A.J. & Veeger, C. (1989), J. Chem. Soc., Faraday Trans. I, 85, 4083-4090.

33. Pierik, A.J., Hagen, W.R., Dunham, W.R. & Sands, R.H. (1992), Eur. J. Biochem., 206, 705-719.

34. Pierik, A.J., Wassink, H., Haaker, H. & Hagen, W.R. (1993), Eur. J. Biochem., 212, 51-61.

35. Holm, R.H. & Ibers, J.A. (1977) in Iron-Sulfur proteins Vol. III. Stucture and Metabolic Mechanisms, (Lovenberg, W., ed.), pp 205-281.

36. Pierik, A.J., Wolbert, R.B.G., Portier, G.L., Verhagen, M.F.J.M. & Hagen, W.R. (1993), Eur. J. Biochem., 212, 237-245.

37. Liu, K.E. & Lippard, S.J. (1991), J. Biol. Chem., 266, 12836-12839.

38. Que, L., Jr. & True, A.E. (1990), Prog. Inorg. Chem., 38, 97-200.

Chapter 9

On the iron-sulfur cluster of adenosine phosphosulfate reductase from *Desulfovibrio vulgaris* (Hildenborough)

Marc F.J.M. Verhagen, Ingeborg M. Kooter, Ronnie B.G. Wolbert and Wilfred R. Hagen

On the iron-sulfur cluster of adenosine phosphosulfate reductase from *Desulfovibrio vulgaris* (Hildenborough)

Marc F. J. M. VERHAGEN, Ingeborg M. KOOTER, Ronnie B. G. WOLBERT and Wilfred R. HAGEN

Department of Biochemistry, Wageningen Agricultural University, The Netherlands

Adenosine phosphosulfate reductase from *Desulfovibrio vulgaris* Hildenborough has been purified to homogeneity and was found to consist of two subunits. The α and β subunits have molecular masses of 67.8 kDa and 25.6 kDa, respectively. The apparent molecular mass of the protein is dependent on the ionic strength of the buffer. At low ionic strength, a high molecular-mass multimer is formed, which reversibly changes into smaller units upon addition of salt. The smallest catalytically active unit of the enzyme has a molecular-mass of 186 kDa, as determined by gel-filtration chromatography and, therefore, an $\alpha_2\beta_2$ stoichiometry is proposed. The protein was found to contain 5.6 ± 1.1 iron and 4.4 ± 0.6 acid-labile sulfur atoms/$\alpha\beta$ heterodimer. The reduced protein exhibits a single, rhombic $S = 1/2$ signal with g values 2.070, 1.932 and 1.891. Lowering the ionic strength of the buffer reversibly changes this spectrum into a complex EPR spectrum, indicating intermolecular, dipolar magnetic coupling. Spin quantification of the reduced protein either at low or at high ionic strength never resulted in more than 1 spin/$\alpha\beta$ heterodimer. Hence, it follows that the iron and sulfur atoms are arranged in one single cluster. The reduction potential of the iron sulfur cluster, measured in an EPR-monitored redox titration, was found to be -19 mV versus the normal hydrogen electrode (NHE) at pH 7.5. The reduction potential of the flavin measured in an optical titration was found to be -59 mV against NHE at pH 7.5. The flavin behaves as a two-electron-transferring group; no evidence was obtained for a stabilization of the intermediate semiquinone state in the enzyme. Determination of the kinetic parameters of adenosine 5'-phosphosulfate (AdoPSO_4) reductase for its substrates resulted in K_m values for sulfite and AMP of 130 μM and 50 μM, respectively. It is proposed that AdoPSO_4 reductase contains a single novel Fe/S structure, possibly with an iron-nuclearity greater than four.

Anaerobic sulfate reducing bacteria like *Desulfovibrio vulgaris* use sulfate as the terminal electron acceptor in their respiration. Sulfate is chemically not very reactive and, therefore, it is activated first by ATP-sulfurylase to adenosine phosphosulfate (AdoPSO_4). This occurs at the expense of one ATP. The thermodynamically unfavourable reaction is thought to be driven by the hydrolysis of pyrophosphate catalyzed by a pyrophosphatase. The AdoPSO_4 formed this way is subsequently reduced by AdoPSO_4 reductase to form bisulfite and AMP ([1] and references therein).

The presence of AdoPSO_4 reductase in sulfate-reducing bacteria has been established for quite some time. Several reports exist on the purification and the biochemical and

Correspondence to W. R. Hagen, Laboratorium voor Biochemie, Landbouwuniversiteit Wageningen, Dreijenlaan 3, NL-6703 HA Wageningen, The Netherlands

Phone: +31 8370 83860.

Fax: +31 8370 84801.

Abbreviations. AdoPSO_4, adenosine 5'-phosphosulfate; MCD, magnetic circular dichroism; NHE, normal hydrogen electrode; ETF, electron transfer flavoprotein; ETF-QO, electron transfer flavoprotein:ubiquinone oxidoreductase.

Enzymes. Adenylylsulfate reductase or adenosine phosphosulfate reductase or AMP, sulfite:(acceptor) oxidoreductase (EC 1.8.99.2); Fe-hydrogenase or H_2:ferricytochrome-c_3 oxidoreductase (EC 1.12.2.1); electron transfer flavoprotein:coenzyme Q_{10} oxidoreductase (EC 1.–.–.–).

physical characterization of this enzyme from different *Desulfovibrio* species [2–5]. Bramlett and Peck found that the enzyme from *D. vulgaris* contained two different subunits with a molecular mass of 72 kDa (α) and 20 kDa (β), respectively. The subunit composition appeared to be dependent on the buffer system and on the presence or absence of substrates such as AMP or AdoPSO_4. The smallest unit of enzyme with catalytic activity had a molecular mass of 220 kDa in sedimentation studies, which let the authors propose a subunit composition of $\alpha_3\beta$. Analysis of the cofactors revealed the presence of 12 iron and 12 acid-labile sulfur atoms/220 kDa unit. The enzyme was also found to contain 1 FAD/220 kDa unit [3].

Later, Lampreia et al. characterized the AdoPSO_4 reductase from *Desulfovibrio gigas* using optical, EPR and Mössbauer spectroscopy [5]. From their experiments, they concluded that the native enzyme was an $\alpha_2\beta_2$ heterotetramer. Analysis of the cofactors resulted in 1 FAD and 7.8 ± 0.8 iron atoms/93 kDa, which is the molecular mass of the $\alpha\beta$ heterodimer. EPR spectroscopy of the native enzyme showed a signal with g values around 2.02, indicative of a $[3Fe\text{-}4S]^{(1+,0)}$ cluster. This signal only integrated to 0.1 spin/$\alpha\beta$ and, therefore, it was considered unlikely that this cluster had a physiological role. On reduction of the enzyme with dithionite, a rhombic $S = 1/2$ signal appeared with g values of 2.079, 1.939 and 1.897. This signal could be titrated in the presence

111

of mediators with a midpoint potential of ≈ 0 mV versus the normal hydrogen electrode (NHE) at pH 9.0. The rhombic EPR spectrum was assigned to a cubane type $[4Fe-4S]^{(2+;1+)}$ cluster despite the, for a cubane in these valency states, high reduction potential. This cluster was named center I. Spin quantification of the $S = 1/2$ signal added up to $0.75-0.9$ spin/$\alpha\beta$ heterodimer. The Mössbauer spectrum of the protein in this redox state contained the spectral components of both a diamagnetic and a paramagnetic species in a ratio of $1:1.1$. The paramagnetic component in the spectrum was associated with center I and it was concluded from the Mössbauer data that this center contained two non-equivalent iron sites. The spectroscopic properties of center I were considered to be typical for a $[4Fe-4S]^{1+}$ cluster, although the values for the quadrupole splitting and isomer shift of the ferrous-like iron sites were unusually high. Prolonged incubation of the protein with dithionite at room temperature was found to result in the simultaneous appearance of a complex EPR spectrum and disappearance of the diamagnetic component in the Mössbauer spectrum. This was taken as evidence for the presence of a second $[4Fe-4S]^{(2+;1+)}$ cluster in the $\alpha\beta$ heterodimer. This second cluster was named center II. The midpoint potential of this putative center II was estimated to be < -400 mV compared to NHE from the appearance of the interaction EPR spectrum during a dye-mediated redox titration. A more accurate determination of this value was not possible since it was reported that the protein could only be reduced by approximately 90% with excess dithionite as estimated from the Mössbauer spectrum. This is, however, not consistent with the simultaneously reported spin quantification of the EPR spectrum of the fully reduced enzyme, which resulted in $1.5-1.7$ spins/$\alpha\beta$ heterodimer, indicating a lower degree of reduction of only $75-85\%$. Finally, the midpoint potential of the FAD in the enzyme was claimed to have the very high value of $+160$ mV compared to NHE, although no data were presented to support this [5].

The present paper describes the results of a study of AdoPSO$_4$ reductase from *D. vulgaris*. The midpoint potentials for the cofactors were determined and compared to the values published for *D. gigas* AdoPSO$_4$ reductase. Also, EPR measurements together with iron and sulfur determinations were performed to establish the stoichiometry of the cluster in the *D. vulgaris* enzyme. Evidence will be presented that this enzyme contains only one single iron sulfur cluster/$\alpha\beta$ heterodimer with a novel structure. A preliminary account of this work has been given in [6].

MATERIALS AND METHODS

Activity

Activity of AdoPSO$_4$ reductase was measured in the AdoPSO$_4$-production assay according to the method described by Peck et al. [7] with some minor modifications. The reaction was measured at 23°C in 3-ml cuvettes at 420 nm. The reaction mixture contained 1 mM potassium ferricyanide, 2 mM sodium sulfite in 0.5 mM EDTA, pH 7.6, 2 mM sodium adenosine monophosphate and 0.5 mM 2-mercaptoethanol in 100 mM Tris/HCl, pH 7.6. The decrease in absorbance at 420 nm was measured with an LKB spectrophotometer connected to a Kipp & Zonen BD 40 recorder. The reduction of ferricyanide was corrected for the blank reaction in the absence of enzyme, and the activity, defined as µmol AdoPSO$_4$ produced/min, was calculated using an $\varepsilon_{420} = 1020$ M^{-1} cm^{-1} for ferricyanide. Ferricyanide was

used to start the reaction after a short incubation of the other components together with the enzyme. The reason for this was to avoid the activation of the enzyme during the assay, which was observed when starting the reaction with enzyme. Using this procedure, the initial absorbance at 420 nm was in good agreement with the initial concentration of ferricyanide.

Purification

D. vulgaris (Hildenborough) NCIB 8303 was maintained on Postgate's medium. For purification of the protein, the cells were grown in 20-l batches on modified Saunders' medium [8]. The yield after a 50-h growth period at 37°C was typically 18 g wet cells. The cells were harvested with a Sharpless continuous-flow centrifuge.

Three different purification schemes have been used in order to obtain pure preparations of the enzyme. First, the method recently described by Odom et al. was used [9]. In their purification scheme, a phenyl-Sepharose hydrophobic-interaction column was used after an ammonium sulphate precipitation. In our hands, however, this column did not show a well defined elution pattern. AdoPSO$_4$ reductase activity was present in several fractions which eluted at different salt or glycerol concentrations. Also, the use of this column resulted in a significant loss of AdoPSO$_4$ reductase, since a substantial amount of the enzyme adsorbed irreversibly. An alternative procedure was based on the purification scheme for *D. gigas* AdoPSO$_4$ reductase described by Lampreia et al. [5]. However, an extra gel-filtration column was added between the two anion-exchange columns and also a DEAE and a Q-Sepharose column (Pharmacia) were used instead of two successive DEAE columns. The elution patterns of the protein on these columns were complex due to the strong tendency of the enzyme to polymerize. We decided, therefore, to alter the latter purification scheme as follows.

Typically 18 g wet cells were suspended in 50 ml Tris/HCl, pH 8.0. The cells were disrupted by passage through a chilled French Press (Aminco) at a pressure of 124 kPa. A small amount of both DNase and RNase (Boehringer) was added. The membrane fraction was separated from the soluble fraction by centrifugation at 100000 g for 60 min. The pH and the conductivity of the supernatant were checked and adjusted if necessary. The soluble protein fraction was applied to a DEAE-anion-exchange column (5 cm × 20 cm; Pharmacia) equilibrated with 10 mM Tris/HCl, pH 8.0. The basic proteins were eluted with starting buffer and subsequently a linear gradient from $0-500$ mM NaCl (2 l) was applied. The fractions eluting over $140-200$ mM NaCl contained AdoPSO$_4$ reductase activity and were pooled. The protein solution was adjusted to pH 6.5 by addition of small amounts of 1 M Mes, pH 6.5, and, after addition of 10% glycerol, the solution was concentrated with an Amicon stirred cell using a YM-30 membrane. The concentrated preparation was subsequently loaded onto a Sephadex 200 PG gel-filtration column (2.6 cm × 91 cm) equilibrated with 10 mM Mes, pH 6.5, and 150 mM NaCl. Mes, pH 6.5, was used as a buffer to avoid polymerization of the enzyme. The fractions eluting at around 200 kDa were pooled, adjusted to the proper ionic strength and loaded onto a Q-Sepharose Hi-load column (2.5 cm × 10 cm; Pharmacia) equilibrated with 10 mM Mes, pH 6.5. A linear gradient of $0-400$ mM NaCl (2 l) was applied and the fractions containing AdoPSO$_4$ reductase eluted over $170-190$ mM NaCl. The fractions were pooled and concentrated (Amicon, YM-30)

after addition of 10% glycerol. After this procedure, the protein was only contaminated with some minor bands around 40 kDa and was judged to be 95% pure by SDS/PAGE electrophoresis. A rerun of small portions of the enzyme on a MonoQ (HR 5/5) anion-exchange column (Pharmacia) resulted in pure protein as judged by SDS/PAGE and by a rerun on an analytical Superose 12 gel-filtration column (HR 10/30; Pharmacia). For pH-dependence and ionic-strength-dependence studies, the buffer of the purified preparations was changed using a small biogel P6DG column (Bio-Rad).

In order to establish whether AdoPSO₄ reductase was affected by oxygen during the aerobic purification, a separate anaerobic purification was performed in which 2 mM dithionite was present in all the buffers. The properties of the preparation obtained this way were identical to the aerobically purified enzyme with respect to activity, metal content, and EPR characteristics.

Redox titrations

The redox titration of the non-heme iron was performed as described by Pierik and Hagen [10]. Freshly prepared sodium dithionite in 0.5 M Hepes, pH 7.5, was used as a titrant for the reduction of the protein. The reversibility of the reduction was checked by oxidation with freshly prepared potassium ferricyanide in 0.5 M Hepes. EPR spectra were measured on a Bruker 200D EPR spectrometer equipped with peripheral instrumentation and data acquisition/quantification as described before [10]. Optically monitored redox titration of the flavin was performed according to the method of Massey [11]. A solution of 1.0 mg/ml AdoPSO₄ reductase in 100 mM Tris/HCl, pH 7.5, was placed in an anaerobic cuvette. To this solution, xanthine and resorufin were added to a final concentration of 250 µM and 20 µM, respectively. A small amount, typically 2.5 µM, of methyl viologen was added to ensure redox equilibrium. The cuvette was sealed with a rubber stopper and made anaerobic by 3 alternating cycles of vacuum and argon. The reduction was started by the addition of a small amount of xanthine oxidase and optical spectra between 300 and 600 nm were taken every 5 minutes on a Aminco DW 2000 spectrophotometer interfaced with an IBM PC. The decrease in absorbance at the isosbestic point of the mediator (355 nm) was used to calculate the degree of reduction of the flavin in AdoPSO₄ reductase. The change in absorbance of the mediator at 572 nm was used to calibrate the potential axis. Only resorufin had a significant absorption at this wavelength and therefore it was possible to calculate the potential from the degree of reduction of the mediator. The validity of this method was checked in a separate experiment by determination of the potential of free FAD (Sigma, grade III) using phenosafranine. The potential thus obtained for free flavin was in good agreement with the previously published values.

Elemental analysis and analytical determinations

Protein was determined with the microbiuret method at 550 nm, [12] after trichloroacetic acid/deoxycholate precipitation [13] or using the method described by Lowry [14]. Bovine serum albumin served as the standard in both cases. Iron was determined colorometrically as described in [15] using 3-(2-pyridyl)-5,6-bis(5-sulfo-2-furyl)-1,2,4-triazine, disodium salt trihydrate ('ferene') as the iron chelator. Acid-labile sulfide was determined aerobically with the metylene-blue coloring method [15, 16]. Polyacrylamide electrophore-
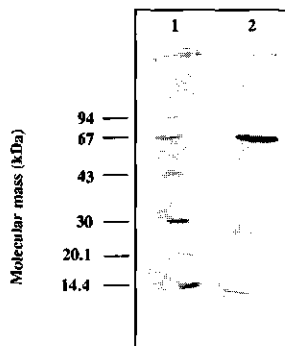

Fig. 1. Homogeneity of AdoPSO₄ reductase from *D. vulgaris* (H) as revealed by SDS/PAGE. Lane 1, low molecular-mass markers; lane 2, 10 µg AdoPSO₄ reductase. The lowest line in both lanes indicates the end of the gel.

sis was performed with a LKB midget-gel electrophoresis system (Pharmcia) using $80 \times 50 \times 0.75$ mm gels. SDS/polyacrylamide gels were according to Laemmli [17]. The composition (mass/vol.) of the stacking gel was 4% acrylamide and 0.1% bisacrylamide; running gels were 12.5% acrylamide and 0.1% bisacrylamide. The molecular mass of the subunits was estimated using low molecular-mass markers (Pharmacia). Analytical gel-filtration chromatography was performed with a Superose 12 (HR 10/30) column attached to a FPLC system (Pharmacia).

RESULTS AND DISCUSSION

Characterization of the enzyme

The subunit composition of the smallest catalytically active form of AdoPSO₄ is controversial [3, 5, 9, 18]. In order to obtain an accurate number for the molecular masses of both the subunits and the native enzyme, we applied our pure preparations to SDS/polyacrylamide gels and performed some gel-filtration experiments. The pure enzyme showed two bands on an SDS/polyacrylamide gel with molecular masses of 67.8 kDa and 25.6 kDa, respectively (Fig. 1). From the gel-filtration experiments it became evident that the overall stoichiometry of the native enzyme depended on the ionic strength of the buffer. Different species, all exhibiting AdoPSO₄ reductase activity, eluted from the gel-filtration column with molecular masses of ± 569, 324 and 186 kDa, respectively (Fig. 2). The molecular mass of the smallest catalytically active unit was 186 kDa, indicating that AdoPSO₄ reductase from *D. vulgaris* (H) is an $\alpha_2\beta_2$ heterotetramer in agreement with the stoichiometry suggested for the AdoPSO₄ reductases from *D. gigas* [5] and *D. desulfuricans* G100A [9]. In order to facilitate comparison of literature values with our results, we will refer to the $\alpha\beta$ heterodimer when discussing the metal and acid-labile sulfide content as well as the spin quantifications.

Activity measurements at variable sulfite or AMP concentrations were performed to obtain the K_m of the enzyme for the two substrates. The K_m for sulfite was found to be 130 µM. This is somewhat lower than the value of 340 µM

113
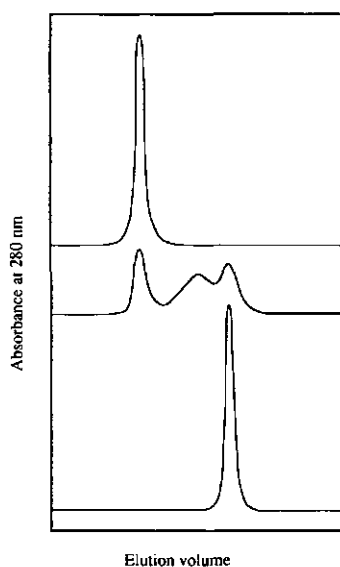
Fig. 2. Gel-filtration profiles from AdoPSO₄ reductase in elution buffers of different ionic strength or pH. Purified AdoPSO₄ reductase (± 200 μg) was loaded onto a Superose 12 (HR 10/30) column equilibrated with the following buffers: (A) 5 mM Tris/HCl, pH 7.5; (B) 5 mM Tris/HCl, 150 mM NaCl, pH 7.5; (C) 10 mM Mes, 150 mM NaCl, pH 6.5.

Table 1. Analytical data of AdoPSO₄ reductase from *D. vulgaris* (H). Protein, iron and acid-labile sulfur were determined as described in the Materials and Methods section. The stoichiometries were calculated using a molecular mass of 93.4 kDa. n.d., not determined.

Pre-paration	Fe/$\alpha\beta$(−)	Labile S^{2-}/$\alpha\beta$(−)	Spins in Fe-S/$\alpha\beta$(−)	Activity
				μmol · AdoPSO$_4^{-1}$ · min^{-1} · mg^{-1}
1	4.5	4.6	0.5	4.0
2	4.8	5.4	0.6	5.5
3	6.3	3.7	0.6	n.d.
4	7.2	4.3	0.9	7.0
5	5.3	4.2	n.d.	4.6
mean ± SD	5.6 ± 1.1	4.4 ± 0.6	0.7 ± 0.2	5.3 ± 1.3
n	5	5	4	4

reported for *D. gigas* AdoPSO₄ reductase [15]. The K_m for AMP was found to be 50 μM which is lower than the value of 300 μM previously reported for the *D. vulgaris* enzyme [3] and also smaller than the value of 160 μM found for the *D. gigas* enzyme [5].

Elemental analysis

The iron and acid-labile sulfide content and the number of unpaired spins of the Fe-S signal after reduction are summarized in Table 1. From this table, it is obvious that there are significantly less than eight iron atoms, necessary for two

cubane clusters, present per $\alpha\beta$ heterodimer. Furthermore, since the spin quantification does not add up to more than 1 spin/$\alpha\beta$ heterodimer, we suggest that these iron atoms are organized in a single cluster. Based on the Lowry-protein-determination method, it was suggested previously that *D. gigas* AdoPSO₄ reductase contains eight iron atoms/$\alpha\beta$ heterodimer [5]. In order to determine if this discrepancy was due to the use of different methods of protein determination, we compared the microbiuret and the Lowry method for the *D. vulgaris* protein. However, the ratio of the concentration obtained with the Lowry method over the value obtained with the microbiuret method was 0.9. This difference does not seem to be sufficient to explain the discrepancy in the Fe-S content.

EPR spectroscopy

The EPR spectrum of *D. vulgaris* AdoPSO₄ reductase in the 'as-isolated' form is characteristic for a [3Fe-4S]$^{(1+;0)}$ cluster with g values 2.02−1.99 (not shown). This spectrum was also found in *D. gigas* AdoPSO₄ reductase [5]. Due to the low value for the spin integration of $\leqslant 0.04$ spins/$\alpha\beta$ heterodimer in our preparations, we do not consider this cluster to have a physiological relevance. Upon reduction with dithionite, AdoPSO₄ reductase gives rise to a rhombic $S = 1/2$ signal with effective g values of 2.070, 1.932 and 1.891 (Fig. 3A). This spectrum was recorded at different temperatures over 4.2−25 K. In this range, the signal remained sharp and no significant broadening of the peaks was observed. No other signals at low field, indicating the presence of high spin systems, were found. Also the typical interaction spectrum, as reported by Lampreia et al. [5], caused by the reduction of the second [4Fe-4S] cluster [5], could not be detected. Even incubation of the enzyme for more than 30 min, with dithionite at room temperature did not alter the shape of the EPR spectrum. Spin quantification of different preparations never resulted in more than one $S = 1/2$ spin/$\alpha\beta$ heterodimer as shown in Table 1. The spectrum shown in Fig. 3A was numerically simulated under the assumption of a single, non-interacting $S = 1/2$ system subject to inhomogeneous broadening by g strain [19]. The result of this simulation and the difference spectrum of the simulated minus the experimental spectrum are shown in Fig. 3B and C, respectively. From the simulation, it can be concluded that the spectrum of AdoPSO₄ reductase is a single-component spectrum. Also, the close fit of the simulation clearly indicates that the slight asymmetry of the peaks at the wings of the spectrum is not caused by magnetic coupling but rather results from g-strain broadening.

Since there was no effect of the time of reduction on the shape of the spectrum, we checked several other conditions. The EPR spectrum proved to be very sensitive to the salt concentration or ionic strength of the buffer. At low ionic strength, the spectrum changed and showed properties typical for an interaction spectrum between magnetically coupled spin systems as shown in Fig. 3D. An increase in ionic strength, however, reversibly changed this spectrum in the earlier observed sharp $S = 1/2$ spectrum. A clue for this ionic-strength-dependent interconversion becomes evident when the results of the EPR experiments are compared with the results of the analytical gel-filtration experiments described earlier in this paper. From the gel-filtration experiments, it was concluded that the enzyme reversibly polymerized at low ionic strength. Therefore, we believe that the interaction EPR spectrum in AdoPSO₄ reductase is not caused by the

g = 2.070 1.932 1.891

A

B

C

D

E

280   300   320   340   360   380   400

B (mT)
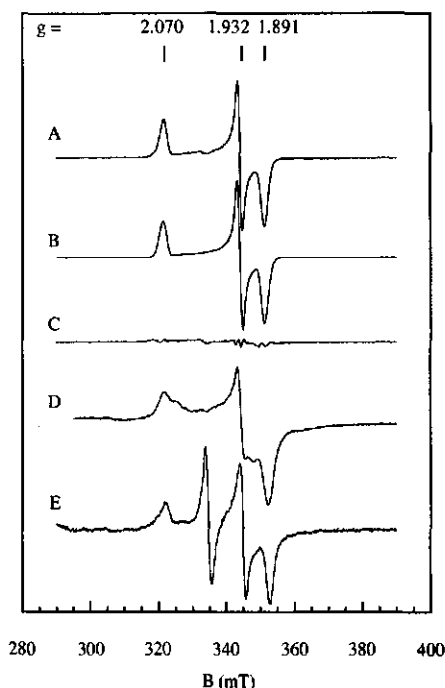
Fig. 3. EPR spectra of reduced AdoPSO₄ reductase. (A) *spectrum of 6 mg/ml AdoPSO₄ reductase in 10 mM Tris/HCl, 1 M NaCl, pH 8.0, after reduction with 2 mM sodium dithionite for 30 min.* (B) Simulation of the spectrum in A. (C) experimental spectrum minus simulated spectrum. (D) EPR spectrum of 4.7 mg/ml AdoPSO₄ reductase after reduction with dithionite in a buffer of low ionic strength (5 mM Tris/HCl, pH 8.0). (E) EPR spectrum of AdoPSO₄ reductase in whole cells. Cells were grown for 50 h, spun down in an EPR tube and frozen. EPR conditions for the experimental spectra: microwave frequency, 9.31 GHz; microwave power, 5.1 mW; modulation amplitude, 0.8 mT; modulation frequency: 100 kHz; temperature; 20 K. Simulation parameters for trace B were 300×100 orientations; g values, 2.070, 1.932, 1.891; g-strain parameters, $\Delta_{zz,yy,xx}$ = −0.0080, 0.0039, 0.0067, $\Delta_{yz,xz,xy}$ = 0.0056, 0.0082, 0.0033; residual broadening, 0.0010.

A

1.2

1

0.8

0.6

0.4

0.2

0

-0.2

rel. EPR intensity at g=2.07 (·)

-500   -300   -100   100   300

E vs NHE (mV)

B

1

0.8

0.6

0.4

0.2

0

rel. optical intensity at 355 nm (·)

-200   -100   0   100

E vs NHE (mV)

Fig. 4. Redox titration of the Fe-S cluster (▲; A) and the flavin (●; B) in AdoPSO₄ reductase from *D. vulgaris* (H). The iron-sulfur cluster was monitored by EPR spectroscopy by measuring the intensity of the line at g = 2.070. EPR conditions, microwave frequency, 9.31 GHz; microwave power 5.1 mW; modulation amplitude, 0.8 mT; modulation frequency, 100 kHz; temperature 20 K. The flavin was monitored by spectroscopy and the reduction was followed by the change of absorption at 355 nm. The potential axis was calibrated using the change of absorbance at 572 nm due to the reduction of resorufin. The first spectrum of the series was taken as 100%. The potentials were calculated versus the NHE. rel., relative.

reduction of a second iron-sulfur cluster in the protein. Instead, we propose that there is only one single iron-sulfur cluster/αβ heterodimer. The magnetic coupling, which is observed in some EPR spectra, is caused by the interaction between single iron-sulfur clusters in different enzyme molecules due to the polymerization at low ionic strength. Indeed, Lampreia et al. [5] mention that they purify the enzyme in a multimeric state with a molecular mass of ±400 kDa. It is, therefore, likely that the interaction EPR spectrum as observed in their preparations is similarly caused by this effect of intermolecular coupling.

The previous would also imply that the Mössbauer studies of Lampreia et al. [5], on what they proposed to be the enzyme with center I reduced and center II oxidized, has in fact been performed on enzyme with center I partially reduced (and center II non existing). They quote a reduction time of 15 s to obtain this intermediate state. In our hands, incubation of AdoPSO₄ reductase with the non-physiological reductant dithionite for 15 s indeed leads to partial reduction

of center I as monitored on the amplitude of the single-component, rhombic EPR signal.

Redox titrations

The result of a redox titration of the iron-sulfur cofactor, performed in 50 mM Hepes and 250 mM NaCl, pH 7.5, is presented in Fig. 4A as the relative EPR intensity of the S = 1/2 signal. The solid line in this figure is a Nernst curve with n = 1. A midpoint potential of −19 mV compared to NHE was determined. This is close to the value of 0 mV determined for *D. gigas* AdoPSO₄ reductase at pH 9.0 [5]. These values are extraordinarily high for cubane type [4Fe-4S]$^{(2+;1+)}$ clusters although there appears to be one precedent. The enzyme electron transfer flavoprotein:ubiquinone oxidoreductase (ETF-QO) has been claimed to contain a [4Fe-4S]$^{(2+;1+)}$ cluster with a midpoint potential of +47 mV relative to NHE at pH 7.5 and 4°C [20]. During the EPR-monitored redox titration of AdoPSO₄ reductase, no other signals other than the S = 1/2 signal were detected. Thus, no signals

115

attributable to a center II were found, and also no signal at $g = 2$ was obtained. The appearance of a signal at $g = 2$ would indicate the formation of the flavin semiquinone radical.

The midpoint potential of the flavin was determined optically as described in the Materials and Methods section. It was assumed that the FeS cluster and the FAD cofactor had separate contributions to the visible spectrum at 356 nm. The result of the titration performed in 100 mM Tris/HCl, pH 7.5, is presented in Fig. 4B. The data points could be fitted with a Nernst curve with $n = 2$, which is shown in Fig. 4B. The calculated midpoint potential was -59 mV relative to NHE. The observation that the flavin could only be reduced in a single two-electron step agrees very well with the absence of a radical signal in the EPR spectrum. We, therefore, conclude that the semiquinone form of the flavin is not stabilized in this enzyme. A consequence of this is that the enzyme has the potential to take up three electrons, although the formation of AdoPSO$_4$ is a two-electron reaction. The midpoint potential for the flavin is rather high, although our value is at least 200 mV lower than the value reported by Lampreia et al. in [5]. Again, as with the iron-sulfur cluster, a comparable value was obtained in the enzyme ETF-QO from pig liver. In this enzyme, the flavin semiquinone is stabilized and the two midpoint potentials are $+28$ and -6 mV respectively, compared to NHE [20].

Our observation that the flavin behaves as a two-electron transferring group complicates the visualization of possible working mechanisms. *In vivo* the enzyme requires two electrons to catalyze the reduction of AdoPSO$_4$ to AMP and HSO^{3-}. Peck and LeGall [1] postulated a mechanism for AdoPSO$_4$ reductase in which the Fe-S cluster is reduced by an electron donor. The reduction of the flavin cofactor occurs subsequently through an intramolecular transfer of electrons [1]. Since the Fe-S cluster can only be reduced by one electron, this mechanism requires a sequential electron transfer from an electron donor to AdoPSO$_4$ reductase and, as a consequence, the occurence of the semiquinone state of the flavin. Since this is not observed by us, an alternative mechanism might be considered in which the iron-sulfur cluster is not redox active during the catalytic cycle. When fresh *D. vulgaris* cells are monitored with EPR spectroscopy, a rhombic $S = 1/2$ signal characteristic for the reduced FeS cluster of AdoPSO$_4$ redtuctase is clearly visible (Fig. 3E). This may be caused by the fact that the enzyme is under turn-over conditions in which the reduction of the cluster is part of the cycle. However, several reports have been published recently in which regulatory functions of iron-sulfur clusters in proteins are proposed [21, 22]. This might also account for the iron-sulfur cluster in this enzyme.

Comparison of AdoPSO$_4$ reductase with ETF-QO oxidoreductase

There are several similarities between AdoPSO$_4$ reductase from *D. vulgaris* and ETF-QO from pig liver or beef heart mitochondria. Since this latter enzyme has been studied extensively spectroscopically as well as biochemically, it is worthwhile to compare the two systems. ETF-QO is a membrane-bound iron-sulfur flavoprotein which resides in the inner mitochondrial membrane. It is composed of a single subunit with a molecular mass of 64.8 kDa. The enzyme has been reported to contain approximately one flavin, four iron and four sulfur atoms/monomer. As a result of spectroscopic studies, it has been suggested that the iron and sulfur atoms

are arranged in a [4Fe-4S]$^{(2+;1+)}$ cluster. The EPR spectrum of the reduced iron-sulfur cluster shows a rhombic $S = 1/2$ signal with effective g values of 2.086, 1.939 and 1.886. The enzyme accepts electrons derived from reactions in, e.g., the fatty acid β-oxidation pathway and amino acid oxidative pathways, which occur in the matrix of the mitochondria, and delivers them to the membrane-bound electron-transport chain through reduction of the ubiquinone pool ([20, 23] and references therein). The electron donor for this enzyme is electron transfer flavoprotein (ETF). Comparing the above-mentioned properties with the properties of AdoPSO$_4$ reductase, we note the following. The molecular mass of 68.4 kDa of the large subunit of AdoPSO$_4$ reductase is close to the value of the pig liver enzyme. However, AdoPSO$_4$ reductase is water soluble and contains a small subunit of 26.6 kDa. Important similarities are, in addition, the resemblance of the EPR spectra of the two enzymes and the almost identical midpoint potentials of both the iron-sulfur cofactor as well as the flavin moiety. The close agreement of the potential values in the two enzymes strongly suggest that these cofactors are in a comparable environment. Furthermore, the similarities in the spectroscopic and redox characteristics of the two enzymes indicate that their iron-sulfur clusters contain similar structural elements. The difference in the iron and sulfur content remains to be explained. The number of iron and acid-labile sulfur atoms in AdoPSO$_4$ reductase has consistently been determined to be 6 ± 1 Fe/$\alpha\beta$ heterodimer and 5 ± 1 S per $\alpha\beta$ heterodimer (this paper; [3]). In ETF-QO, the number of iron atoms determined/FAD was found to be ≤ 4 [23−25]. Therefore, either the cluster in ETF-QO is similar to a substructure of the cluster in AdoPSO$_4$ reductase or ETF-QO looses part of its iron and sulfur upon purification. However, no data have been reported to support the latter view. Based on the iron-sulfur content of AdoPSO$_4$ reductase determined by us, we propose that these elements are organized in an Fe-S cluster with a novel structure and possibly a novel stoichiometry. Additional support for this proposal is obtained from the earlier mentioned temperature dependence of the $S = 1/2$ signal in AdoPSO$_4$ reductase and from a comparison of this signal with the EPR spectra from Fe-hydrogenase from *D. vulgaris* (H). Upon activation of this hydrogenase, a transient $S = 1/2$ rhombic EPR signal appears with g values of 2.07, 1.96 and 1.89 [26]. This signal, almost identical in shape to the signal from AdoPSO$_4$ reductase, was associated with the H cluster which forms the active site of this enzyme. The exact nature of this cluster has not been identified yet but it has been hypothesized that it bears resemblance to the [6Fe-6S] model compounds ([26] and references therein). It seems unlikely, however, that the cluster in AdoPSO$_4$ reductase resembles the putative [6Fe-6S] cluster as observed in the recently discovered prismane cluster containing protein from *D. vulgaris* [15, 27]. This cluster can exist in four redox states and this is not observed in redox titrations of AdoPSO$_4$ reductase. Furthermore, this prismane cluster is high spin in certain redox states, and we have not detected any high spin signals in AdoPSO$_4$ reductase.

CONCLUSIONS

For the redox couple AdoPSO$_4$/(HSO$_3^-$ + AMP), a redox potential of -60 mV has been calculated [28]. This value is in close agreement to the value obtained by us for the flavin cofactor of AdoPSO$_4$ reductase. Our results indicate that only a single iron-sulfur cluster is present per $\alpha\beta$ heterodimer in AdoPSO$_4$ reductase. Its structure, redox characteristics, and

function remain enigmatic. Elemental analysis indicates 5—7Fe and 4—5 S^{2-}. We propose that the Fe-S cluster in AdoPSO$_4$ reductase is different from the well-known cubane-type. The nearly identical EPR spectra of the reduced Fe-S cofactors in AdoPSO$_4$ reductase, ETF-QO from pig liver mitochondria and activating Fe-hydrogenase from *D. vulgaris*, (H) suggest that the clusters in these three enzymes have comparable (sub)stuctures. From the appearance of the interaction EPR spectrum at low ionic strength, it follows that the iron-sulfur cluster in AdoPSO$_4$ reductase is located at the surface of the enzyme.

REFERENCES

1. Peck, H. D. Jr & LeGall, J. (1982) Biochemistry of dissimilatory sulphate reduction, *Phil. Trans. Roy. Soc. London 298*, 443–466.
2. Ishimoto, M. & Fujimoto, D. (1961) Biochemical studies on sulfate reducing bacteria: X. Adenosine-5'-Phosphosulfate reductase, *J. Biochem. 50*, 299–304.
3. Bramlett, R. N. & Peck, H. D. Jr (1975) Some physical and kinetic properties of adenylyl sulfate reductase from *Desulfovibrio vulgaris*, *J. Biol. Chem. 250*, 2979–2986.
4. Michaels, C. B., Davidson, J. T. & Peck, H. D. Jr (1970) in *Flavins and flavoproteins: proceedings of the third international symposium on flavins and flavoproteins* (Kamin, N. ed.) pp. 555–580, University Park Press, Baltimore.
5. Lampreia J., Moura, I., Teixeira, M., Peck, H. D. Jr, LeGall, J., Huynh, B. H. & Moura, J. J. G. (1990) The active centers of adenylylsulfate reductase from *Desulfovibrio gigas*: Characterization and spectroscopic studies, *Eur. J. Biochem. 188*, 653–664.
6. Verhagen, M. F. J. M., Kooter, I., Wolbert, R. B. G. & Hagen, W. R. (1993) Spectroscopic and redox properties of adenosine phosphosulfate reductase from *Desulfovibrio vulgaris* (H), *J. Inorg. Biochem. 51*, 19.
7. Peck, H. D. Jr, Deacon, T. E. & Davidson, J. T. (1965) Studies on adenosine 5'-phosphosulfate reductase from *Desulfovibrio desulfuricans* and *Thiobacillus thioparus*: I. The assay and purification, *Biochim. Biophys. Acta 96*, 429–446.
8. van der Westen, H. M., Mayhew, S. G. & Veeger, C. (1978) Separation of hydrogenase from intact cells of *Desulfovibrio vulgaris*: purification and properties, *FEBS Lett. 86*, 122–126.
9. Odom, J. M., Jessie, K., Knodel, E. & Emptage, M. (1991) Immunological cross-reactivities of adenosine-5'-phosphosulfate reductases from sulfate-reducing and sulfide-oxidizing bacteria, *Appl. Environ. Microbiol. 57*, 727–733.
10. Pierik, A. J. & Hagen, W. R. (1991) S = 9/2 EPR signals are evidence against coupling between the siroheme and the Fe/S cluster prosthetic groups in *Desulfovibrio vulgaris* (Hildenborough) dissimilatory sulfite reductase, *Eur. J. Biochem. 195*, 505–516.
11. Massey, V. (1990) in *Flavins and flavoproteins: proceedings of the tenth international symposium on flavins and flavoproteins* (Curti, B., Ronchi, S. & Zanetti, G., eds.) pp. 59–66, Walter de Gruyter & Co., Berlin.
12. Goa, J. (1953) A micro-biuret method for protein determination: determination of total protein in cerebrospinal fluid, *Scand. J. Clin. Lab. Invest. 5*, 219–222.
13. Bensadoun, A. & Weinstein, D. (1976) Assays of proteins in the presence of interfering materials, *Anal. Biochem. 70*, 241–250.
14. Lowry, O. H., Rosebrough, N. J., Farr, A. L. & Randall, R. J. (1951) Protein measurement with the Folin Phenol reagent, *J. Biol. Chem. 193*, 265–275.
15. Pierik, A. J., Wolbert, R. B. G., Mutsaers, P. H. A., Hagen, W. R. & Veeger, C. (1992) Purification and biochemical characterization of a putative [6Fe-6S] prismane-cluster-containing protein from *Desulfovibrio vulgaris* (Hildenborough), *Eur. J. Biochem. 206*, 697–704.
16. Lovenberg, W., Buchanan, B. B. & Rabinowitz, J. C. (1963) Studies on the chemical nature of Clostridial ferredoxin, *J. Biol. Chem. 238*, 3899–3913.
17. Laemmli, U. K. (1970) Cleavage of structural proteins during the assembly of the head of bacteriophage T 4, *Nature 227*, 680–685.
18. Lampreia, J., Moura, I., Xavier, A. V., Le Gall, J., Peck, H. D. Jr & Moura, J. J. G. (1992) in *Chemistry and biochemistry of flavoenzymes*, (Müller, F., ed.) vol. 3, pp. 333–355, CRC press, Baton Rouge.
19. Hagen, W. R., Hearshen, D. O., Harding, L. J. & Dunham, W. R. (1985) Quantitative numerical analysis of g strain in the EPR of distributed systems and its importance for multicenter metalloproteins, *J. Magn. Reson. 61*, 233–244.
20. Paulsen, K. E., Orville, A. M., Frerman, F. E., Lipscomb, J. D. & Stankovich, M. T. (1992) Redox properties of Electron Transfer Flavoprotein Ubiquinone Oxidoreductase as determined by EPR-spectroelectrochemistry, *Biochemistry 31*, 11755–11761.
21. Klausner, R. D. & Rouault, T. A. (1993) A double life: Cytosolic aconitase as a regulatory RNA binding protein, *Mol. Biol. Chem. 252*, 8440–8445.
22. Thomson, A. J. (1991) Does ferredoxin I (Azotobacter) represent a novel class of DNA-binding proteins that regulate gene expression in response to cellular iron (II), *FEBS Lett. 285*, 230–236.
23. Ruzicka, F. J. & Beinert, H. (1977) A new iron-sulfur flavoprotein of the respiratory chain: A component of the fatty acid β oxidation pathway, *J. Biol. Chem. 252*, 8440–8445.
24. Ruzicka, F. J. & Beinert, H. (1975) A new membrane iron-sulfur flavoprotein of the mitochondrial electron transfer system, *Biochem. Biophys. Res. Commun. 66*, 622–631.
25. Beckmann, J. D. & Frerman, F. E. (1985) Electron-Transfer Flavoprotein-Ubiquinone Oxidoreductase from Pig Liver: Purification and molecular, redox, and catalytic properties, *Biochemistry 24*, 3913–3921.
26. Pierik, A. J., Hagen, W. R., Redeker, J. S., Wolbert, R. B. G., Boersma, M., Verhagen, M. F. J. M., Grande, H. J., Veeger, C., Mutsaers, P. H. A., Sands, R. H. & Dunham, W. R. (1992) Redox properties of the iron-sulfur clusters in activated Fe-hydrogenase from *Desulfovibrio vulgaris* (Hildenborough), *Eur. J. Biochem. 2*, 63–72.
27. Pierik, A. J., Hagen, W. R., Dunham, W. R. & Sands, R. H. (1992) Multi-frequency EPR and high resolution Mössbauer spectroscopy of a putative [6Fe-6S] prismane-cluster-containing protein from *Desulfovibrio vulgaris* (Hildenborough), *Eur. J. Biochem. 206*, 705–719.
28. Thauer, R. K. (1982) Dissimilatory sulphate reduction with acetate as electron donor, *Phil. Trans. Roy. Soc. Lond. 298*, 467–471.

117

Chapter 10

Axial coordination and reduction potentials of the sixteen hemes in high-molecular-mass cytochrome *c* from *Desulfovibrio vulgaris* (Hildenborough)

Marc F.J.M. Verhagen, Antonio J. Pierik, Ronnie B.G. Wolbert, Leonard F. Mallée, Wilfried G.B. Voorhorst and Wilfred R. Hagen

Axial coordination and reduction potentials
of the sixteen hemes in high-molecular-mass cytochrome c
from *Desulfovibrio vulgaris* (Hildenborough)

Marc F. J. M. VERHAGEN, Antonio J. PIERIK, Ronnie B. G. WOLBERT, Leonard F. MALLÉE, Wilfried G. B. VOORHORST and Wilfred R. HAGEN

Department of Biochemistry, Wageningen Agricultural University, The Netherlands

A spectroelectrochemical study is described of the sixteen hemes in the high-molecular-mass, monomeric cytochrome c (Hmc) from the periplasmic space of *Desulfovibrio vulgaris*, strain Hildenborough. One of the hemes has special properties. In the oxidized state at pH 7 it is predominantly high-spin, $S = 5/2$, with a $g_\perp$ value of less than 6 indicative of quantum-mechanical mixing with a low-lying (800 cm^{-1}) $S = 3/2$ state; the balance is probably a low-spin derivative. The high-spin heme has an $E_{m,7.5}$ value of $+61$ mV. The fifteen other hemes are low-spin bis-histidine coordinated with $E_{m,7.5}$ values of approximately -0.20 V. Two of these hemes exhibit very anisotropic EPR spectra with a g_1 value of 3.65 characteristic for strained bis-histidine coordination. A previous proposal, namely that methionine is coordinated to one of the hemes [Pollock, W. B. R., Loufti, M. Bruschi, M. Rapp-Giles, B. J., Wall, J. & Voordouw, G. (1991) *J. Bacteriol.* 173, 220] is disproved using spectroscopic evidence. Contrasting electrochemical data sets from two previous studies [Tan, J. & Cowan, J. A. (1990) *Biochemistry* 29, 4886; Bruschi, M., Bertrand, P., More, C., Leroy, G., Bonicel, J., Haladjian, J., Chottard, G., Pollock, W. B. R. & Voordouw, G. (1992) *Biochemistry* 31, 3281] are not consistent with our EPR titration results and are not reproducible. Hmc can be reduced by *D. vulgaris* Fe-hydrogenase in the presence of molecular hydrogen.

Sulfate reducers in general have a high heme content. The heme porphyrin structure is used by these bacteria in two ways. Sirohydrochlorin, the basic component of siroheme, is the prosthetic group of dissimilatory and assimilatory sulfite reductases in the cytoplasm. Protoporphyrin IX is the basic component for b-type and c-type cytochromes in the periplasm, in the cytoplasmic membrane, and also possibly in the cytoplasm. Although some of these proteins have been studied in considerable detail, our knowledge of the number, type, location, biosynthesis, and, especially, the function of these cytochromes is incomplete [1].

For example, in the intensively studied *Desulfovibrio vulgaris*, strain Hildenborough, no cytochromes have yet been identified in the cytoplasm or in the cytoplasmic membrane. Export to the periplasm has been found for three c-type cytochromes, monoheme c_{553} [2], tetraheme c_3 [3], and multiheme high-molecular-mass cytochrome c (Hmc) [4]; the functions of these cytochromes are either debatable or unknown. The existence of a proposed fourth cytochrome, cytochrome c_3 (26 kDa) [5], has been questioned [4].

A Hmc was first alluded to by Yagi for *D. vulgaris*, strain Miyazaki F, initially as a 70-kDa cytochrome c-553 [6], and later as a 60-kDa protein with otherwise unspecified properties [7]. Higuchi et al. have purified and crystallized a similar monomeric Hmc from *D. vulgaris*, strain Hildenborough, and have estimated the heme content to be approximately 16 with a considerable possibility for error in this estimate due to uncertainty in the molecular mass [8]. Since this initial report on crystallization in 1987, no further X-ray data on the protein have been reported. More recently Tan and Cowan have claimed that *D. vulgaris* (Hildenborough) Hmc contains not 16 but only three hemes, and they have renamed the protein as 'triheme cytochrome' [9]. Subsequently, however, the structural gene for Hmc was sequenced by Pollock et al., who found 16 regions encoding Cys-Xaa-Xaa-Cys-His motifs for the potential covalent binding of 16 hemes [4]. Furthermore, with this gene transferred to *Desulfovibrio desulfuricans*, strain G200, an overexpression system was constructed and the purified recombinant Hmc contained 13–16 hemes by chemical analysis [10].

Although the heme stoichiometry of Hmc is thus reestablished at approximately 16, several other basic properties are not yet properly determined. In addition to the 16 Cys-Xaa-Xaa-Cys-His sequences for the thioether binding to the porphyrin side chains, Pollock et al. found 15 histidine residues as putative axial ligands to the 16 hemes. They concluded that one out of the 16 hemes must have (His, Met) axial coordination [4]. This proposal was repeated in the subsequent study by Bruschi et al. on the overexpressed protein, where it was also proposed that the protein contains one or

two high-spin hemes on the basis of EPR data [10]. These two proposals appear to be mutually inconsistent as both bis-histidine and (His, Met) axial coordination commonly determine a low-spin configuration. Another problem exists with the redox properties of the hemes, which were studied both by Tan and Cowan [9] and by Bruschi et al. [10] by means of direct voltammetric techniques. This approach is nowadays well established for small electron-transferring proteins, e.g. cytochromes [11]. However, application to larger proteins, especially enzymes, is still in its infancy. It is therefore perhaps not surprising that the two groups have obtained completely different results. Furthermore, each of these sets appear quantitatively inconsistent with the notion of one or two high-spin hemes out of a total of 16. With respect to these problems, we have re-examined some of the characteristics of the Hmc from wild-type *D. vulgaris* (Hildenborough). A preliminary account of this study has already appeared [12].

Recently, a more detailed characterization has been carried out of Hmc from *D. vulgaris*, substrain Miyazaki [13]. The optically determined redox properties differ from the two sets of data determined electrochemically for *D. vulgaris*, Hildenborough [9, 10] and from the EPR-determined data presented in this study.

MATERIALS AND METHODS

Organism, growth and isolation

The sulfate reducer *D. vulgaris* (Hildenborough) NCIB 8303 was maintained on Postgate's medium [14]; large-scale growth at 35°C on lactate/sulfate was in modified Saunders' medium [15]. Stirred batch cultures of 240 l were grown under nitrogen to an A_{600} value of approximately 0.8 in 60 h from a 1% inoculum in a home-built anaerobic glass fermentor. Using a Sharples continuous-flow centrifuge, 150–200 g wet cells were collected over a 10-h period and directly processed after completing the harvesting. The cells were resuspended in three volumes of 10 mM Tris/HCl, pH 8.0, plus a spatula of $MgCl_2$, DNase, RNase, and 0.1 mM protease inhibitor phenylmethylsulfonyl fluoride. The cells were disrupted by three passages through a chilled Manton-Gaulin press at 84 MPa. The supernatant was freed of membranes by centrifugation at $120000 \times g$ for 60 min. The pH was adjusted to pH 8.0 with 1 M Tris/HCl, pH 9, and the supernatant was diluted with water to yield a conductivity of 1.2 mS/cm.

Purification of cytochromes

All column operations were performed at 4°C with a computerized Pharmacia FPLC system. The whole-cell extract (0.5 l) was applied onto a diethylaminoethyl (DEAE) Sepharose Fast Flow column (5 cm × 20 cm; flow rate 15 ml/min) equilibrated with 10 mM Tris/HCl, pH 8.0. Cytochromes were eluted with this buffer. In subsequent steps, Hmc was monitored by SDS/PAGE. The pH of the eluate was adjusted to pH 6.0 with 0.1 M Mes. The pooled fractions were centrifuged at $20000 \times g$ for 20 min, and applied onto a carboxymethyl–cellulose column (2.6 cm × 15 cm; flow rate, 1 ml/cm) equilibrated with 10 mM Mes, pH 6.0 (standard buffer). A gradient of 0–1 M NaCl in standard buffer (25 column volumes) was applied, and Hmc was eluted at approximately 0.12 M NaCl. A pooled sample of 60 ml was diluted with standard buffer to 120 ml, concentrated by elu-

tion with 1 M NaCl in standard buffer from a small carboxymethyl–cellulose column (2.5 cm × 4 cm), further concentrated over Amicon YM-30 to 5 ml and applied onto a gel-filtration column (Superdex G-75 Hiload; 2.6 cm × 61 cm; flow rate, 1.5 ml/min). With Mes standard buffer plus 150 mM NaCl, Hmc was eluted at an elution volume of approximately 140 ml corresponding to an apparent molecular mass of 68 kDa. Prolonged elution also yielded cytochrome c_3 and cytochrome c_{553} as pure fractions. A pool of 20 ml Hmc was concentrated over an Amicon YM-30 column to 5 ml, and was applied onto a strong cation exchanger (Mono S; volume 1 ml; flow rate 1 ml/min). A gradient of 0–1 M NaCl in standard buffer (50 column volumes) was applied, and Hmc was eluted at approximately 0.1 M NaCl. The final preparation was judged to be pure using SDS/PAGE. The purity index $[(A_{553}red - A_{570}red)/A_{280}ox]$ was 2.8 for Hmc, 2.6 for cytochrome c_3, and 1.0 for cytochrome c_{553}.

Analytical determinations

The concentration of Hmc was determined from the absorbance at 553 nm (a peak) of the dithionite-reduced protein using an absorption coefficient, ε, of 428 mM^{-1} cm^{-1} according to Higuchi et al. [8] and Bruschi et al. [10].

The purity of the protein was determined by SDS/PAGE (the composition of the stacking gel was 4% acrylamide and 0.1% bisacrylamide; the composition of the running gel was 20% acrylamide and 0.07% bisacrylamide) and native PAGE (the composition of the stacking gel was 4% acrylamide and 0.1% bisacrylamide; the composition of the running gel was 10% acrylamide and 0.13% bisacrylamide) using 80 × 50 × 0.75 mm gels in an LKB midget gel-electrophoresis system (Pharmacia). Isoelectric focussing was carried out with a Servalyt Precote (3-11) on a flat-bed Ultrophor Unit from Pharmacia.

Gel filtration on a Superose 12 HR 10/30 column was carried out to determine the molecular mass of the native protein using cytochrome c (12.4 kDa), trypsin inhibitor (20.1 kDa), ovalbumin (43 kDa) and bovine serum albumin (68 kDa) as the markers. The column was equilibrated with 50 mM potassium phosphate, pH 7.5, containing 150 mM NaCl before use.

Nitrite reductase and hydroxylamine reductase activities were measured as described in [16]; reduction by hydrogenase in the presence of hydrogen was measured as in [17].

Spectroscopy

Optical spectra were obtained with a computerized SLM Aminco DW 2000 ultraviolet/visible spectrophotometer.

EPR spectra were obtained with a Bruker ER-200 D spectrometer, with peripheral instrumentation and data acquisition as described before [18]. Since high accuracy is required to quantify heme signals with a resolution of 1 in 16, the following precautions were taken. The ceramic side walls of the standard rectangular cavity were rebuilt by the manufacturer (Bruker, Karlsruhe, Germany) to produce an initial high-quality baseline; a non-linearity of a few percent in the electronic-gain dial and in the 60-dB attenuator was determined using the strong pitch sample at ambient temperature and was corrected for in the heme quantifications; tubes for samples and external reference were taken from the same quartz batch and filled to the same volume in order for the resonator to always have the same loaded Q factor.
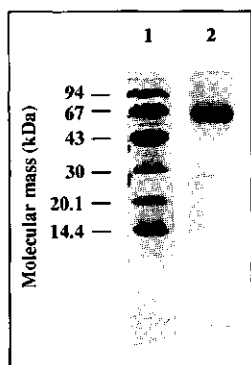
Fig. 1. Characterization of high-molecular-mass cytochrome *c* from *D. vulgaris* (Hildenborough) by SDS/PAGE. Lane 1, molecular-mass markers; lane 2, 10 µg Hmc.

Electrochemistry

EPR-monitored mediated redox titrations were performed as previously described [18]. The reductant was buffered sodium dithionite and the oxidant was potassium ferricyanide.

Cyclic voltammetry and differential pulse voltammetry were performed at 22°C in the three-electrode micro-cell (10 µl) with a nitric-acid-activated glassy carbon disc as the working electrode, as previously described [19]. The cell was driven by a computerized potentiostat (Autolab 110, Eco Chemie, Utrecht, The Netherlands).

RESULTS AND DISCUSSION

Purification and characterization of Hmc

The original isolation scheme given by Higuchi et al. is a five-step procedure that starts with an efficient step to separate a cytochrome fraction by its inability to bind to DEAE [8]. Similarly, our four-step procedure starts with DEAE chromatography. However, we have eliminated Higuchi's second step involving ammonium-sulfate precipitation. The rest of our procedure differs only slightly from the procedure described in [8]. Tan and Cowan have reported a different procedure that starts with chromatography on hydroxylapatite [9]. This three-step procedure was repeated by Bruschi et al. who found the purification to be insufficient, and who subsequently added two more chromatographic steps [10]. We have obtained a purity index $[(A_{553}red - A_{570}red)/A_{280}ox]$ of 2.8, which is identical to the value reported by Bruschi et al. [10]. Tan and Cowan have reported a reciprocal purity index $[A_{280}ox/A_{553}red]$ of 3.4, which is possibly erroneous. Neither this value nor its inverse is consistent with the published spectra in this study (Fig. 2 in [9] from which we read an $A_{280}ox/A_{553}red$ value of approximately 0.55).

Purified Hmc exhibited a single band after SDS/PAGE, native PAGE, and isoelectric focussing in this study. We present the result of SDS/PAGE in Fig. 1 in view of the purity-index problem just mentioned, and also because it has not been given before. The molecular mass determined from SDS/PAGE is 64.1 kDa, which is close to the value of 55.7 kDa calculated for the mature apoprotein on the basis of the gene sequence [4]. After gel filtration on Superose, a mass of 62 kDa was determined in good agreement with the mass of 65.5 kDa calculated for the holoprotein carrying 16

hemes [4]. After isoelectric focussing at 4°C, a single band with a pI value of 9.2 ± 0.1 was found; this value is consistent with the literature values of 9.2 (temperature not specified) [8], 8.9 (10°C) [9], and 9.2 (temperature not specified) [10].

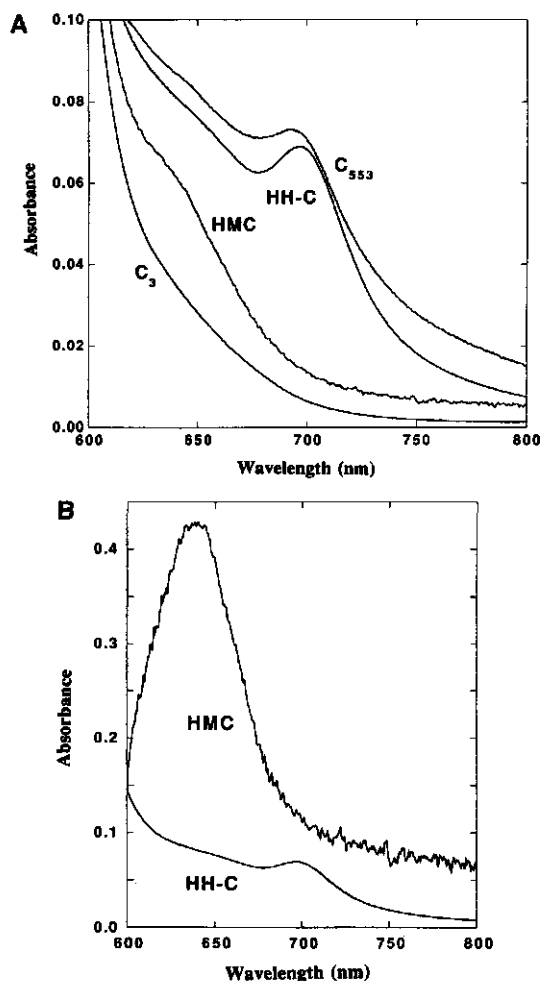### Absorption spectra are inconsistent with Met coordination

All *c*-type cytochromes with (His, Met) axial coordination have a weak absorption band in the near-infrared at approximately 695 nm due to electron transfer from the methionine sulfur to the ferric ion [20]. Axial (His, Met) coordination to one out of the 16 hemes has been proposed for *D. vulgaris* Hildenborough Hmc [4, 10]. However, in previous studies the near-infrared region has not been examined. The near-infrared spectra from four oxidized *c*-type cytochromes is shown (Fig. 2A). Horse heart cytochrome *c* and *D. vulgaris* cytochrome c_{553} have a single heme with (His, Met) coordination, and both exhibit a clear absorption band near 695 nm. *D. vulgaris* cytochrome c_3 has four bis-His coordinated hemes and does not exhibit a band at approximately 695 nm. Also, in the spectrum of Hmc no 695-nm band can be discerned.

However, if such a band was present, it would be intrinsically difficult to observe, as the protein also contains 15 bis-His coordinated hemes. Therefore, the graphical experiment shown in Fig. 2B was performed. The cytochrome spectra were normalized with respect to their amplitude at 530 nm. A difference spectrum was constructed from the spectra of Hmc and cytochrome c_3. This difference was multiplied by a factor of 16 and compared to the original spectrum of horse heart cytochrome *c*. From this comparison in Fig. 2B we conclude that, with a signal-to-noise ratio of approximately 5, oxidized Hmc exhibits no absorption band near 695 nm and therefore that none of the 16 hemes has (His, Met) coordination.

EPR spectroscopy of low-spin hemes

In Fig. 3B, the complete EPR spectrum of oxidized Hmc is given. We have made six Hmc preparations from six different batch cultures, and the EPR spectrum in each case was invariant. The spectrum is essentially identical to that reported by Tan and Cowan [9] for their triheme cytochrome and to that reported by Bruschi et al. for the 16-heme recombinant Hmc expressed in *D. desulfuricans* G200 [10]. For comparison, the spectrum of *D. vulgaris* cytochrome c_3 is presented in Fig. 3C. It is clear that the electronic structure of the iron in the bulk of the hemes in Hmc is quite similar to that for the bis-histidine coordinated hemes in cytochrome c_3. However, there are additional features (see also Figs 4 and 5), notably around $g \approx 6$, typical for high-spin heme, a positive peak around $g \approx 3.6$, typical for strained bis-histidine coordination (with the two imidazole rings in perpendicular planes [20]), and a positive peak at $g = 2.63$ with a negative peak around $g \approx 1.89$ indicative of (His, oxygen) coordination [22].

In Fig. 3 the spectrum of *D. vulgaris* cytochrome c_{553} (axial coordination: His, Met) is also given (Fig. 3D). It appears that the major feature of this spectrum, i.e. a peak at $g \approx 3.3$ has no counterpart in the spectrum of Hmc. Our presentation of this spectrum is also meant to be a correction to literature data on cytochrome c_{553} apparently flawed by a mix-up of species; Bertrand et al. have published a spectroelectrochem-

123

Fig. 3. EPR spectra of *D. vulgaris* cytochromes Hmc (A and B), c_3 (C), and c_{553} (D). The buffer was 10 mM Hepes, pH 7.0. A is the integral of the low-spin heme part of trace B (see text). The EPR conditions were as follows: microwave frequency, 9.33 MHz; microwave power, 1.3 mW (B) and 20 mW (C, D); modulation frequency, 100 kHz; modulation amplitude, 1.0 mT; temperature, 20 K (B) and 15 K (C, D).

Fig. 2. Near-infrared spectra of *D. vulgaris* cytochromes c_{553}, c_3, Hmc, and horse heart cytochrome *c* (HH-C). The buffer was 10 mM Hepes, pH 7.0. (A) The spectra were normalized with respect to the amplitude at 530 nm (of diluted samples). The absorbance scale applies to 0.34 mg/ml Hmc. (B). A difference spectrum of Hmc minus cytochrome c_3 was multiplied 16-fold (HMC) and compared to horse heart cytochrome *c* (HH-C).

ical study on *D. vulgaris* (Hildenborough) cytochrome c_{553} with an EPR spectrum (Fig. 1 in [23]) whose legend specifies *Desulfovibrio gigas* as the bacterial source. No reference is made to *D. gigas* in the description of the experiments. The spectrum presented by Bertrand et al. is different in *g* values (*g* values of 3.154 and 2.065) and in shape to our spectrum (Fig. 3D; *g* values of 3.285 and 1.96) of *D. vulgaris* (Hildenborough) cytochrome c_{553}.

Only two out of three *g* values are observed in the spectrum of cytochrome c_{553}. This is common for low-spin heme spectra [24], whose shape is dominated by the inhomogeneous broadening mechanism of *g* strain [25]. Under the assumption that *g* strain is isotropic, the apparent line width

in field-swept spectra approximately varies in field units proportional to g^{-2} [25]. Under this simple model, and using Griffith's theorem that the sum of the squared *g* values equals approximately 16 [24], it is easily calculated from the line width of the first peak at a *g* value of 3.285 that the third peak is broadened beyond detection. This problem of detectability and spin quantification becomes more severe the more the first *g* value moves downfield with increasing *g* anisotropy towards its theoretical maximum of 4. This problem is particularly apparent in the quantification of low-spin EPR from Hmc.

In Fig. 4 the low-field peaks of the low-spin hemes are examined in detail. The weak peak at $g = 3.65$ can be optimized by running at high incident microwave power levels with the peaks of the other low-spin hemes partially saturated. The shape of the $g = 3.65$ peak exhibits the characteristic cutoff at low field due to the theoretical maximum of $g = 4$ for these systems. The other two *g* values are not determined as the corresponding spectral features are too broad for detection. De Vries and Albracht have shown that the Aasa-Vänngård method of spin quantification on a single peak [26] is still possible for these highly anisotropic spectra provided that the first *g* value is greater than 3.3 [24]. Using their procedure, we find the $S = 1/2$ concentration represented by the $g = 3.65$ peak to be approximately twice the optically determined concentration of Hmc (Table 1). The other low-spin hemes can be quantified with the common single-peak integration method [26] since from the spectra a
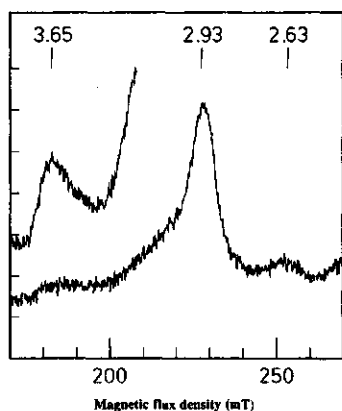
Fig. 4. Details of the low-field EPR spectrum of the low-spin hemes in *D. vulgaris* Hmc. The low-field expanded spectrum up is from the strained bis-histidine hemes ($g = 3.65$). A weak peak at $g = 2.63$ is from a putative (N, O) derivative. The EPR conditions were as follows: microwave frequency, 9323 MHz; microwave power, 1.3 mW and (expanded region) 51 mW; modulation frequency, 100 kHz; modulation amplitude, 1.0 mT; temperature, 20 K.

Fig. 5. Low-field EPR of the high-spin heme in *D. vulgaris* Hmc. The EPR conditions were as follows: microwave frequency, 9326 MHz; microwave power, 2 mW; modulation frequency, 100 kHz; modulation amplitude, 1.25 mT; temperature, 4.2 K.

Table 1. Stoichiometries, g values, and reduction potentials of the 16 hemes in high-molecular-mass cytochrome c from *D. vulgaris* (Hildenborough). The species assignment is putative. The stoichiometry is obtained by dividing the EPR-determined heme concentration over the optically determined Hmc concentration. Total EPR is the integral up to and including the last detectable peak, i.e. at $g \approx 1.5$. n.d., not determined.

Heme species	Stoichiometry	g values	E_m
			mV
Strained bis-His	2.2	3.65	≈ -200
bis-His	12	3.12−2.95, 2.25, 1.50−1.52	−201
His, O	0.7	2.63, 2.19, 1.87	n.d.
High-spin	0.4	5.8 (6.19; 5.81; 5.53)	+ 61
Total EPR	≈17	−	−

reasonable estimate can be made of all g values; the bulk of the low-spin hemes have $g_1 = 3.12-2.93$, $g_2 \approx 2.25$, $g_3 = 1.52-1.50$ (Figs 3 and 4). Quantification of the first peak gives approximately 12 hemes/Hmc. A minor component has $g_1 = 2.63$ and $g_3 = 1.89$ with the second g value probably at $g_2 \approx 2.19$. This g tensor is characteristic for low-spin (N, O) derivatives of high-spin hemes [22]. Quantification of the $g_1 = 2.63$ peak gives approximately half a low-spin heme/ Hmc, which indicates that this is part of a high-spin/low-spin set. A complete double integration of the low-spin spectrum is not strictly possible as the $g = 3.65$ spectrum is only partially detected and is expected to extend beyond the field limit of the electromagnet. However, a reasonable estimate can be made by an integration from the low-field side of the $g = 3.65$ line up to the high-field limit of the $g = 1.5$ peak. This integral is shown in Fig. 3A; it encompasses the complete spectrum of the bis-histidine hemes, the complete spectrum of the putative (N, O) derivative, and part of the spectrum of the strained bis-histidine hemes. The second in-
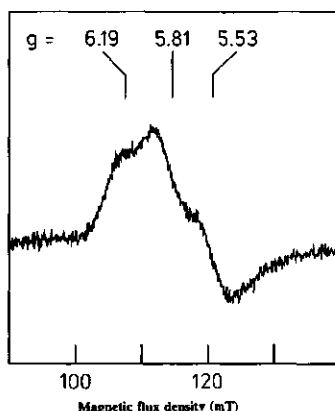
tegral corresponds to a total of approximately 17 low-spin hemes/optically determined Hmc.

EPR spectroscopy of the high-spin heme

The g_{xy} region of the high-spin heme spectrum is presented in Fig. 5. The details of this spectrum are remarkable, e.g. the g_{xy} feature is not centered around an effective g value (g_{eff}) of 6. Bruschi et al. have reported a g value of 5.57. However, no comment was made on this unusual value [10]. We find a similar g_{eff} value of approximately 5.8. Also, the fine structure of the spectrum is unusual, a positive peak at $g_{eff} = 6.19$ and derivative features at $g_{eff} = 5.81$ and 5.53. A possible explanation would be to assume two rhombicities, one essentially axial form with $g_{xy} = 5.81$ and one rhombic form with $g_x = 5.53$ and $g_y = 6.19$. The real g tensor for high-spin Fe^{3+} in an approximately octahedral ligand field is commonly near-isotropic and very close to the free-electron value $g_e = 2.0023$ [27]. High-spin ferric heme systems experience a strong zero-field interaction resulting in an isolated $m_s = \pm 1/2$ doublet with g_{eff} centered around $3 \cdot g_{xy} [1-(h\nu/D)^2/2]$ [28]. For X-band EPR, $h\nu$ is approximately 0.3 cm^{-1}; Bruschi et al. have determined in a depopulation experiment that D is approximately 12 cm^{-1} for Hmc [10]. With a real g value approximately equal to g_e this gives a perpendicular g_{eff} of approximately 6.01. The observed value of $g_{eff} \approx 5.8$ is a significant deviation from 6.01.

The deviation implies that this high-spin heme is not purely high spin, but is a mild case of quantum-mixed spin; i.e. an excited quartet ($S = 3/2$) electronic state is sufficiently close to the ground state to be quantum mechanically mixed with this ground state by spin-orbit interaction. The numerical condition for this is that the ligand-field splitting Δ is comparable in magnitude to the spin-orbit coupling constant λ. The classical example of quantum mechanical mixed spin in biology is cytochrome c' which represents a case of strong mixing, i.e. $\Delta/\lambda \approx 1$ [29]. Other less well defined, weaker cases of quantum mechanical spin mixing are found in the hemeprotein peroxidases [29]. Interestingly, the unusual shape of the Hmc spectrum (compare Fig. 5) is quite similar

125

to that of cytochrome c' (compare [29]). The present identification of the high-spin heme in Hmc as a quantum spin mixture is the second example of such a system from sulfate-reducing bacteria. We have recently reported the first example, i.e. high-spin siroheme in the dissimilatory sulfite reductase from *Desulfosarcina variabilis* [30]. According to a model calculation by Maltempo and Moss for tetragonal symmetry [29], the $g \approx 5.8$ signal in Hmc defines $\Delta/\lambda = 1.94$ and therefore $\Delta \approx 800$ cm^{-1}.

The high-spin heme spectrum is partially obscured by the low-spin components; the parallel g value (expected at $g \approx 2$) is not readily identified. Therefore, the amount of high-spin heme cannot be determined by double integration. Bruschi et al. have proposed numerical simulations of the spectrum in order to study the integrated intensity as a function of temperature [10]. Their algorithm is based on the statistical theory of g strain. However, this theory was developed explicitly for $S = 1/2$ systems [31]. No justification has ever been given in the literature for its application to high-spin systems. Aasa et al. have made the point that partial integration of the experimental trace up to a defined effective g value is an acceptable way of quantifying this type of spectra [32]. We have followed their procedure by integrating the high-spin EPR spectra of Hmc approximately over the range shown in Fig. 5 and comparing this to the partial integral over the same range of a metmyoglobin standard. Data taken at a temperature of 4.2 K were used to avoid the complication of depopulation of the ground state Kramers doublet at higher temperatures. With this method, the $g \approx 5.8$ signal represented less than half a high-spin system/Hmc molecule. We propose that the balance (i.e. adding up to one spin system/Hmc) is found in the low-spin (N, O) derivative (Table 1).

EPR redox titration

An equilibrium reductive/oxidative titration of Hmc was carried out with buffered sodium dithionite as the reductant and potassium ferricyanide as the oxidant in the presence of 13 different dye-stuff mediators (see [18] for experimental details), and samples were removed at defined potentials for EPR samples. No changes in individual EPR line shapes, only in intensities, were observed in the course of the titration. The amplitude (peak-to-trough) of the high-spin signal around $g \approx 5.8$ and the amplitude (baseline-to-peak) of the bulk of the low-spin signals at $g = 2.93$ are plotted as intensities versus solution potential (Fig. 6). The intensity of the shoulder at $g \approx 3.1$ essentially follows the intensity of the $g = 2.93$ peak. The strained bis-histidine hemes are more difficult to monitor because of the intrinsically low intensity of the spectrum. The peak at $g = 3.65$ also appeared to follow the $g = 2.93$ peak. In order to corroborate this observation, a separate purification of Hmc was carried out and all of the purified protein was used to prepare five samples of concentrated protein at potentials of approximately -0.2 V. The relative amplitude of the $g = 3.65$ peak from these samples is also plotted in Fig. 6.

The $g = 2.93$ peak represents several different hemes. It is therefore to be expected that its intensity versus potential profile will not exactly follow a Nernst relationship for a single, one-electron transferring center. The $g = 2.93$ data have been fitted to a Nernst curve with $E_{m7.5} = -201$ mV and $n = 0.6$ in Fig. 6. It is concluded that all 15 bis-histidine hemes have a reduction potential at pH 7.5 within a maximal band of 100 mV full width around $E_m = -0.20$ V.

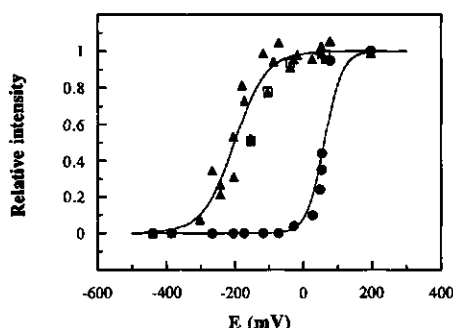The reduction potential of the high-spin heme is approximately 0.3 V more positive, namely at $E_{m7.5} = +61$ mV when the data are fitted with $n = 1$ (Fig. 6). However, the present signal-to-noise ratio precludes an accurate determination of the n value. The putative (N, O) derivative also appears to become reduced early in the titration. However, we have been unable to quantitatively follow the amplitude reduction of its weak EPR signal.

Voltammetry

The application of cyclic voltammetry and related techniques to the study of redox properties of small (approximately $6-20$ kDa) electron-transferring proteins has become possible over the last decade. At least for some of these proteins, stable, reproducible, and electrochemically reversible direct responses have been obtained at solid electrodes especially of the carbon type [12, 19, 32].

This applicability is certainly not true at the present time for voltammetry on larger proteins (greater than 20 kDa), especially enzymes. Despite considerable efforts in this area over the last years, very few direct electrochemical responses have been reported so far. Some of the determined responses are extremely complicated [34], others are poorly characterized and are not consistent with data obtained by other methods (compare hemoglobin in [35] versus [36], and superoxide dismutase in [37] versus [38]). It should be obvious that studies involving novel, direct electrochemistry of a larger protein must include a description of reproducibility and reversibility of the response and consistency with data obtained by other methods.

Tan and Cowan [9] and Bruschi et al. [10] have reported the direct electrochemistry of Hmc on carbon electrodes. These reports do not fit the criteria of quality just formulated. Only single scans at a single potential scan rate are given and thus reversibility is not documented. One of the two transitions found by Tan and Cowan can only be observed once, namely in the very first reduction [9]. Bruschi et al. found three different transitions of approximately equal current density ($E_m \approx 0$, -100, -250 mV), none of which corresponded to either one of the two transitions of approximately equal current density ($E_m = -59$, -400 mV) reported by Tan and Cowan. No comparison was made with E_m values

determined by other methods. Both electrochemical studies are qualitatively and quantitatively inconsistent with the EPR data reported in this study. In a reversible system, all 16 hemes should contribute quantitatively to the electrochemical response. Our EPR results predict for the electrochemistry a broad feature at approximately $E_m = -201$ mV and a single transition at $E_m = +61$ mV with an integrated maximal current intensity 1/16 times that of the broad feature.

We have attempted to reproduce the electrochemical experiments on Hmc using activated glassy carbon as previously described [19]. A variety of conditions were tried including slow-scanning cyclic voltammetry, fast-scanning cyclic voltammetry, differential-pulse voltammetry, bare electrodes, the addition of promotors (e.g. neomycin), variation in protein concentrations, pH variation, temperature variation, and ionic-strength variation. These experiments produced variable results. Reproducibility was poor with respect to the number of redox steps and their apparent E_m values and current density. The development of the response with respect to time was also erratic. In a very qualitative sense, the cyclic voltammograms and the differential-pulse voltammograms have the shape expected on the basis of the EPR titration, namely they are dominated by a broad feature centered at a potential approximately (i.e., ± -150 mV) corresponding to the $E_m \approx -201$ mV for the low-spin hemes.

In conclusion, there is an indication that direct electrochemistry of this 65-kDa protein (as may also be the case for many other larger proteins) may become practical in the future if the proper conditions are established for these type of experiments. Currently, no meaningful information can be determined from the electrochemistry of Hmc; the reports by Tan and Cowan and by Bruschi et al. have been premature [9, 10]. Loufti et al. have reported the electrochemistry of a 26-kDa cytochrome c_3 from *D. vulgaris* [5]. Bruschi et al. have suggested that this protein is a breakdown product of Hmc [10]. Interestingly, the differential pulse voltammetry of the 26-kDa cytochrome indicates an average reduction potential of approximately -180 mV at pH 7.6 [5]; this value is close to the average value that we find in EPR titration.

Nomenclature

The protein characterized in this study poses a nomenclature probleme. The name 'high-molecular-weight cytochrome' was introduced by Yagi for a protein isolated from *D. vulgaris*, strain Miyazaki F [6]. It was subsequently adopted by Higuchi et al. for the protein from *D. vulgaris*, strain Hildenborough [8]. Alternatively, these authors also used the name hexadecahemoprotein, and this was later adopted by Pollock et al. as hexadecacytochrome c in their work on the structural-gene sequence [4]. Tan and Cowan re-named the protein triheme cytochrome [9]. Subsequently, Bruschi et al. reverted to the original name, extending it with the epitaph 'c' to 'high-molecular-weight cytochrome c', and shortened this to Hmc most probably in analogy to the common practice in the naming of genes [10]. Finally, Ogata et al. have re-assigned the abbreviation Hmc to high-molecular-mass cytochrome c_3.

The name triheme cytochrome is obviously incorrect due to an erroneous determination of the heme content. The trivial name cytochrome c_3 is an unfortunate relic from the time that this tetraheme cytochrome was thought to contain only three hemes. The proposed usage of in the name high-molecular-mass cytochrome c_3 is, in our view, particularly unfortunate, not only because of its analogy to the erroneous triheme
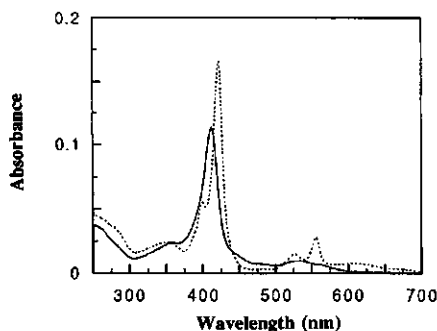

Fig. 7. Optically detected reduction of *D. vulgaris* Hmc by Fe-hydrogenase in the presence of molecular hydrogen. (——) Hmc (4.2 µg/ml) as isolated (i.e. oxidized); (– – –) Hmc was mixed with hydrogenase (30 U) and incubated under 120 kPa H_2 for 5 min at 22°C.

cytochrome, but also because it suggests a structural and/or functional similarity between Hmc and cytochrome c_3. A structural similarity between cytochrome c_3 and certain domains of Hmc has been proposed [4]. However, this cannot possibly apply to the whole structure of Hmc which includes a high-spin heme.

Although cytochrome may not be a proper label for a putative enzyme, we propose to retain the trivial name Hmc, meaning high-molecular-mass cytochrome, as long as the biological function of the protein has not been established.

Putative function of Hmc

The 16 hemes of the high-molecular-mass cytochrome c from the periplasmic space of *D. vulgaris*, strain Hildenborough, have been quantitatively identified with EPR spectroscopy. There are 13 low-spin hemes with bis-His coordination and two low-spin hemes with strained bis-histidine coordination. Methionine is not an axial ligand. All 15 low-spin hemes have a reduction potential $E_{m,7.5}$ of -201 ± 50 mV. The 16-th heme is clearly different from the other hemes in that it is high spin (or, rather, quantum-mixed spin close to the high-spin limit), and it has a 0.3-V higher reduction potential $E_{m,7.5}$ of $+61$ mV. This configuration suggests that Hmc is not a simple electron-tranferring cytochrome, but rather a redox enzyme (the high-spin heme) combined in a single polypeptide with an electron-transfer chain (15 low-spin hemes). Tan and Cowan have claimed the detection of nitrite reductase activity and hydroxylamine reductase activity (unpublished observations quoted in [9]). We have not been able to detect any nitrite reductase or hydroxylamine reductase activity in our Hmc preparations.

Rossi et al. have recently determined the nucleotide sequence of what they named the *hmc* operon of *D. vulgaris* (Hildenborough), an operon consisting of eight open-reading frames the first of which encodes Hmc. On the basis of comparison of the translated protein sequences with proteins of known or proposed function, Rossi et al. proposed that Hmc is part of a transmembrane protein complex that allows electron flow from the periplasmic hydrogenases to the cytoplasmic enzymes that catalyze the reduction of sulfate [39]. Unfortunately, there are no enzymological data to support this detailed proposal. We have, therefore, attempted to mea-

sure electron transfer of Hmc from/to the Fe-hydrogenase (i.e. the only periplasmic hydrogenase thus far identified in *D. vulgaris*). Indeed, addition of a catalytic amount of hydrogenase to a solution of Hmc and subsequent incubation under molecular hydrogen resulted in essentially complete reduction of the Hmc as detected by optical spectroscopy (Fig. 7). Thus, the proposal of Rossi et al. is consistent with but not proved by our observation. More elaborate kinetic experimentation will be required to verify the possible significance of Hmc and to establish the biological function of this protein.

REFERENCES

1. LeGall, J. & Fauque, G. (1988) Dissimilatory reduction of sulfur compounds, in *Biology of anaerobic microorganisms* (Zehnder, A. J. B., ed.) pp. 587–639, Wiley, New York.
2. Van Rooijen, G. J. H., Bruschi, M. & Voordouw, G. (1989) Cloning and sequencing of the gene encoding cytochrome c_{553} from *Desulfovibrio vulgaris* Hildenborough, *J. Bacteriol. 171*, 3575–3578.
3. Voordouw, G. & Brenner, S. (1986) Cloning and sequencing of the gene encoding cytochrome c_3 from *Desulfovibrio vulgaris* Hildenborough, *Eur. J. Biochem. 159*, 347–351.
4. Pollock, W. B. R., Loufti, M., Bruschi, M., Rapp-Giles, B. J., Wall, J. & Voordouw, G. (1991) Cloning, sequencing, and expression of the gene encoding the high-molecular-weight cytochrome *c* from *Desulfovibrio vulgaris* Hildenborough, *J. Bacteriol. 173*, 220–228.
5. Loufti, M., Guerlesquin, F., Bianco, P., Haladjian, J. & Bruschi, M. (1989) Comparative studies of polyhemic cytochromes *c* isolated from *Desulfovibrio vulgaris* (Hildenborough) and *Desulfovibrio desulfuricans* (Norway), *Biochem. Biophys. Res. Commun. 159*, 670–676.
6. Yagi, T. (1969) Formate:cytochrome oxidoreductase of *Desulfovibrio vulgaris*, *J. Biochem. (Tokyo) 66*, 473–478.
7. Yagi, T. (1979) Purification and properties of cytochrome *c*-553, an electron acceptor for formate dehydrogenase of *Desulfovibrio vulgaris*, Miyazaki, *Biochim. Biophys. Acta 548*, 96–105.
8. Higuchi, Y., Inaka, K., Yasuoka, N. & Yagi, T. (1987) Isolation and crystallization of high molecular mass cytochrome from *Desulfovibrio vulgaris* Hildenborough, *Biochim. Biophys. Acta 911*, 341–348.
9. Tan, J. & Cowan, J. A. (1990) Coordination and redox properties of a novel trihene cytochrome from *Desulfovibrio vulgaris* (Hildenborough), *Biochemistry 29*, 4886–4892.
10. Bruschi, M., Bertrand, P., More, C., Leroy, G., Bonicel, J., Haladjian, J., Chottard, G., Pollock, W. B. R. & Voordouw, G. (1992) Biochemical and spectroscopic characterization of the high molecular mass cytochrome *c* from *Desulfovibrio vulgaris* Hildenborough expressed in *Desulfovibrio desulfuricans* G200, *Biochemistry 31*, 3281–3288.
11. Armstrong, F. (1990) Probing metalloproteins by voltammetry, *Struct. Bonding 72*, 137–230.
12. Hagen, W. R., Verhagen, M. F. J. M., Pierik, A. J., Wolbert, R. B. G., Mallée, L. F. & Voorhorst, W. G. B. (1993) Axial coordination and reduction potentials of the 16 hemes in high-molecular-weight cytochrome *c* from *Desulfovibrio vulgaris*, *J. Inorg. Biochem. 51*, 28.
13. Ogata, M., Kiuchi, N. & Yagi, T. (1993) Characterization and redox properties of high molecular mass cytochrome c_3 (Hmc) isolated from *Desulfovibrio vulgaris* Miyazaki, *Biochimie (Paris) 75*, 977–983.
14. Postgate, J. R. (1951) On the nutrition of *Desulphovibrio desulfuricans*, *J. Gen. Microbiol. 5*, 714–724.
15. Van der Westen, H. M., Mayhew, S. G. & Veeger, C. (1978) Separation of hydrogenase from intact cells of *Desulfovibrio vulgaris*. Purification and properties, *FEBS Lett. 86*, 122–126.
16. Odom, J. M. & Peck, H. D. Jr (1981) Localization of dehydrogenases, reductases, and electron transfer components in the sulfate-reducing bacterium *Desulfovibrio gigas*, *J. Bacteriol. 147*, 161–169.
17. Verhagen, M. F. J. M., Wolbert, R. B. G. & Hagen, W. R. (1994) Cytochrome c_{553} from *Desulfovibrio vulgaris* (Hildenborough): electrochemical properties and electron transfer with hydrogenase, *Eur. J. Biochem. 221*, 821–829.
18. Pierik, A. J. & Hagen, W. R. (1991) $S = 9/2$ EPR signals are evidence against coupling between the siroheme and the Fe/S cluster prosthetic groups in *Desulfovibrio vulgaris* (Hildenborough) dissimilatory sulfite reductase, *Eur. J. Biochem. 195*, 505–516.
19. Hagen, W. R. (1989) Direct electron transfer of redox proteins at the bare glassy carbon electrode, *Eur. J. Biochem. 182*, 523–530.
20. Pettigrew, G. W. & Moore, G. R. (1990) *Cytochromes c: evolutionary, structural and physicochemical aspects*, Springer, Berlin.
21. Walker, F. A., Huynh, B. H., Scheidt, W. R. & Osvath, S. R. (1986) Models of the cytochromes *b*. Effect of axial ligand plane orientation on the EPR and Mössbauer spectra of low-spin ferrihemes, *J. Am. Chem. Soc. 108*, 5288–5297.
22. Palmer, G. (1985) The electron paramagnetic resonance of metalloproteins, *Biochem. Soc. Trans. 13*, 548–560.
23. Bertrand, P., Bruschi, M., Denis, M., Gayda, J.-P. & Manca, F. (1982) Cytochrome c_{553} from *Desulfovibrio vulgaris*: potentiometric characterization by optical and EPR studies, *Biochem. Biophys. Res. Commun. 106*, 756–760.
24. De Vries, S. & Albracht, S. P. J. (1979) Intensity of highly anisotropic low-spin heme EPR signals, *Biochim. Biophys. Acta 546*, 334–340.
25. Hagen, W. R. (1981) Dislocation strain broadening as a source of anisotropic line width and asymmetrical line shape in the electron paramagnetic resonance spectrum of metalloproteins and related systems, *J. Magn. Reson. 44*, 447–469.
26. Aasa, R. & Vänngård, T. (1975) EPR signal intensity and powder shapes: a reexamination, *J. Magn. Reson. 19*, 308–315.
27. Abragam, A. & Bleaney, B. (1970) *Electron paramagnetic resonance of transition ions*, Clarendon Press, Oxford.
28. Von Waldkirch, T., Müller, K. A. & Berlinger, W. (1972) Analysis of the Fe^{3+}-V_O center in the tetragonal phase of $SrTiO_3$, *Phys. Rev. B 5*, 4324–4334.
29. Maltempo, M. M. & Moss, T. H. (1976) The spin 3/2 state and quantum spin mixtures in haem proteins, *Quart. Rev. Biophys. 9*, 181–215.
30. Arendsen, A. F., Verhagen, M. F. J. M., Wolbert, R. B. G., Pierik, A. J., Stams, A. J. M., Jetten, M. S. M. & Hagen, W. R. (1993) The dissimilatory sulfite reductase from *Desulfosarcina variabilis* is a desulforubidin containing uncoupled metallated sirohemes and $S = 9/2$ iron-sulfur clusters, *Biochemistry 32*, 10323–10330.
31. Hagen, W. R., Hearshen, D. O., Sands, R. H. & Dunham, W. R. (1985) A statistical theory for powder EPR in distributed systems, *J. Magn. Reson. 61*, 220–232.
32. Aasa, R., Albracht, S. P. J., Falk, K.-E., Lanne, B. & Vänngård, T. (1976) EPR signals from cytochrome *c* oxidase, *Biochim. Biophys. Acta 422*, 260–272.
33. Link, T. A., Hagen, W. R., Pierik, A. J., Assmann, C. & von Jagow, G. (1992) Determination of the redox properties of the Rieske [2Fe-2S] cluster of bovine heart bc_1 complex by direct electrochemistry of a water-soluble fragment, *Eur. J. Biochem. 208*, 685–691.
34. Sucheta, A., Ackrell, B. A. C., Cochran, B. & Armstrong F. A. (1992) Diode-like behaviour of a mitochondrial electron-transport enzyme, *Nature 356*, 361–362.

35. Song, S. & Dong, S. (1988) Spectroelectrochemistry of the quasi-reversible reduction and oxidation of hemoglobin at a methylene blue adsorbed modified electrode, *J. Electroanal. Chem.* 253, 337–346.
36. Taylor, J. F. & Hastings, A. B. (1939) Oxidation-reduction potentials of the methemoglobin-hemoglobin system, *J. Biol. Chem.* 131, 649–662.
37. Borsari, M. & Azab, H. A. (1992) Voltammetric behaviour of bovine erythrocyte superoxide dismutase, *J. Electroanal. Chem.* 342, 229–233.
38. Fee, J. A. & DiCorletto, P. E. (1973) Observations on the oxidation-reduction properties of bovine erythrocyte superoxide dismutase, *Biochemistry 12*, 4893–4899.
39. Rossi, M., Pollock, W. B. R., Reij, M. W., Keon, R. G., Fu, R. & Voordouw, G. (1993) The *hmc* operon of *Desulfovibrio vulgaris* subsp. *vulgaris* Hildenborough encodes a potential transmembrane redox protein complex, *J. Bacteriol. 175*, 4699–4711.

Chapter 11

Summary
Samenvatting

Summary

The use of electrochemical techniques in combination with proteins started approximately a decade ago and has since then developed into a powerfull technique for the study of small redox proteins. In addition to the determination of redox potentials, electrochemistry can be used to obtain information about the kinetics of electron transfer between proteins and about the dynamic behaviour of redox cofactors in proteins. This thesis describes the results of a study, initiated to get a better insight in the conditions necessary to obtain electron transfer between solid state electrodes and proteins.

Flavin Adenine Dinucleotide (FAD) is the subject of chapter 2. The electrochemical behavior of this cofactor, which is present in some flavoproteins, appeared to be dependent on its solution concentration. At concentrations of 1 μM the voltammetry showed all the characteristics of a species adsorbed to the surface. At a thousandfold higher concentration the voltammetry became completely diffusion controlled. From experiments at intermediate concentrations it was concluded that part of the FAD molecules adsorb to the electrode. Furthermore, it was shown that electron transfer between the molecules in solution and the electrode can only take place through the adsorbed molecules, which act as mediators. A comparison with results obtained with a 2 [4Fe-4S] ferredoxin from *Megasphaera elsdenii* suggested that, under certain conditions, a similar mechanism of selfmediation can be valid for proteins.

The results of a study of cytochrome c 553 from *D. vulgaris* (H) are presented in chapter 3. The cytochrome was characterized by cyclic voltammetry and the same technique was used to determine the rate of electron transfer between the cytochrome and the Fe-hydrogenase from the same organism. The results indicated that the cytochrome was a physiologically competent redox partner dependent on the *in vivo* function of the hydrogenase. Since the function of the hydrogenase is still an issue of debate it is not known whether this new electron transfer pathway has physiological relevance.

The reinvestigation of the protein desulfoferrodoxin from *D. vulgaris* (H) is described in chapter 4. This protein was reported to contain two iron atoms one of which was coordinated by four cysteine residues in a distorted tetrahedron. By comparison with model compounds using EPR spectroscopy and by using cyclic voltammetry at different pH values it was shown that this is very unlikely. Instead it is proposed that the iron atom is coordinated in a pentagonal bipyramid (surrounded by 5 ligands in a plane and 2 ligands perpendicular to and on both sides of this plane). Furthermore the controversy about the protein having a mixed N-terminus was elucidated and it was established that the protein was a homodimer instead of the reported monomer.

The conditions necessary for the use of direct electrochemistry to study small redox proteins become more and more established. The application of this technique to enzymes is, however, not straightforward. The reason for this is not clear, but one possibility is that a large

enzyme adsorbs more easily to the electrode than a small protein. Another possible explanation is that the redox cofactors in enzymes are shielded more by the protein matrix. In order to circumvent this latter problem we tried to establish conditions for the electron transfer between cytochrome P-450 from *P. putida* and glassy carbon electrodes. This bacterial cytochrome P-450 has a ferredoxin as a physiological electron donor and has therefore a docking place where the electrons can enter the enzyme. When using the right conditions it should be possible to let the electrode be the "substrate" for the enzyme. Unfortunately the enzyme adsorbed to the electrode and the obtained value for the potential was much more positive than the literature value. An EPR redox titration of the cytochrome P-450 indicates that the literature value needs a correction. However, there still remains a difference between the value obtained from the titration in homogeneous solution and the value determined electrochemically.

Recent reports about electrochemical characterization of superoxide dismutase from bovine erythrocytes incited the study described in chapter 6. The conditions used in the reported electrochemical experiments were rather extreme i.e. low pH. EPR monitored redox titrations of the enzyme at different pH values indicated that the oxidation and reduction at low pH values is not reversible. Furthermore, it was found that the reported potentials at pH 7.0 needed to be corrected. A redox titration was also performed with the iron enzyme from *E. coli* as a comparison with the copper zinc containing enzyme. After reduction, however, it was not possible to reoxidize the enzyme again indicating that the redox reaction is not reversible. This can explain the huge differences in potentials reported so far in the literature.

The use of a redox active promotor can give some insight in its mechanism of action. The lanthanide europium proved to be a potent promotor of rubredoxin. The latter is a small purple redox protein containing a single iron coordinated to 4 cysteine residues. At high pH values the reduction and oxidation of rubredoxin is readily obtained despite the fact that the europium ion does not show any reduction or oxidation anymore. This is not consistent with the models used to explain the promotor function of cations. These models all assume that the cation provides charge compensation and sandwiches both between the protein and the electrode as well as between different protein molecules. The results from this study are presented in chapter 7.

A great advantage of electrochemistry using glassy carbon electrodes is that it is possible to vary the potential between approximately -1 V and +0.8 V. This makes it possible to study redox couples with potentials more negative than the commonly used chemical reductants like dithionite or titanium citrate. This led to the discovery of the superreduction of the Rieske cluster in the soluble fragment of the *bc1* complex of beef heart as described in chapter 8. This protein contains an [2Fe-2S] cluster with a redox potential of + 312 mV versus SHE. At low potential (-840 mV versus SHE) it is possible to reduce this cluster with a second electron. The physiological relevance of this superreduced state is not clear but its characterization can give insight in the mechanism of multiple electron transfer by iron sulfur clusters.

The final two chapters are used to describe the biochemical and spectroscopic characterization of two proteins from *D. vulgaris* . Adenylyl sulphate reductase (*AdoPSO4* reductase) is an enzyme which is involved in the sulfate respiration of the bacterium. It reduces the activated sulfate (*AdoPSO4*) to AMP and sulfite. Literature reports indicated that the protein contained one FAD and two [4Fe-4S] clusters. The presence of two clusters was based on the observation of a complicated EPR spectrum which indicates interaction between two paramagnetic centers. In our studies however this "interaction" spectrum only appeared when the enzyme solution was at low ionic strength. Upon raising the ionic strength with an inert salt like NaCl the complicated EPR spectrum changed into a spectrum of a single S=1/2 species. This indicated that the interaction between the paramagnetic centers was intermolecular rather than intramolecular. This observation led us to propose that *AdoPSO4* reductase contains one FAD and one Fe-S cluster. Since the average metal analysis showed the presence of 6 iron atoms and 5 acid labile sulfur atoms it was proposed that the Fe-S cluster may have an iron content greater than 4.

Chapter 10 describes the results of a study of high molecular weight cytochrome *c* . This protein resides in the periplasmic space of *D. vulgaris* and contains sixteen hemes. Its function is up till now unknown. In previous reports midpoint potentials were reported for the different hemes based on single scan differential pulse voltammetry. These values might be erroneous due to the absence of reversibility. Indeed an equilibrium redox titration monitored by EPR indicated that the reported values were incorrect. Furthermore, it was not possible to reproduce the reported voltammograms. This confirmed our observation that the electrochemistry of large proteins or enzymes is often difficult to interpret and difficult to reproduce. It is also a good example of how important it is to check whether or not reversibility applies during electrochemical experiments.

Samenvatting

De aandacht voor het gebruik van electrochemische technieken bij het karakteriseren van redoxeiwitten bestaat al tientallen jaren. Daarvoor was electrochemie een techniek die voorbehouden was aan fysisch chemische laboratoria. In deze laboratoria wordt electrochemie tot op de dag van vandaag gebruikt voor het bestuderen van processen zoals de redoxchemie van metaal ionen, corrosie van metalen voorwerpen en de werking van batterijen. De belangstelling van de biochemici voor electrochemie kwam voort uit de behoefte naar betere en snellere methodes om de eigenschappen van redoxeiwitten te bestuderen. Redoxeiwitten zijn essentieel voor alle levensvormen op aarde en maken het onder andere mogelijk om de energie opgeslagen in de voeding te benutten voor groei, deling en warmte.

Een intrinsieke eigenschap van redoxeiwitten is de redoxpotentiaal. De redoxpotentiaal is een maat voor de energie nodig om een bepaalde verbinding te reduceren (= een electron op te laten nemen). Een manier om deze potentiaal te bepalen is het uitvoeren van een evenwichts redoxtitratie. In zo'n titratie wordt het eiwit met behulp van een chemische reductor in kleine stapjes gereduceerd waarbij de potentiaal van de oplossing gemeten wordt met behulp van twee electrodes en een voltmeter. Bij verschillende potentiaalwaarden worden monsters genomen en deze worden met een spectroscopische techniek (Electron Paramagnetische Resonantie (EPR) of optische spectroscopie) gekarakteriseerd. Van elk monster wordt bepaald welk percentage is gereduceerd. Onder gecontroleerde omstandigheden (constante temperatuur en pH) levert dit de zogenaamde 'midpoint' potentiaal op als de waarde waarbij 50% van het monster is gereduceerd. Met behulp van de eerder genoemde electrochemische technieken kan deze 'midpoint' potentiaal echter op een veel eenvoudiger en minder kostbare manier worden bepaald. Men begon de mogelijkheden hiervan dan ook te onderzoeken, maar voordat de electrochemie daadwerkelijk toegepast kon worden op eiwitten dienden eerst een aantal aanpassingen te worden doorgevoerd. Zo bedroeg het meetvolume van de commercieel verkrijgbare apparatuur enige milliliters terwijl de biochemici in het algemeen veel kleinere volumes beschikbaar hebben. Kwik werd bovendien veelvuldig gebruikt als electrode materiaal. Eiwitten denatureren over het algemeen op een kwikoppervlak en de combinatie van kwik en eiwit is dus niet bruikbaar. Deze problemen konden echter goed worden opgelost door het gebruik van geminiaturiseerde electrochemische cellen en alternatieve electrode materialen. Het grootste probleem bleek te schuilen in het verkrijgen van een goede electronenoverdracht tussen het redoxeiwit en de vaste stof electrode.

Een doorbraak kwam eind jaren zeventig toen er werd ontdekt dat het mogelijk was om cytochroom c, een klein rood electron transporterend eiwit met een heem groep, te reduceren en oxideren met behulp van een goud electrode waarop een coating van een organisch molekuul was aangebracht. Een goud electrode zonder deze coating bleek niet geschikt. Het idee werd gepostuleerd dat het mogelijk was om alle soorten redoxeiwitten met behulp van de electrochemie te bestuderen indien een geschikte coating werd gebruikt. Naarstig werden vele

136

organische stoffen getest op hun bruikbaarheid in de eiwit electrochemie. De interesse van de biotechnologische industrie was gewekt want eiwit electrochemie zou mogelijkheden op kunnen leveren om biosensoren te ontwikkelen. In deze sensoren worden enzymen gebruikt om, heel specifiek, een bepaalde stof in een mengsel te detecteren. Het best ontwikkelde en meest bekende voorbeeld is de glucosesensor. Deze sensor wordt door suikerpatienten gebruikt om de concentratie glucose in het bloed vast te stellen. De basis van deze sensor is de oxidatie van het enzym glucose oxidase met behulp van een vaste stof electrode.

In de loop van de tijd werd duidelijk dat het gebruik van organische hulpstoffen tijdens de electrochemische metingen geen goede oplossing is. Het blijkt slechts mogelijk om zeer globale regels op te stellen voor de combinatie van eiwit en hulpstof. Dit maakt het noodzakelijk om voor elk afzonderlijk eiwit een serie stoffen te testen op hun bruikbaarheid. Uiteraard is dit een tijdrovende bezigheid. Een gedeeltelijke oplossing is gevonden in het gebruik van een ander type electrode. De toepassing van een koolstofelectrode ('glassy carbon') in plaats van een goud electrode maakt het gebruik van hulpstoffen voor een aantal eiwitten overbodig. In dit proefschrift staan de resultaten beschreven verkregen uit het bestuderen van verschillende eiwitten met behulp van dit type koolstofelectrode.

In hoofdstuk 1 worden de redoxeigenschappen van de cofactor Flavin Adenine Dinucleotide (FAD) beschreven . Deze cofactor komt voor in flavoproteïnen waar het onderdeel uitmaakt van het actieve centrum. In de meeste gevallen is deze cofactor niet covalent gebonden aan het enzym. Dit is ook het geval in het enzym glucose oxidase dat gebruikt wordt in de eerder genoemde glucose sensoren. In experimenten met dit enzym kan er dus niet-gebonden FAD aanwezig zijn. Voor een juiste interpretatie van de electrochemische experimenten met dit soort enzymen is het daarom belangrijk dat het gedrag van dit ongebonden FAD tijdens de reductie en oxidatie met behulp van een koolstofelectrode bekend is. Het ongebonden FAD blijkt, wanneer het aanwezig is in lage concentraties, te adsorberen aan de electrode. Deze geadsorbeerde laag kan zeer snel electronen opnemen en afgeven aan de electrode. Bij hogere concentraties FAD fungeert de geadsorbeerde laag als een doorgeefluik. Alhoewel het gehele electrode oppervlak in contact staat met de oplossing blijkt het FAD in oplossing slechts electronen op te kunnen nemen via de geadsorbeerde laag. Aangezien deze laag niet het gehele electrode oppervlak bedekt lijkt de electrode kleiner dan het geometrische oppervlak. Dit effect van "oppervlakte mediatie" is ook waargenomen voor sommige eiwitten.

Cytochroom c553 is een klein rood heem eiwit dat voorkomt in de periplasmatische ruimte van de sulfaatreduceerder *Desulfovibrio vulgaris* . De functie van dit eiwit is niet bekend. Tijdens de electrochemische studies van dit eiwit, die beschreven zijn in hoofdstuk 2, bleek er een zeer efficiënte electronenoverdracht mogelijk te zijn tussen dit cytochroom en het enzym hydrogenase. Dit enzym katalyseert de reversibele reaktie

$$H_2 <\text{-}> 2H^+ + 2e^-$$

137
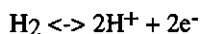
Alhoewel de precieze functie van dit enzym in deze bacterie niet bekend is wordt al geruime tijd aangenomen dat cytochroom c3 de natuurlijke redox partner voor het hydrogenase is. Deze veronderstelling is gebaseerd op het feit dat er een snelle electronenoverdracht mogelijk is tussen dit cytochroom en hydrogenase. De waarneming dat de electronen overdracht tussen hydrogenase en de twee verschillende cytochromen met vergelijkbare snelheid plaats vindt zet dit idee op losse schroeven. Afhankelijk van de functie van het hydrogenase kunnen beide cytochromen optreden als redoxpartners.

In hoofdstuk 3 wordt de spectroscopische en electrochemische karakterisering van het eiwit 'desulfoferrodoxine' beschreven. Dit eiwit, met een tot nog toe onbekende functie, is geïsoleerd uit *Desulfovibrio vulgaris*. In de literatuur werd beschreven dat dit eiwit twee ijzer ionen (Fe) bevat die op een specifieke manier zijn gecoördineerd. Voor één van de ijzers werd voorgesteld dat deze aan het eiwit gebonden is door middel van 4 in het eiwit aanwezige zwavel liganden (S). Met behulp van 'Electron Paramagnetische Resonantie' (EPR), een techniek waarmee o.a. ijzerionen bestudeerd kunnen worden en die erg gevoelig is voor de direct omgeving waarin dit ijzerion zich bevindt, en met cyclische voltammetrie bij verschillende pH's werd aangetoond dat de eerder voorgestelde coördinatie niet juist is. Door vergelijking met modelverbindingen werden aanwijzingen verkregen dat het ijzerion gecoördineerd is in een pentagonale bipyramide (omringd door 7 liganden waarvan 5 in een horizontaal vlak en 2 aan weerskanten van dit vlak) en naast zwavel nog andere liganden heeft, die bovendien geprotoneerd kunnen worden.

De tot nu toe beschreven electrochemische experimenten hebben alle betrekking op relatief kleine eiwitten zonder katalytische activiteit. Als een vervolg hierop is gezocht naar mogelijkheden om directe electrochemische technieken toe te passen op enzymen. Dit zou het bestuderen van deze enzymen zonder meer vergemakkelijken en bovendien eventuele biotechnologische toepassingen op kunnen leveren. Een tweetal enzymen werden gezuiverd met het doel de verworven mogelijkheden van directe electrochemie uit te proberen. Een van de enzymen was cytochroom P-450 uit *Pseudomonas putida* . Deze grondbacterie kan kamfer als koolstofbron gebruiken. Hiertoe dient deze verbinding echter eerst gehydroxyleerd te worden. Cytochroom P-450 neemt deze hydroxyleringsreaktie voor zijn rekening. De specifieke reden om dit enzym te gebruiken was tweeledig. Het enzym is relatief klein met een molekuulgewicht van 45000 Da en heeft een ferredoxine als natuurlijke electrondonor. Het idee was dat het mogelijk zou moeten zijn om de electrode de rol van dit ferredoxine over te laten nemen. De tweede, meer triviale reden, was dat het enzym in relatief grote hoeveelheden voorkomt in de bacterie en derhalve makkelijk te zuiveren is. De resultaten verkregen met cytochroom P-450 staan beschreven in hoofdstuk 4. Alleen onder zeer specifieke omstandigheden bleek het mogelijk om electronenoverdracht te verkrijgen tussen het enzym en de electrode. De uit deze experimenten verkregen 'midpoint'potentiaal was bovendien niet in overeenstemming met waarden uit de literatuur, verkregen door middel van andere methoden. Het bepalen van de redoxpotentiaal met een zogenaamde redoxtitratie gevolgd met behulp van EPR spectroscopie

leverde weliswaar een bijstelling van de in de literatuur genoemde waarde op, maar een verschil met de electrochemisch bepaalde waarde bleef bestaan.

Een ander enzym dat gebruikt werd voor electrochemische experimenten was superoxide dismutase. Dit enzym, verkregen uit de bacterie *Escherichia coli* en uit rode bloedlichaampjes van runderen, katalyseert de vorming van waterstofperoxide (H_2O_2) en zuurstof (O_2) uit twee superoxide ionen (O_2^-). Er wordt verondersteld dat superoxide dismutase betrokken is bij het onschadelijk maken van het zeer giftige superoxide ion. Het enzym uit *E. coli* bevat een ijzeratoom in het actieve centrum in tegenstelling tot het runderenzym dat een redox actief koper ion en een structureel zink ion bevat. Een reden om deze enzymen te gebruiken voor electrochemie was de recente beschrijving van een aantal electrochemische experimenten onder zeer extreme condities (bij zeer lage pH). Een andere reden was dat er in de literatuur verschillende waarden voor de 'midpoint' potentiaal waren vermeld. Aangezien deze potentiaal een intrinsieke eigenschap van een redox enzym is, zou er een consistent getal gevonden moeten worden. In hoofdstuk 5 staan de resultaten beschreven van cyclische voltammetrie en evenwichts redoxtitraties gevolgd met behulp van EPR spectroscopie. Runder erythrocyten superoxide dismutase bleek alleen bij zeer lage pH een voltammogram op te leveren. Uit de redoxtitratie onder vergelijkbare condities bleek de reductie van het enzym niet reversibel. Het EPR spectrum veranderde drastisch van vorm na oxidatie van het gereduceerde enzym. De in de literatuur verschenen data verkregen uit electrochemische experimenten bij lage pH zijn daarom niet bruikbaar. Evenwichts redoxtitraties van het enzym, uitgevoerd bij pH 7.0 gaven aan dat de tot nu bekende literatuurwaarde voor de redox potentiaal van dit enzym bijgesteld diende te worden. Het bleek niet mogelijk om voor superoxide dismutase uit *Escherichia coli* condities te vinden waaronder electronen overdracht met een electrode mogelijk werd. Uit de resultaten van een evenwichts redoxtitratie bleek dat het enzym alleen zeer traag te reduceren is met een chemische reductor. Reoxidatie blijkt bovendien niet mogelijk en dit geeft aan dat de redox reactie niet reversibel is. Dit kan de oorzaak zijn van de grote onderlinge verschillen tussen de in de literatuur vermelde waarden voor de redox potentiaal.

In hoofdstuk 6 en 7 wordt de electrochemische karakterisering beschreven van een tweetal kleine eiwitten die betrokken zijn bij electronenoverdracht. Rubredoxine uit *Megasphaera elsdenii* is een paars gekleurd eiwit van 6000 Da. Het eiwit bevat een redoxactief ijzerion dat gecoördineerd wordt door 4 zwavelatomen. Uit de kristallografie blijkt dat het ijzerion in het midden zit van een tetraëder met de zwavelatomen op de hoekpunten. Bij neutrale pH is de netto lading van het eiwit sterk negatief. Dit levert een probleem op tijdens de electrochemie aangezien gebruik gemaakt wordt van een eveneens negatieve koolstofelectrode. De afstoting tussen het eiwit en de electrode wordt algemeen beschouwd als de reden waarom geen goede electrochemie verkregen kan worden. Zoals aan het begin van deze samenvatting is beschreven wordt soms gebruik gemaakt van hulpstoffen die naar wordt aangenomen het contact tussen de electrode en het eiwit verbeteren. Voor eiwitten met een negatieve lading zijn

139

een aantal positief geladen ionen beschreven, die de electrochemische respons bevorderen. De huidige hypothese is dat ladingscompensatie hierbij een belangrijke rol speelt alhoewel definitief bewijs hiervoor nog niet geleverd is. De resultaten verkregen uit experimenten met rubredoxine in aanwezigheid van het redox actieve kation europium (Eu^{3+}) staan beschreven in hoofdstuk 6. De mogelijkheid om de potentiaal, en eventuele veranderingen hierin, van zowel het eiwit als het kation te volgen geeft inzicht in het werkingsmechanisme van het kation als promotor. Bij hoge pH waarden bleek het kation geen electrochemische respons meer te geven terwijl de respons van het eiwit onveranderd bleef. Dit is aanleiding om te veronderstellen dat ladingscompensatie niet zonder meer de belangrijkste voorwaarde is van de promotor werking van een kation.

De mogelijkheden van het gebruik van een electrode blijken uit de experimenten met het 'Rieske' eiwit. Dit eiwit is eigenlijk een onderdeel van een groot eiwitcomplex dat geïsoleerd kan worden uit runderharten. Dit complex is membraan-gebonden, maar met behulp van eiwitsplitsende enzymen kan een fragment afgesplitst worden ter grootte van 14521 Da. Dit fragment bevat een [2Fe-2S] cluster en verondersteld wordt dat deze cluster betrokken is bij de electronenoverdracht van het membraan gebonden complex naar electron carriers in oplossing . De [2Fe-2S] cluster wordt *in vivo* slechts half gereduceerd:

$$Fe(III)\text{-}Fe(III) + 1e^- \longrightarrow Fe(III)\text{-}Fe(II) \qquad (E_m' = 0.3 \text{ V vs. SHE})$$
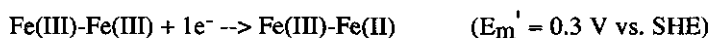
De vraag rijst of het mogelijk is om de cluster verder te reduceren tot de 2-electron gereduceerde vorm. Wanneer dit mogelijk is dan valt het te verwachten dat deze tweede potentiaal beduidend lager ligt dan de eerste. Het is dan ook de vraag of deze waarde met chemische reductiemiddelen bereikt kan worden. Met behulp van een electrode kan de potentiaal in principe onbegrensd gevarieerd worden. In praktijk blijken de grenzen bepaald tussen -1 V en + 0.8 V vanwege optredende electrolyse reacties (de vorming van waterstof bij lage potentiaal en de vorming van zuurstof bij hoge potentiaal). De resultaten verkregen met het Rieske eiwit staan beschreven in hoofdstuk 7 en geven aan dat reductie met twee electronen inderdaad mogelijk is. De potentiaal van deze tweede reductie is echter extreem laag met een waarde van -800 mV vs. SHE. Het lijkt daarom niet waarschijnlijk dat deze tweede reductie overgang een fysiologische relevantie heeft. De karakterisering van deze 'superreductie' moet dan ook meer gezien worden als een bijdrage aan de pogingen om inzicht te krijgen in de manieren waarop eiwitten in staat zijn de redox potentialen van bepaalde metaalionen te beïnvloeden.

Het laatste gedeelte van dit proefschrift bevat nog twee hoofdstukken waarin de aandacht ligt op de spectroscopische karakterisering van een tweetal eiwitten uit de sulfaatreduceerder *D. vulgaris* (Hildenborough). De al eerder in deze samenvatting genoemde EPR spectroscopie werd uitgebreid toegepast om de aard van de redox actieve cofactor in beide eiwitten vast te stellen. In hoofdstuk 8 is een EPR studie van 'hoog molekuulgewicht cytochroom *c* ' uit *D. vulgaris* (H) beschreven. Cytochromen zijn in het algemeen kleine

eiwitten die één tot vier hemen bevatten. De heem veroorzaakt de karakteristieke dieprode kleur. Al geruime tijd is bekend dat *D. vulgaris* (H) een eiwit bevat met een molekuulgewicht van 64 kDa waarin zestien heemgroepen zitten gebonden. De functie van dit eiwit is tot nu toe onbekend en daarom heeft het de naam hoog molekuulgewicht cytochroom *c* gekregen. Deze naam suggereert weliswaar dat dit eiwit, evenals andere *c* cytochromen, alleen betrokken zou zijn bij electronen transport. Een rol als enzym lijkt echter waarschijnlijker gezien het molekuulgewicht. De coordinatie van de ijzerionen in de heemgroepen is niet voor alle 16 hemen gelijk en hierover is in de literatuur onduidelijkheid ontstaan. EPR spectroscopie van geconcentreerde preparaten in combinatie met optische spectroscopie en evenwichts redoxtitraties hebben inzicht gegeven in de precieze coordinatie. Uit vergelijking van de redoxpotentialen bepaald uit de redoxtitraties bleek bovendien dat de in de literatuur beschreven electrochemische experimenten niet voldeden aan de criteria van reversibiliteit en reproduceerbaarheid. Tot nu toe is het niet mogelijk gebleken een biologische functie voor dit eiwit vast te stellen.

In het laatste hoofdstuk is tenslotte de karakterisering beschreven van het enzym adenylyl phosphosulfaat reductase (APS reductase). Dit enzym is betrokken bij de 'ademhaling' van *Desulfovibrio vulgaris* . Bij deze ademhaling wordt echter geen gebruik gemaakt van zuurstof als terminale electron acceptor zoals bij aërobe organismen maar van sulfaat. Sulfaat wordt door de bacterie omgezet in het corrosieve H_2S dat de, voor deze bacterie karakteristieke, rotte eieren lucht veroorzaakt. De bacterie is aanwezig in gebieden waar geen zuurstof beschikbaar is zoals bijv. op de bodem van vijvers of in moerasgebieden. Ook in de nabijheid van ondergrondse pijpleidingen is deze bacterie te vinden en veroorzaakt hier veel schade door corrosie. APS reductase is een van de eerste enzymen in de ademhalingsketen van de bacterie en is betrokken bij de reductiestap van het geactiveerde sulfaat (APS) tot sulfiet. APS reductase werd in de literatuur beschreven als een enzym bestaande uit vier subeenheden gerangschikt als $\alpha_2\beta_2$. Per $\alpha\beta$ zou het enzym twee [4Fe-4S] clusters (cubanen) bevatten en één FAD cofactor. De aanwezigheid van twee cubanen was gebaseerd op een ijzeranalyse, die 7.8 Fe per $\alpha\beta$ opleverde, en op het verschijnen van een ingewikkeld EPR interactie spectrum. Dit interactie spectrum wordt vaker waargenomen wanneer twee clusters dicht bij elkaar in de buurt zitten. De door ons uitgevoerde ijzerbepalingen leverden een iets lager getal op van gemiddeld 6 ijzers en 5 zwavels per $\alpha\beta$. Dit was aanleiding om ook de spectroscopie opnieuw onder de loep te nemen. Aangetoond kon worden dat het ingewikkelde EPR interactiespectrum afhankelijk was van de aanwezigheid van inert zout zoals NaCl. Bovendien kon op grond van de intensiteit van het EPR spectrum vastgesteld worden dat er maar één cluster aanwezig kon zijn per $\alpha\beta$. Dit was aanleiding om voor te stellen dat APS reductase niet twee maar één ijzer zwavel cluster bevat mogelijk met meer dan 4 ijzer- en zwavelatomen.

Curriculum vitae

Marcus Franciscus Josefus Maria Verhagen werd geboren op 14 september 1965 te Boxtel. In 1983 behaalde hij het diploma atheneum B aan het Jacob Roelandslyceum in Boxtel. In hetzelfde jaar werd begonnen met de studie Moleculaire Wetenschappen aan de toenmalige Landbouwhogeschool in Wageningen. De doctoraalfase bestond uit afstudeervakken bij de vakgroepen Biochemie (Dr. W.R. Hagen, Prof. Dr. C. Veeger; De invloed van NO en CO op de kinetiek van hydrogenase uit *Desulfovibrio vulgaris* (Hildenborough)) en Proceskunde (Dr. M. Fontijn, Prof Dr. Ir. K. van 't Riet, Prof Dr. B. Bijsterbosch; De invloed van vervuiling op de poriegrootte verdeling van ultrafiltratie membranen). Tevens werd er een stage uitgevoerd bij de Biophysics Research Division van de University of Michigan, Ann Arbor, USA (Dr. W.R. Dunham en Prof. R.H. Sands; Magnetische eigenschappen en structuur van enkele metaal-chelator complexen). Het doctoraal examen werd afgelegd in maart 1989.

In de periode van april 1989 tot januari 1994 werd er gewerkt als assistent in opleiding bij de vakgroep Biochemie van de Landbouwuniversiteit in Wageningen. Het promotie onderzoek werd uitgevoerd binnen het Innovatief Onderzoeks Programma biotechnologie (IOP-b) en heeft geleid tot dit proefschrift. Vanaf januari 1994 is de auteur werkzaam als Post-Doc bij het Department of Biochemistry van de University of Georgia (Prof. M.W.W. Adams) gedeeltelijk gefinancierd door een NATO stipendium toegekend door NWO.

List of publications

Full papers:

M.F.J.M. Verhagen and W.R. Hagen, Electron transfer mechanism of flavin adenine dinucleotide at the glassy carbon electrode; a model study for protein electrochemistry, *Journal of Electroanalytical Chemistry and Interfacial Electrochemistry*, 334 (1992) 339-350.

M.F.J.M. Verhagen, W.G.B. Voorhorst, J.A. Kolkman, R.B.G. Wolbert and W.R. Hagen, On the two iron centers of Desulfoferrodoxin, *FEBS Letters*, 336 (1993) 13-18.

M.F.J.M. Verhagen, R.B.G. Wolbert and W.R. Hagen, Cytochrome *c* 553 from *Desulfovibrio vulgaris* (Hildenborough): Electrochemical properties and electron transfer with hydrogenase, *European Journal of Biochemistry*, 221 (1994) 821-829.

M.F.J.M. Verhagen, I.M. Kooter, R.B.G. Wolbert and W.R. Hagen, On the iron-sulfur cluster of adenosine phosphosulfate reductase from *Desulfovibrio vulgaris* (Hildenborough), *European Journal of Biochemistry*, 221 (1994) 831-837.

M.F.J.M. Verhagen, A.J. Pierik, R.B.G. Wolbert, L.F. Mallée, W.G.B. Voorhorst and W.R. Hagen, Axial coordination and reduction potentials of the sixteen hemes in high-molecular-mass cytochrome *c* from *Desulfovibrio vulgaris* (Hildenborough), *European Journal of Biochemistry*, 225 (1994) 311-319

M.F.J.M. Verhagen, E.M. Meussen and W.R. Hagen, On the reduction potentials of Fe and Cu-Zn containing superoxide dismutases, *Biochimica et Biophysica Acta*, in the press.

A.F. Arendsen, M.F.J.M. Verhagen, R.B.G. Wolbert, A.J. Pierik, A.J.M. Stams, M.S.M. Jetten and W.R. Hagen, The dissimilatory sulfite reductase from *Desulfosarcina variabilis* is a desulforubidin and it contains uncoupled metallated sirohemes and S=9/2 iron-sulfur clusters, *Biochemistry*, 32 (1993) 10323-10330.

A.J. Pierik, R.B.G. Wolbert, G.L. Portier, M.F.J.M. Verhagen and W.R. Hagen, Nigerythrin and Rubrerythrin from *Desulfovibrio vulgaris* each contain two rubredoxin-like centers and two dinuclear iron centers, *European Journal of Biochemistry*, 212 (1993) 237-245.

A.J. Pierik, W.R. Hagen, J.S. Redeker, R.B.G. Wolbert, M. Boersma, M.F.J.M. Verhagen, H.J. Grande, C. Veeger, P.H.A. Mutsaers, R.H. Sands and W.R. Dunham, Redox properties of the iron-sulfur clusters in activated Fe-hydrogenase from *Desulfovibrio vulgaris* (Hildenborough), *European Journal of Biochemistry*, 209 (1992), 63-72.

W.A.M. van de Berg, A.A.M. Stevens, M.F.J.M. Verhagen, W.M.A.M. van Dongen and W.R. Hagen, Overproduction of the prismane protein from *Desulfovibrio desulfuricans* ATCC 27774 in *Desulfovibrio vulgaris* (Hildenborough) and EPR spectroscopy of the [6Fe-6S] cluster in different redox states, *Biochimica et Biophysica Acta*, 1206 (1994) 240-246.

M.F.J.M. Verhagen, T.A. Link and W.R. Hagen, Electrochemical study of the redox properties of [2Fe-2S] ferredoxins; evidence for superreduction of the Rieske [2Fe-2S] cluster, submitted to *FEBS Letters*.

M.F.J.M. Verhagen and W.R. Hagen, Redox properties of rubredoxin from *Megasphaera elsdenii* studied at the glassy carbon electrode in the presence of europium, submitted to *Journal of Electroanalytical Chemistry and Interfacial Electrochemistry*.

Abstracts

M.F.J.M. Verhagen, I.M. Kooter, R.B.G. Wolbert and W.R. Hagen, Spectroscopic and redox properties of adenosine phosphosulfate reductase from *Desulfovibrio vulgaris* (Hildenborough), *Journal of Inorganic Biochemistry*, 51, 1993, 19.

A.F. Arendsen, M.F.J.M. Verhagen, R.B.G. Wolbert, A.J. Pierik, A.J.M. Stams, M.S.M. Jetten and W.R. Hagen, The dissimilatory sulfite reductase from *Desulfosarcina variabilis* is a desulforubidin and it contains uncoupled metallated sirohemes and S=9/2 iron-sulfur clusters, *Journal of Inorganic Biochemistry*, 51, 1993, 469.

W.R. Hagen, M.F.J.M. Verhagen, A.J. Pierik, R.B.G. Wolbert, L.F. Mallée and W.G.B. Voorhorst, Axial coordination and reduction potentials of the 16 hemes in high-molecular-weight cytochrome *c* from *Desulfovibrio vulgaris* (H), *Journal of Inorganic Biochemistry*, 51, 1993, 28.

W.R. Hagen, A.J. Pierik, R.B.G. Wolbert, M.F.J.M. Verhagen and C. Veeger, A reinvestigation of the redox properties of the periplasmic Fe-hydrogenase from *Desulfovibrio vulgaris* (Hildenborough), *Abstracts of the third international conference on the molecular biology of hydrogenases, Troia, Portugal*, 1991, 72-75.

W.R. Hagen, A.J. Pierik, W.M.A.M. van Dongen, M.G. Duyvis, M.F.J.M. Verhagen and H. Haaker, The redox and magnetic properties of the prosthetic groups in the MoFe-protein of *Azotobacter vinelandii* nitrogenase, *New horizons in nitrogen fixation* (Palacios, R., Mora, J. & Newton, W.E. eds.) Nijhoff/Junk, Dordrecht (The Netherlands), 1993, 137.